1991 William Barclay Parsons Fellowship
Parsons Brinckerhoff
Monograph 7

Seismic Design of Tunnels

A Simple State-of-the-Art Design Approach

Jaw-Nan (Joe) Wang, Ph.D., P.E.
Professional Associate
Parsons Brinckerhoff Quade & Douglas, Inc.
June 1993

First Printing 1993

Published by
Parsons Brinckerhoff Inc.
One Penn Plaza
New York, New York

CONTENTS

LIST OF FIGURES

LIST OF TABLES

FOREWORD

For more than a century, Parsons Brinckerhoff (PB) has been instrumental in advancing state-of-the-art design and construction of underground structures, and the fields of seismic design and earthquake engineering are no exceptions. Almost three decades ago PB's engineers pioneered in these fields in the design and construction of the San Francisco BART system, whose toughness during earthquakes, including the recent Loma Prieta event, has been amply tested. Recently, PB developed state-of-the-art, two-level seismic design philosophy in its ongoing Los Angeles Metro and Boston Central Artery/Third Harbor Tunnel projects, taking into account both performance-level and life-safety-level earthquakes.

This monograph represents PB's continuous attempts in the seismic design and construction of underground structures to:

- Improve our understanding of seismic response of underground structures
- Formulate a consistent and rational seismic design procedure

Chapter 1 gives general background information including a summary of earthquake performance data for underground structures.

Chapter 2 presents the seismic design philosophy for tunnel structures and the rationale behind this philosophy. Differences in seismic considerations between surface structures and underground structures, and those between a seismic design and a static design are also discussed.

Chapter 3 focuses on the seismic design considerations in the longitudinal direction of the tunnels. Axial and curvature deformations are the main subjects. The free-field deformation method and the methods accounting for tunnel-ground interaction effects are reviewed for their applicability.

Chapter 4 takes a look at the ovaling effect on circular tunnel linings. Closed-form solutions considering soil-lining interaction effects are formulated and presented in the form of design charts to facilitate the design process.

Chapter 5 moves to the evaluation of racking effect on cut-and-cover rectangular tunnels. This chapter starts with a review of various methods of analysis that are currently in use, followed by a series of dynamic finite-element analyses to study the various factors influencing the tunnel response. At the end, simplified frame analysis models are proposed for this evaluation.

Chapter 6 ends this monograph with a general summary.

Acknowledgments

I wish to express my thanks to the Career Development Committee and Paul H. Gilbert, the original initiator of the William Barclay Parsons Fellowship Program, for selecting my proposal and providing continuous support and guidance throughout this study. Thanks are also due to the Board of Directors of Parsons Brinckerhoff Inc. for making the growth and flowering of an engineer's idea possible.

The fruitful results of this exciting study would never have been possible without technical guidance from three individuals — my fellowship mentors, Dr. George Munfakh and Dr. Birger Schmidt, and the technical director of underground structures, Dr. James E. Monsees. Their constant critiques and advice were sources of inspiration and motivation.

Appreciation is due also to Tom Kuesel, who gave constructive technical comments on the content of this study, and to Tim Smirnoff, who provided much of the tunnel structural data of the LA Metro project. Ruchu Hsu and Rick Mayes deserve my thanks for generously giving their time and comments on the draft of this monograph. Gratitude is offered to many other individuals for numerous technical discussions on real world seismic design issues for the ongoing Central Artery/Third Harbor Tunnel project and the Portland Westside LRT project. They include: Louis Silano, Vince Tirolo, Anthony Lancellotti, Dr. Sam Liao, Brian Brenner, Alexander Brudno, Mike Della Posta, Dr. Edward Kavazanjian, Richard Wilson, and many others.

Very special thanks to Willa Garnick for her exquisite editing of the manuscript, and to Randi Aronson who carefully proofread the final draft of the monograph. Their wonderful work gave this fellowship study a beautiful finish. I also acknowledge the support and contribution of personnel of the New York office Graphics Department, particularly Pedro Silva who prepared the graphics and tables and laid out the text.

I simply could not put a period to this study without expressing thanks to my wife Yvonne Yeh, my son Clinton and my daughter Jolene. Their sacrificing support of my work through many late nights and weekends contributed the greatest part to this monograph.

Jaw-Nan (Joe) Wang, Ph.D., P.E.
Professional Associate
Parsons Brinckerhoff Quade & Douglas, Inc.
June 1993

1.0 INTRODUCTION

1.0 INTRODUCTION

1.1 Purpose

The purpose of this research study was to develop a rational and consistent seismic design methodology for lined transportation tunnels that would also be applicable to other underground lined structures with similar characteristics. The results presented in this report provide data for simple and practical application of this methodology.

While the general public is often skeptical about the performance of underground structures, tunnel designers know that underground structures are among the safest shelters during earthquakes, based primarily on damage data reported in the past. Yet one certainly would not want to run away from a well designed building into a buried tunnel when seismic events occur if that tunnel had been built with no seismic considerations.

Most tunnel structures were designed and built, however, without regard to seismic effects. In the past, seismic design of tunnel structures has received considerably less attention than that of surface structures, perhaps because of the conception about the safety of most underground structures cited above. In fact, a seismic design procedure was incorporated into a tunnel project for the first time in the 1960s by PB engineers.

In recent years, however, the enhanced awareness of seismic hazards for underground structures has prompted an increased understanding of factors influencing the seismic behavior of underground structures. Despite this understanding, significant disparity exists among engineers in design philosophy, loading criteria, and methods of analysis.

Therefore, this study, geared to advance the state of the art in earthquake engineering of transportation tunnels, has the following goals:

- To maintain a consistent seismic design philosophy and consistent design criteria both for underground structures and other civil engineering facilities.
- To develop simple yet rational methods of analysis for evaluating earthquake effects on underground structures. The methodology should be consistent for structures with different section geometries.

1.2 Scope of this Study

The work performed to achieve these goals consisted of:

- *A summary of observed earthquake effects on underground structures.*
- *A comparison of seismic design philosophies for underground structures and other civil engineering facilities.* Based on this comparison, seismic design criteria were developed for underground tunnels.
- *A quantitative description of ground behavior during traveling seismic waves.* Various modes of ground deformations and their engineering implications for tunnel design are discussed.
- *A review of current seismic design methodology for both circular mined tunnels and cut-and-cover rectangular tunnels.* Examples were used to study the applicability of these conventionally used methods of analysis.
- *The development of a refined (yet simple) method for evaluating the earthquake ovaling effect on circular linings.* This method considers the soil-structure interaction effects and is built from a theory that is familiar to most mining/underground engineers. To ease the design process, a series of design charts was developed, and these theoretical results were further validated through a series of numerical analyses.
- *The development of a simplified frame analysis model for evaluating the earthquake racking effect on cut-and-cover rectangular tunnels.* During the process of this development, an extensive study using dynamic finite-element, soil-structure interaction analyses was conducted to cover a wide range of structural, geotechnical and ground motion parameters. The purpose of these complex and time consuming analyses was not to show the elegance of the mathematical computations. Rather, these analyses were used to generate design data that could be readily incorporated into the recommended simplified frame analysis model.

1.3 Background

Importance of Seismic Design

One of the significant aspects of the 1989 Loma Prieta earthquake in the San Francisco area was its severe impact on the aboveground transportation system:

- The collapse of the I-880 viaduct claimed more than 40 lives.
- The direct damage costs to the transportation facilities alone totalled nearly $2 billion (Werner and Taylor, 1990).
- The indirect losses were several times greater as a result of major disruptions of transportation, particularly on the San Francisco-Oakland Bay Bridge and several major segments of the Bay area highway system.

The San Francisco Bay Area Rapid Transit (BART) subway system was found to be one of the safest places during the event, and it became the only direct public transportation link between Oakland and San Francisco after the earthquake. Had BART been damaged and rendered inoperative, the consequences and impact on the Bay area would have been unthinkable.

The 60-mile BART system was unscathed by the earthquake because PB engineers had the foresight 30 years ago to incorporate state-of-the-art seismic design criteria in their plans for the subway tunnels (SFBARTD, 1960; Kuesel, 1969; and Douglas and Warshaw, 1971). The Loma Prieta earthquake proved the worth of their pioneering efforts.

Seismic Design Before the '90s

Based on the performance record, it is undoubtedly fair to say that underground structures are less vulnerable to earthquakes than surface structures (Dowding and Rozen, 1978; Rowe, 1992). Interestingly, some tunnels and shafts built without special earthquake provisions have survived relatively strong earthquakes in the past — for example, the Mexico City subway during the 1985 Mexico City earthquake. On the other hand, some underground structures have been damaged severely in other events (see Section 1.5).

Limited progress has been made in seismic design methodology for underground tunnels since the work for BART, possibly because of favorable performance data, and limited research work has been done toward a practical solution. The lack of a rational methodology for engineers and the nonexistence of applicable codes has led to widely varied measures taken by different engineers. For example:

- Some ignore seismic effects and fail to check the resistance of the structures to earthquakes, even in highly seismic areas.
- Others conduct their seismic design for underground structures using the same methodology developed for aboveground structures, without recognizing that underground structures are constrained by the surrounding medium.

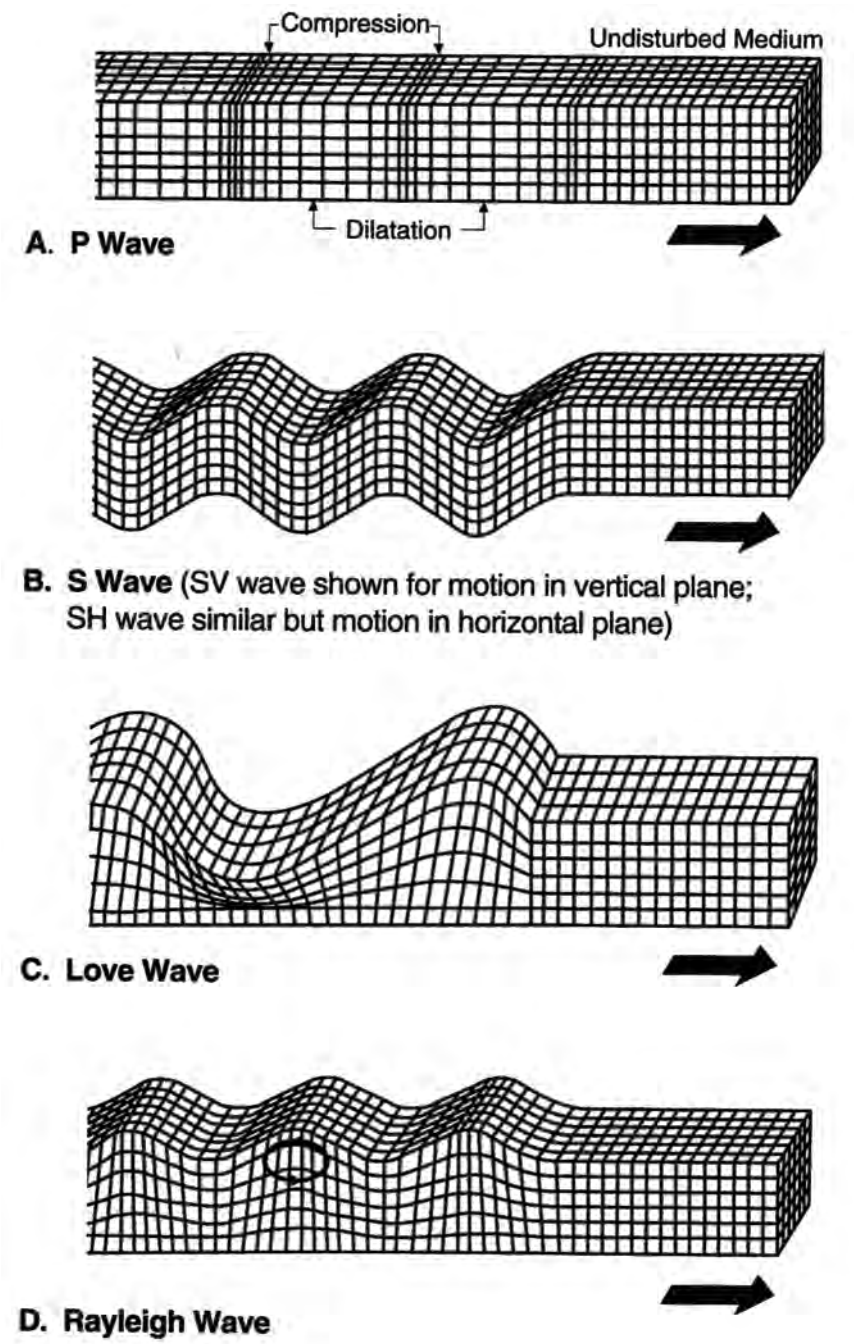

Figure 1.
Ground Response to Seismic Waves

(Source: Bolt, 1978)

Design based on such inappropriate measures may lead to the construction of unsafe structures or structures that are too conservatively designed.

Although the progress of underground seismic design methodology is lagging, the earthquake awareness in the country is not. Recent discoveries in seismology, geology and geotechnical engineering have led to the belief that earthquake hazard is no longer only a California problem. Many regions throughout the United States, Puerto Rico and the Virgin Islands are now known to have the potential for tremors of similar or larger magnitude than that of the Loma Prieta. This situation demands rethinking of the current seismic design practice for our underground transportation systems.

1.4 General Effects of Earthquakes

In a broad sense, earthquake effects on underground tunnel structures can be grouped into two categories – ground shaking and ground failure.

Ground Shaking

Ground shaking refers to the vibration of the ground produced by seismic waves propagating through the earth's crust. The area experiencing this shaking may cover hundreds of square miles in the vicinity of the fault rupture. The intensity of the shaking attenuates with distance from the fault rupture. Ground shaking motions are composed of two different types of seismic waves, each with two subtypes. Figure 1 shows the ground response due to the various types of seismic waves:

- Body waves travel within the earth's material. They may be either longitudinal P waves or transverse shear S waves and they can travel in any direction in the ground.
- Surface waves travel along the earth's surface. They may be either Rayleigh waves or Love waves.

As the ground is deformed by the traveling waves, any tunnel structure in the ground will also be deformed. If the imposed deformation were the sole effect to be considered, ductility and flexibility would probably be the only requirements for the design of tunnel structures (from a structural standpoint). However, tunnel structures also must be designed to carry other sustained loads and satisfy other functional requirements. A proper and efficient tunnel structural design, therefore, must consider the structural members' capacity in terms of strength as well as ductility and flexibility of the overall configuration.

Ground Failure

Ground failure broadly includes various types of ground instability such as faulting, landslides, liquefaction, and tectonic uplift and subsidence. Each of these hazards may be potentially catastrophic to tunnel structures, although the damages are usually localized. Design of a tunnel structure against ground instability problems is often possible, although the cost may be high. For example, it may be possible to remedy the ground conditions against liquefaction and landslides with proper ground improvement techniques and appropriate earth retaining measures.

It may not be economically or technically feasible, however, to build a tunnel to resist potential faulting displacements. As suggested by Rowe (1992), the best solution to the problem of putting a tunnel through an active fault is —- don't. Avoidance of faults may not always be possible, however, because a tunnel system may spread over a large area. In highly seismic areas such as California, tunnels crossing faults may be inevitable in some cases. The design approach to this situation is to accept the displacement, localize the damage, and provide means to facilitate repairs (Kuesel, 1969).

1.5 Performance Record in Earthquakes

Information on the performance of underground openings during earthquakes is relatively scarce, compared to information on the performance of surface structures, and information on lined underground tunnels is even more scarce. Therefore, the summaries of published data presented in this section may represent only a small fraction of the total amount of data on underground structures. There may be many damage cases that went unnoticed or unreported. However, there are undoubtedly even more unreported cases where little or no damage occurred during earthquakes.

Dowding and Rozen (1978)

The authors reported 71 cases of tunnel response to earthquake motions. The main characteristics of these case histories are as follows:

- These tunnels served as railway and water links with diameters ranging from 10 feet to 20 feet.
- Most of the tunnels were constructed in rock with variable rock mass quality.
- The construction methods and lining types of these tunnels varied widely. The permanent ground supports ranged from no lining to timber, masonry brick, and concrete linings.

Based on their study, Dowding and Rozen concluded, primarily for rock tunnels, that:

- Tunnels are much safer than aboveground structures for a given intensity of shaking.
- Tunnels deep in rock are safer than shallow tunnels.
- No damage was found in both lined and unlined tunnels at surface accelerations up to 0.19g.
- Minor damage consisting of cracking of brick or concrete or falling of loose stones was observed in a few cases for surface accelerations above 0.25g and below 0.4g.
- No collapse was observed due to ground shaking effect alone up to a surface acceleration of 0.5g.
- Severe but localized damage including total collapse may be expected when a tunnel is subject to an abrupt displacement of an intersecting fault.

Owen and Scholl (1981)

These authors documented additional case histories to Dowding and Rozens', for a total of 127 case histories. These added case histories, in addition to rock tunnels, included:

- Damage reports on cut-and-cover tunnels and culverts located in soil
- Data on underground mines, including shafts

The authors' discussion of some of the damaged cut-and-cover structures is of particular interest. These structures have the common features of shallow soil covers and loose ground conditions:

- A cut-and-cover railroad tunnel with brick lining (two barrels, each approximately 20 feet wide) was destroyed by the 1906 San Francisco earthquakes. In this case, where brick lining with no moment resistance was used, the tunnel structure collapsed.
- Five cases of cut-and-cover conduits and culverts with reinforced concrete linings were damaged during the 1971 San Fernando earthquake. The damages experienced by the linings included:
    - The failure of longitudinal construction joints
    - Development of longitudinal cracks and concrete spalling

- Formation of plastic hinges at the top and bottom of walls

The conclusions made by Owen and Scholl, based on their study, echoed the findings by Dowding and Rozen discussed above. In addition, they suggested the following:

- Damage to cut-and-cover structures appeared to be caused mainly by the large increase in the lateral forces from the surrounding soil backfill.

- Duration of strong seismic motion appeared to be an important factor contributing to the severity of damage to underground structures. Damage initially inflicted by earth movements, such as faulting and landslides, may be greatly increased by continued reversal of stresses on already damaged sections.

Wang (1985)

In describing the performance of underground facilities during the magnitude 7.8 Tang-Shan earthquake of 1976, the author reported the following:

- An inclined tunnel passing through 13 feet of soil into limestone was found to have cracks up to 2 cm wide on the side wall. The plain concrete floor heaved up 5 to 30 cm.

- Damage to underground facilities decreased exponentially with depth to 500 m. Schmidt and Richardson (1989) attributed this phenomenon to two factors:

    - The increasing competence of the soil/rock with depth

    - The attenuation of ground shaking intensity with depth

Sharma and Judd (1991)

The authors extended Owen and Scholl's work and collected qualitative data for 192 reported observations from 85 worldwide earthquake events. They correlated the vulnerability of underground facilities with six factors: overburden cover, rock type (including soil), peak ground acceleration, earthquake magnitude, epicentral distance, and type of support. It must be pointed out that most of the data reported are for earthquakes of magnitude equal to 7 or greater. Therefore, the damage percentage of the reported data may appear to be astonishingly higher than one can normally conceive.

The results are summarized in the following paragraphs. Readers should be aware that these statistical data are of a very qualitative nature. In many cases, the damage statistics, when correlated with a certain parameter, may show a trend that violates an engineer's intuition. This may be attributable to the statistical dependency on other parameters which may be more influential.

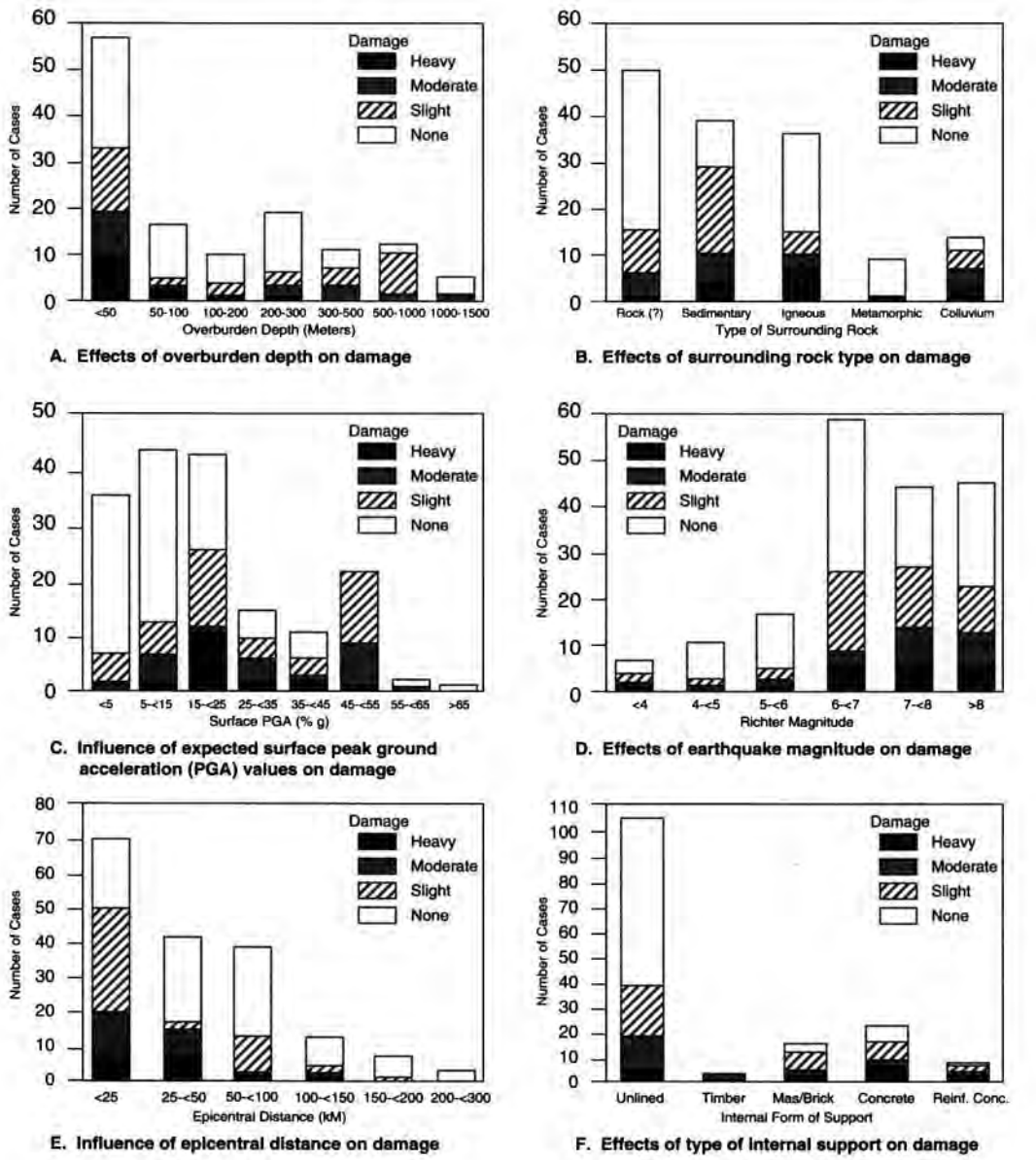

Figure 2.
Damage Statistics

(Source: Sharma and Judd, 1991)

- The effects of overburden depths on damage are shown in Figure 2A for 132 of the 192 cases. Apparently, the reported damage decreases with increasing overburden depth.

- Figure 2B shows the damage distribution as a function of material type surrounding the underground opening. In this figure, the data labeled “Rock (?)” were used for all deep mines where details about the surrounding medium were not known. The data indicate more damage for underground facilities constructed in soil than in competent rock.

- The relationship between peak ground acceleration (PGA) and the number of damaged cases are shown in Figure 2C.

    - For PGA values less than 0.15g, only 20 out of 80 cases reported damage.

    - For PGA values greater than 0.15g, there were 65 cases of reported damage out of a total of 94 cases.

- Figure 2D summarizes the data for damage associated with earthquake magnitude. The figure shows that more than half of the damage reports were for events that exceeded magnitude M=7.

- The damage distribution according to the epicentral distance is presented in Figure 2E. As indicated, damage increases with decreasing epicentral distance, and tunnels are most vulnerable when they are located within 25 to 50 km from the epicenter.

- Among the 192 cases, unlined openings account for 106 cases. Figure 2F shows the statistical damage data for each type of support. There were only 33 cases of concrete-lined openings including 24 openings lined with plain concrete and 9 cases with reinforced concrete linings. Of the 33 cases, 7 were undamaged, 12 were slightly damaged, 3 were moderately damaged, and 11 were heavily damaged.

  It is interesting to note that, according to the statistical data shown in Figure 2F, the proportion of damaged cases for the concrete and reinforced concrete lined tunnels appears to be greater than that for the unlined cases. Sharma and Judd attributed this phenomenon to the poor ground conditions that originally required the openings to be lined. Richardson and Blejwas (1992) offered two other possible explanations:

    -Damage in the form of cracking or spalling is easier to identify in lined openings than in unlined cases.

    -Lined openings are more likely to be classified as damaged because of their high cost and importance.

2.0 SEISMIC DESIGN PHILOSOPHY FOR TUNNEL STRUCTURES

2.0 SEISMIC DESIGN PHILOSOPHY FOR TUNNEL STRUCTURES

2.1 Seismic Design vs. Conventional Design

The purpose of seismic design, like any civil engineering design, is to give the structure the capacity to withstand the loads or displacements/deformations applied to it. The philosophy employed in seismic design is different, however, from standard structural engineering practice because:

- Seismic loads cannot be calculated accurately. Seismic loads are derived with a high degree of uncertainty, unlike dead loads, live loads, or other effects such as temperature changes. Any specified seismic effect has a risk (probability of exceedance) associated with it.

- Seismic motions are transient and reversing (i.e., cyclic). The frequency or rate of these cyclic actions is generally very high, ranging from less than one Hz to greater than ten Hz.

- Seismic loads are superimposed on other permanent or frequently occurring loads. Although seismic effects are transient and temporary, seismic design has to consider the seismic effects given the presence of other sustained loads.

Conventional design procedure under permanent and frequently occurring loads calls for the structure to remain undamaged (i.e., more or less within elastic range). Because of the differences discussed above, however, proper seismic design criteria should consider the nature and importance of the structure, cost implications, and risk assessment associated with such factors as public safety, loss of function or service, and other indirect losses (Nyman, et al, 1984).

2.2 Surface Structures vs. Underground Structures

For underground structures such as tunnels, the seismic design approach differs from that of the surface structures (e.g., bridges and buildings).

Surface Structures

In the seismic design practice for bridges, the loads caused by an extreme event (earthquake) in a seismically active region are often several times more severe than the

loads arising from other causes. To design a bridge to remain elastic and undamaged for such infrequent loads is uneconomical and sometimes not possible (Buckle, et al, 1987). Therefore, it is clearly not practical to use the same design approach to earthquakes as is used for other types of loads. The seismic design philosophy developed for bridges (AASHTO, 1991) is discussed briefly in Section 2.3.

Surface structures are not only directly subjected to the excitations of the ground, but also experience amplification of the shaking motions depending on their own vibratory characteristics. If the predominant vibratory frequency of the structures is similar to the natural frequency of the ground motions, the structures are excited by resonant effects.

Underground Structures

In contrast, underground structures are constrained by the surrounding medium (soil or rock). It is unlikely that they could move to any significant extent independently of the medium or be subjected to vibration amplification. Compared to surface structures, which are generally unsupported above their foundations, the underground structures can be considered to display significantly greater degrees of redundancy thanks to the support from the ground. These are the main factors contributing to the better earthquake performance data for underground structures than their aboveground counterparts.

Design and Analysis Approaches

The different response characteristics of aboveground and underground structures suggest different design and analysis approaches:

- *Force Method for Surface Structures.* For aboveground structures, the seismic loads are largely expressed in terms of inertial forces. The traditional methods generally involve the application of equivalent or pseudostatic forces in the analysis.

- *Deformation Method for Underground Structures.* The design and analysis for underground structures should be based, however, on an approach that focuses on the displacement/deformation aspects of the ground and the structures, because the seismic response of underground structures is more sensitive to such earthquake induced deformations.

  The deformation method is the focus of this report.

2.3 Seismic Design Philosophies for Other Facilities

Bridges and Buildings

The design philosophy adopted in bridge and building codes (e.g., AASHTO and UBC) is such that:

- *For small to moderate earthquakes*, structures are designed to remain elastic and undamaged

- *For more severe earthquakes*, the intent is to avoid collapse but to accept that structural damage will occur. This means that in a severe earthquake, the stresses due to seismic loads will exceed the yield strength of some of the structural members and inelastic deformations such as plastic hinges will develop (Buckle, et al, 1987).

Using this design philosophy for a severe earthquake, the structural members are designed for seismic forces that are lower than those anticipated if the structures were to remain elastic. This reduction in seismic forces is expressed by the response modification factor in the codes. At the same time, these codes also require that catastrophic failures be prevented by using good detailing practice to give the structures sufficient ductility. Normally, the larger a response modification factor used in the design of a member, the greater the ductility that should be incorporated in the design of this member. With this ductility the structures are able to hang together, even when some of the members are strained beyond their yield point.

Although the two-level design concept (small versus severe earthquake) is adopted in the bridge and building codes, the explicit seismic design criteria specified in these codes are based only on a single level of design earthquake — the severe earthquake. Typical design shaking intensity specified in these codes (ATC, 1978; UBC, 1992; AASHTO, 1983 and 1991) is for an earthquake of about a 500-year return period, which can be translated into an event with a probability of exceedance of about 10 percent during the next 50 years.

Nuclear Power Facilities

Two-level earthquake design philosophy is adopted for nuclear power facilities:

- *For the Operating Basis Earthquake (OBE)*, the lower-level event, the allowable stresses in all structural members and equipment should be within two-thirds of the ultimate design values.

- *For the Safe Shutdown Earthquake (SSE)*, the higher-level event, stresses caused by seismic loads should not exceed the ultimate strength of the structures and equipment.

Port and Harbor Facilities

Neither standard seismic codes nor universally accepted seismic design criteria exist for waterfront facilities such as berthing (wharf) structures, retaining structures, and dikes. Recent advances in seismic design practice for other facilities, however, have prompted the development of several project specific seismic design criteria for waterfront facilities in high seismic areas (POLA, 1991; Wittkop, 1991; Torseth, 1984).

The philosophy employed in the design, again, is based on two-level criteria:

- *Under an Operating Level Earthquake (OLE)*, *a smaller earthquake*, the structures should experience little to no damage and the deformations of wharf structures should remain within the elastic range. Generally, the OLE is defined to have a probability of exceedance of 50 percent in 50 years.

- *Under a Contingency Level Earthquake (CLE)*, *a larger earthquake*, the structures should respond in a manner that prevents collapse and major structural damage, albeit allowing some structural and nonstructural damage. Damage that does occur should be readily detectable and accessible for inspection and repair. Damage to foundation elements below ground level should be prevented (POLA, 1991).

Generally, the CLE is to have a probability of exceedance of 10 percent in 50 years. The risk level defined for the CLE is similar to that of the design earthquake adopted in bridge and building design practice.

Oil and Gas Pipeline Systems

The seismic design guidelines recommended by ASCE (Nyman, et al, 1984) for oil and gas pipeline systems are in many ways similar to the principles used in the design for other important facilities. For important pipeline systems, the design should be based on two-level earthquake hazard:

- *The Probable Design Earthquake (PDE), the lower level*, is generally associated with a return period of 50 to 100 years.

- *The Contingency Design Earthquake (CDE), the higher level*, is represented by an event with a return period of about 200 to 500 years. The general performance requirements of the pipeline facilities under the two design events are also similar to those for other facilities.

2.4 Proposed Seismic Design Philosophy for Tunnel Structures

Two-Level Design Criteria

Based on the discussion presented above, it is apparent that current seismic design philosophy for many civil engineering facilities has advanced to a state that dual (two-level) design criteria are required. Generally speaking, the higher design level is aimed at life safety while the lower level is intended for continued operation (i.e., an economical design goal based on risk considerations). The lower-level design may prove to be a good investment for the lifetime of the structures.

The two-level design criteria approach is recommended to ensure that transportation tunnels constructed in moderate to high seismic areas represent functional adequacy and economy while reducing life-threatening failure. This design philosophy has been employed successfully in many of PB's recent transportation tunnel projects (LA Metro, Taipei Metro, Seattle Metro, and Boston Central Artery/Third Harbor Tunnel). In these projects the two design events are termed as:

- *The Operating Design Earthquake (ODE)*, defined as the earthquake event that can reasonably be expected to occur during the design life of the facility (e.g., at least once). The ODE design goal is that the overall system shall continue operating during and after an ODE and experience little to no damage.

- *The Maximum Design Earthquake (MDE)*, defined as an event that has a small probability of exceedance during the facility life (e.g., 5 percent). The MDE design goal is that public safety shall be maintained during and after an MDE.

Note, however, that the design criteria aimed at saving lives alone during a catastrophic earthquake are sometimes considered unacceptable. There are cases where more stringent criteria are called for under the maximum design earthquake, such as requiring rapid repairs with relatively low cost. A good example would be the existing San Francisco BART structures. As described in Chapter 1, BART warrants such stringent criteria because it has an incalculable value as possibly the only reliable direct public transportation system in the aftermath of a catastrophic earthquake.

Therefore, the actual acceptable risk and the performance goals during and after an MDE depend on the nature and the importance of the facility, public safety and social concerns, and potential direct and indirect losses.

Loading Criteria

Maximum Design Earthquake (MDE). Given the performance goals of the MDE (i.e., public safety), the recommended seismic loading combinations using the load factor design method are as follows:

For Cut-and-Cover Tunnel Structures

$$U = D + L + E1 + E2 + EQ \qquad \text{(Eq. 2-1)}$$

Where U = required structural strength capacity

D = effects due to dead loads of structural components

L = effects due to live loads

E1 = effects due to vertical loads of earth and water

E2 = effects due to horizontal loads of earth and water

EQ = effects due to design earthquake (MDE)

For Mined (Circular) Tunnel Lining

$$U = D + L + EX + H + EQ \qquad \text{(Eq. 2-2)}$$

where U, D, L, and EQ are as defined in Equation 2-1

EX = effects of static loads due to excavation (e.g., O'Rourke, 1984)

H = effects due to hydrostatic water pressure

Comments on Loading Combinations for MDE

- The structure should first be designed with adequate strength capacity under static loading conditions.
- The structure should then be checked in terms of ductility as well as strength when earthquake effects, EQ, are considered. The "EQ" term for conventional surface structure design reflects primarily the inertial effect on the structures. For tunnel structures, the earthquake effect is governed by the displacements/deformations imposed on the tunnels by the ground.
- In checking the strength capacity, the effects of earthquake loading should be

expressed in terms of internal moments and forces, which can be calculated according to the lining deformations (distortions) imposed by the surrounding ground. If the "strength" criteria expressed by Equation 2-1 or 2-2 can be satisfied based on elastic structural analysis, no further provisions under the MDE are required. Generally the strength criteria can easily be met when the earthquake loading intensity is low (i.e., in low seismic risk areas) and/or the ground is very stiff.

- If the flexural strength of the tunnel lining, using elastic analysis and Equation 2-1 or 2-2, is found to be exceeded (e.g., at certain joints of a cut-and-cover tunnel frame), one of the following two design procedures should be followed:

  (1) Provide sufficient ductility (using proper detailing procedure) at the critical locations of the lining to accommodate the deformations imposed by the ground in addition to those caused by other loading effects (see Equations 2-1 and 2-2). The intent is to ensure that the structural strength does not degrade as a result of inelastic deformations and the damage can be controlled at an acceptable level.

  In general the more ductility is provided, the more reduction in earthquake forces (the "EQ" term) can be made in evaluating the required strength, U. As a rule of thumb, the force reduction factor can be assumed equal to the ductility provided. This reduction factor is similar by definition to the response modification factor used in bridge design code (AASHTO).

  Note, however, that since an inelastic "shear" deformation may result in strength degradation, it should always be prevented by providing sufficient shear strengths in structure members, particularly in the cut-and-cover rectangular frame.

  (2) Re-analyze the structure response by assuming the formation of plastic hinges at the joints that are strained into inelastic action. Based on the plastic-hinge analysis, a redistribution of moments and internal forces will result.

  If new plastic hinges are developed based on the results, the analysis is re-run by incorporating the new hinges (i.e., an iterative procedure) until all potential plastic hinges are properly accounted for. Proper detailing at the hinges is then carried out to provide adequate ductility. The structural design in terms of required strength (Equations 2-1 and 2-2) can then be based on the results from the plastic-hinge analysis.

  As discussed earlier, the overall stability of tunnel structures during and after the MDE has to be maintained. Realizing that the structures also must have sufficient capacity (besides the earthquake effect) to carry static loads (e.g., D, L, E1, E2 and H terms), the potential modes of instability due to the development of plastic

hinges (or regions of inelastic deformation) should be identified and prevented (Monsees, 1991; see Figure 21 for example).

- The strength reduction factor, ϕ, used in the conventional design practice may be too conservative, due to the inherently more stable nature of underground structures (compared to surface structures), and the transient nature of the earthquake loading.

- For cut-and-cover tunnel structures, the evaluation of capacity using Equation 2-1 should consider the uncertainties associated with the loads E1 and E2, and their worst combination. For mined circular tunnels (Equation 2-2), similar consideration should be given to the loads EX and H.

- In many cases, the absence of live load, L, may present a more critical condition than when a full live load is considered. Therefore, a live load equal to zero should also be used in checking the structural strength capacity using Equations 2-1 and 2-2.

Operating Design Earthquake (ODE). For the ODE, the seismic design loading combination depends on the performance requirements of the structural members. Generally speaking, if the members are to experience little to no damage during the lower-level event (ODE), the inelastic deformations in the structure members should be kept low. The following loading criteria, based on load factor design, are recommended:

For Cut-and-Cover Tunnel Structures

$$U = 1.05D + 1.3L + \beta_1 (E1 + E2) + 1.3EQ \qquad \text{(Eq. 2-3)}$$

where D, L, E1, E2, EQ, and U are as defined in Equation 2-1.

β_1 = 1.05 if extreme loads are assumed for E1 and E2 with little uncertainty. Otherwise, use β_1 = 1.3.

For Mined (Circular) Tunnel Lining

$$U = 1.05D + 1.3L + \beta_2 (EX + H) + 1.3EQ \qquad \text{(Eq. 2-4)}$$

where D, L, EX, H, EQ, and U are as defined in Equation 2-2.

β_2 = 1.05 if extreme loads are assumed for E1 and E2 with little uncertainty. Otherwise, use β_2 = 1.3.

Comments on Loading Combinations for ODE

- The structure should first be designed with adequate strength capacity under static loading conditions.

- For cut-and-cover tunnel structures, the evaluation of capacity using Equation 2-3 should consider the uncertainties associated with the loads E1 and E2, and their worst combination. For mined circular tunnels (Equation 2-4), similar consideration should be given to the loads EX and H.

  When the extreme loads are used for design, a smaller load factor is recommended to avoid unnecessary conservatism. Note that an extreme load may be a maximum load or a minimum load, depending on the most critical case of the loading combinations. Use Equation 2-4 as an example. *For a deep circular tunnel lining*, it is very likely that the most critical loading condition occurs when the maximum excavation loading, EX, is combined with the minimum hydrostatic water pressure, H. *For a cut-and-cover tunnel*, the most critical seismic condition may often be found when the maximum lateral earth pressure, E2, is combined with the minimum vertical earth load, E1. If a very conservative lateral earth pressure coefficient is assumed in calculating the E2, the smaller load factor $b_1 = 1.05$ should be used.

- Redistribution of moments (e.g., ACI 318) for cut-and-cover concrete frames is recommended to achieve a more efficient design.

- If the "strength" criteria expressed by Equation 2-3 or 2-4 can be satisfied based on elastic structural analysis, no further provisions under the ODE are required.

- If the flexural strength of the tunnel lining, using elastic analysis and Equation 2-3 or 2-4, is found to be exceeded, the structure should be checked for its ductility to ensure that the resulting inelastic deformations, if any, are small. If necessary, the structure should be redesigned to ensure the intended performance goals during the ODE.

- Zero live load condition (i.e., L = 0) should also be evaluated in Equations 2-3 and 2-4.

3.0 RUNNING LINE TUNNEL DESIGN

3.0 RUNNING LINE TUNNEL DESIGN

3.1 Overview

Discussions of the earthquake shaking effect on underground tunnels, specifically the "EQ" term in Equations 2-1 through 2-4, are presented in a quantitative manner in this chapter and in Chapters 4 and 5.

The response of tunnels to seismic shaking motions may be demonstrated in terms of three principal types of deformations (Owen and Scholl, 1981):

- Axial
- Curvature
- Ovaling (for circular tunnels) or racking (for rectangular tunnels such as cut-and-cover tunnels)

The first two types — axial and curvature — are considered in this chapter. Analytical work developed in previous studies for tunnel lining design is presented. The work is applicable to both circular mined tunnels and rectangular cut-and-cover tunnels.

Discussions of the third type — the ovaling effect on circular tunnels and the racking effect on rectangular tunnels — are presented in detail in Chapters 4 and 5, respectively.

3.2 Types of Deformations

Axial and Curvature Deformations

Axial and curvature deformations develop in a horizontal or nearly horizontal linear tunnel (such as most tunnels) when seismic waves propagate either parallel or obliquely to the tunnel. The tunnel lining design considerations for these types of deformations are basically in the longitudinal direction along the tunnel axis.

Figure 3 shows the idealized representations of axial and curvature deformations. The general behavior of the linear tunnel is similar to that of an elastic beam subject to deformations or strains imposed by the surrounding ground.

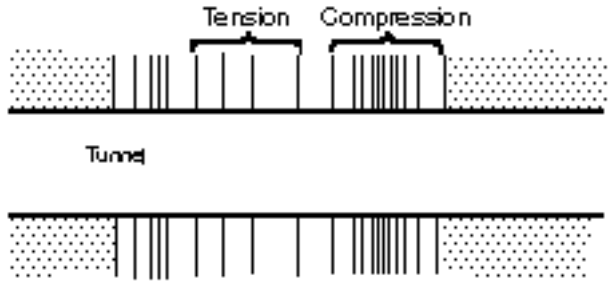

A. Axial Deformation Along Tunnel

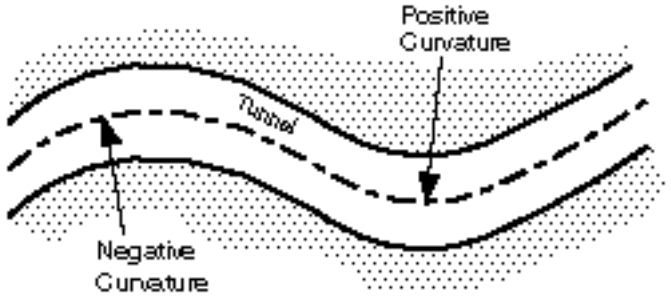

B. Curvature Deformation Along Tunnel

Figure 3.
Axial and Curvature Deformations

(Source: Owen and Scholl, 1981)

Ovaling or Racking Deformations

The ovaling or racking deformations of a tunnel structure may develop when waves propagate in a direction perpendicular or nearly perpendicular to the tunnel axis, resulting in a distortion of the cross-sectional shape of the tunnel lining. Design considerations for this type of deformation are in the transverse direction.

Figure 4 shows the ovaling distortion and racking deformation associated with circular tunnels and rectangular tunnels, respectively. The general behavior of the lining may be simulated as a buried structure subject to ground deformations under a two-dimensional, plane-strain condition.

Ovaling and racking deformations may be caused by vertically, horizontally or obliquely propagating seismic waves of any type. Many previous studies have suggested, however, that the vertically propagating shear wave is the predominant form of earthquake loading that governs the tunnel lining design against ovaling/racking. The following reasons are given:

- Ground motion in the vertical direction is generally considered less severe than its horizontal component. Typically, vertical ground motion parameters are assumed to be 1/2 to 2/3 of the horizontal ones. (Note that a vertically propagating shear wave causes the ground to shake in the horizontal direction.) This relation is based on observation of California earthquakes, which are most commonly of the strike-slip variety in which horizontal motion predominates.

  For thrust faults, in which one rock block overrides another, vertical effects may equal or exceed the horizontal ones. The effects of thrust faulting are usually more localized, however, than those of the strike-slip faulting, and they are attenuated more rapidly with distance from the focus.

- For tunnels embedded in soils or weak media, the horizontal motion associated with vertically propagating shear waves tends to be amplified. In contrast, the ground strains due to horizontally propagating waves are found to be strongly influenced by the ground strains in the rock beneath. Generally, the resulting strains are smaller than those calculated using the properties of the soils.

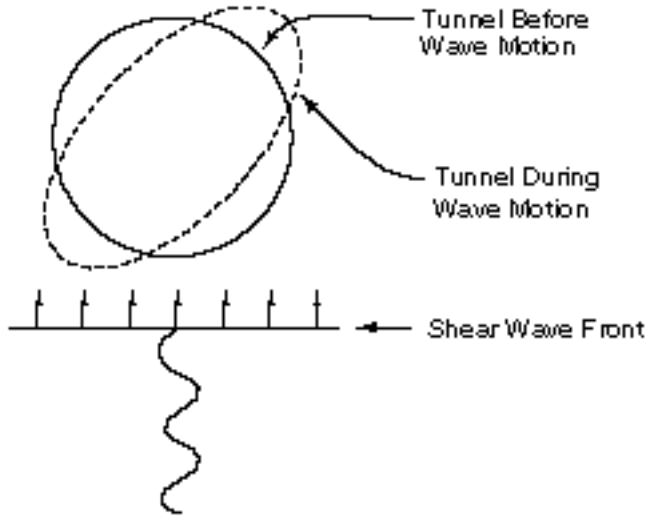

A. Ovaling Deformation of a Circular Cross Section

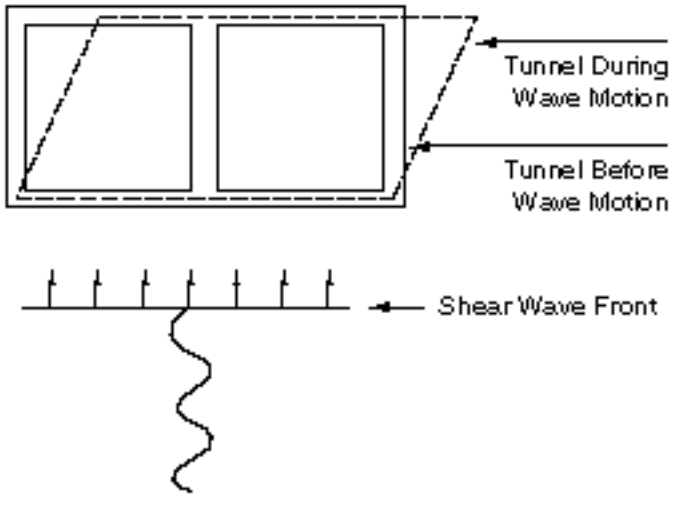

B. Racking Deformation of a Rectangular Cross Section

Figure 4.
Ovaling and Racking Deformations

3.3 Free-Field Axial and Curvature Deformations

Background

The intensity of earthquake ground motion is described by several important parameters, including peak acceleration, peak velocity, peak displacement, response spectra, duration and others. For aboveground structures, the most widely used measure is the peak ground acceleration and the design response spectra, as the inertial forces of the structures caused by ground shaking provide a good representation of earthquake loads.

Peak ground acceleration is not necessarily a good parameter, however, for earthquake design of underground structures such as tunnels, because tunnel structures are more sensitive to the distortions of the surrounding ground than to the inertial effects. Such ground distortions — referred to in this report as free-field deformations/strains — are the ground deformations/strains caused by the traveling seismic waves without the structures being present. The procedure used to derive these deformations/strains is discussed below.

A Practical Approach to Describing Ground Behavior

To describe the free-field ground behavior rigorously, even without the consideration of ground structure interaction, is an extremely complex problem that would generally require a three-dimensional dynamic analysis for solution. The earthquake source characteristics and the transmission paths of various types of waves should also be included in the model. This type of complex analysis, however, is rarely justified economically.

For practical purposes, a simplified approach was proposed by Newmark (1968) and has been considered by others (Sakurai and Takahashi, 1969; Yeh, 1974; and Agrawal et. al, 1983). This approach is based on theory of wave propagation in homogeneous, isotropic, elastic media. The ground strains are calculated by assuming a harmonic wave of any wave type propagating at an angle (angle of incidence) with respect to the axis of a planned structure.

Figure 5 (Kuesel, 1969) represents free-field ground deformations along a tunnel axis due to a sinusoidal shear wave with a wavelength, L, a displacement amplitude, D, and an angle of incidence, ϕ. A conservative assumption of using the most critical angle of incidence, and therefore the maximum values of strain, is often made, because the angle of incidence for the predominant earthquake waves cannot be determined reliably.

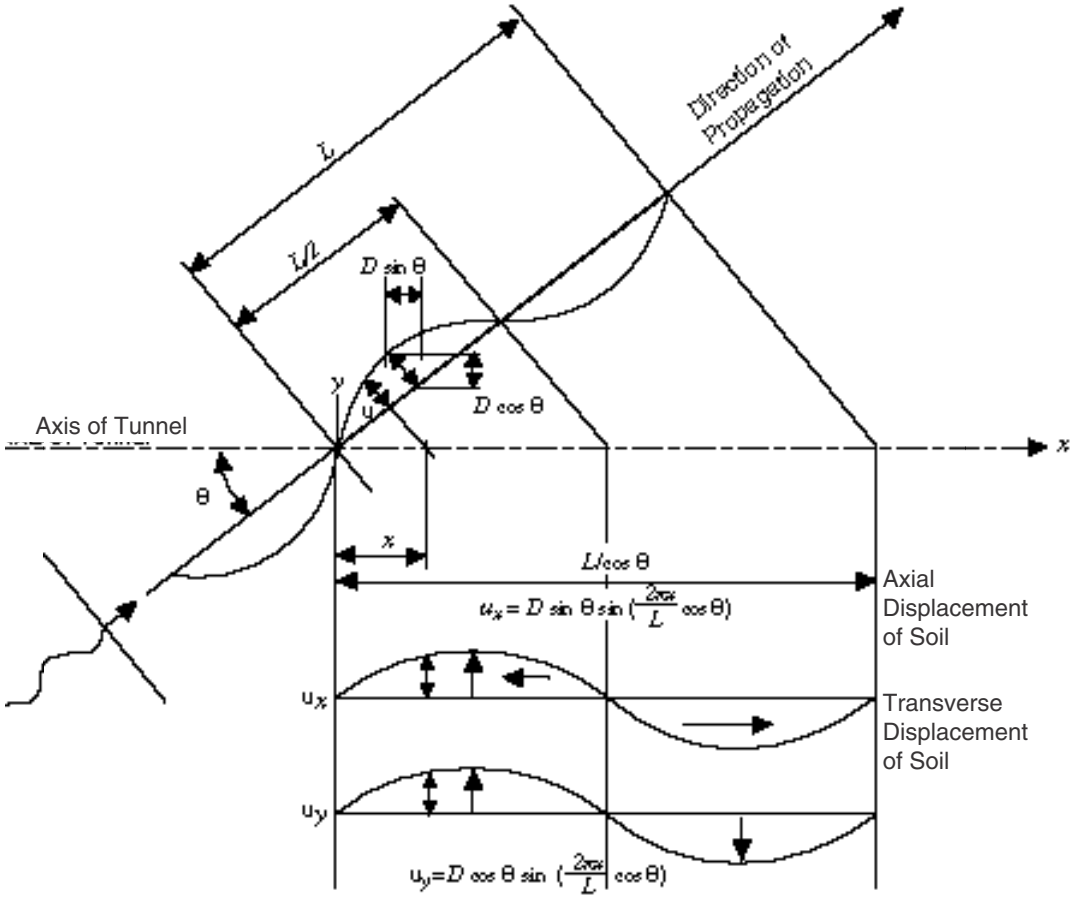

Figure 5.
Geometry of a Sinusoidal Shear Wave Oblique to Axis of Tunnel

(Source: SFBARTD, 1960)

Simplified Equations for Axial Strains and Curvature

Using the simplified approach, the free-field axial strains and curvature due to shear waves and Rayleigh waves (surface waves) can be expressed as a function of angle of incidence, as shown in Table 1. The most critical angle of incidence and the maximum values of the strains are also included in the table.

Equations caused by compressional P-waves are also available, but it is generally considered that they would not control the design. It is difficult to determine which type of wave will dominate due to the complex nature of the characteristics associated with different wave types. Generally, strains produced by Rayleigh waves may govern only when the site is at a large distance from the earthquake source and the structure is built at shallow depth.

Application of the strain equations presented in Table 1 requires knowledge of:

- The effective wave propagation velocity
- The peak ground particle velocity
- The peak ground particle acceleration

The peak velocity and acceleration can be established through empirical methods, field measurements, or site-specific seismic exposure studies. The effective wave propagation velocity in rock can be determined with reasonable confidence from in-situ and laboratory tests.

Estimating the effective wave propagation velocity in soil overburden presents the major difficulty. Previous studies have shown that, except possibly for vertically propagating shear waves, the use of soil properties in deriving the wave velocity in soil overburden may be overly conservative.

It has been suggested that for horizontally or obliquely propagating waves the propagation velocities in soil overburden are affected significantly by the velocities in the underlying rock. That is to say, the actual velocity values in the soils may be much higher than those calculated based on the soil properties alone (Hadjian and Hadley, 1981). This phenomenon is attributable to the problem of deformation compatibility. The motion of a soil particle due to a horizontally propagating wave above the rock cannot differ greatly from the motion of the rock, unless the soil slides on top of the rock (a very unlikely occurrence) or the soil liquifies. For a very deep (thick) soil stratum, however, the top of the soil stratum is less coupled to the rock and is more free to follow a motion that is determined by its own physical properties.

Wave Type		Longitudinal Strain (Axial)	Curvature
Shear Wave	General Form	$\varepsilon = \frac{V_s}{C_s}\sin\theta\cos\theta$	$\frac{\hat{\varepsilon}_1}{r} = \frac{A_s}{C_s^2}\cos^3\theta$
	Maximum Value	$\varepsilon_{max} = \frac{V_s}{2C_s}$ *for* $\theta = 45$	$\left(\frac{\hat{\varepsilon}_1}{r}\right)_{max} = \frac{A_s}{C_s^2}$ *for* $\theta = 0$
Rayleigh Wave	General Form	$\varepsilon = \frac{V_R}{C_R}\cos^2\theta$	$\frac{\hat{\varepsilon}_1}{r} = \frac{A_R}{C_R^2}\cos^2\theta$
	Maximum Value	$\varepsilon_{max} = \frac{V_R}{C_R}$ *for* $\theta = 0$	$\left(\frac{\hat{\varepsilon}_1}{r}\right)_{max} = \frac{A_R}{C_R^2}$ *for* $\theta = 0$

θ = Angle of Incidence with respect to Tunnel Axis

r = Radius of Curvature

V_S, V_R = Peak Particle Velocity for Shear Wave and Rayleigh Wave, respectively

C_S, C_R = Effective Propagation Velocity for Shear Wave and Rayleigh Wave, respectively

A_S, A_R = Peak Particle Acceleration for Shear Wave and Rayleigh Wave, respectively

Table 1.
Free-Field Ground Strains

3.4 Design Conforming to Free-Field Axial and Curvature Deformations

Background and Assumptions

The free-field ground strain equations, originally developed by Newmark (Table 1), have been widely used in the seismic design of underground pipelines. This method has also been used successfully for seismic design of long, linear tunnel structures in several major transportation projects (Monsees, 1991; Kuesel, 1969).

When these equations are used, it is assumed that the structures experience the same strains as the ground in the free-field. The presence of the structures and the disturbance due to the excavation are ignored. This simplified approach usually provides an upper-bound estimate of the strains that may be induced in the structures by the traveling waves. The greatest advantage of this approach is that it requires the least amount of input.

Underground pipelines, for which this method of analysis was originally developed, are flexible because of their small diameters (i.e., small bending rigidity), making the free-field deformation method a simple and reasonable design tool. For large underground structures such as tunnels, the importance of structure stiffness sometimes cannot be overlooked. Some field data indicated that stiff tunnels in soft soils rarely experience strains that are equal to the soil strains (Nakamura, Katayama, and Kubo, 1981). A method to consider tunnel stiffness will be presented and discussed later in Section 3.5.

Design Example 1: The Los Angeles Metro

For the purpose of illustration, a design example modified from the seismic design criteria for the LA Metro project (SCRTD, 1984) is presented here. In this project, it was determined that a shear wave propagating at 45 degree (angle of incidence) to the tunnel axis would create the most critical axial strain within the tunnel structure. Although a P-wave (compressional wave) traveling along the tunnel axis might also produce a similar effect, it was not considered because:

- Measurement of P-wave velocity can be highly misleading, particularly when a soil deposit is saturated with water (Monsees, 1991).
- The magnitudes of soil strains produced by a nearly horizontally propagating P-wave are generally small and about the same as those produced in the underlying rock and, therefore, not as critical as the shear-wave generated axial strains (SFBART, 1960). This phenomenon was discussed previously in Section 3.3.

Other assumptions and parameters used in this example are:

- Design Earthquake Parameters: Peak Ground Acceleration, A_s = 0.6 (Maximum Design Earthquake, MDE)
- Peak Ground Velocity, V_s = 3.2 ft/sec
- Soil surrounding Tunnel: Fernando Formation
- Effective Shear Wave Velocity: C_s = 1360 ft/sec (in Fernando Formation under MDE)
- Tunnel Structure: Cast-in-place circular segmented reinforced lining, with Radius R =10 feet

From Table 1, the combined maximum axial strain and curvature strain would be:

$$\varepsilon_{max} = \pm \frac{V_s}{2C_s} \pm \frac{A_s R}{C_s^2} \cos^3\theta$$

$$= \pm \frac{3.2}{2 \times 1360} \pm \frac{0.6 \times 32.2 \times 10}{(1360)^2} \cos^3 45$$

$$= \pm 0.00118 \pm 0.000037$$

$$= \pm 0.00122$$

As the results of calculations indicate, the curvature (bending) component (0.000037) is, in general, relatively insignificant for tunnel structures under seismic loads. According to the LA Metro criteria, the maximum usable compression strain (under MDE) in the concrete lining is ε_{allow} =0.002, since the strain is almost purely axial. With $\varepsilon_{max} < \varepsilon_{allow}$, the lining is considered adequate in compression under the Maximum Design Earthquake (MDE).

The calculated maximum axial strain (=0.00122) is cyclic in nature. When tension is in question, a plain concrete lining would obviously crack. The assumed lining is reinforced, however, and the opening of these cracks is transient due to the cyclic nature of seismic waves. As long as no permanent ground deformation results, these cracks will be closed by the reinforcing steel at the end of the shaking. Even in the unreinforced concrete lining cases, the lining generally is considered adequate as long as:

- The crack openings are small and uniformly distributed
- The resulting tension cracks do not adversely affect the intended performance goals of the lining

Applicability of the Free-Field Deformation Approach

The example presented above demonstrates the simplicity of the free-field deformation approach. Because it is an upper-bound assessment of the tunnel response, it often becomes the first tool an engineer would use to verify the adequacy of his design. This approach offers a method for verification of a design rather than a design itself.

Note, however, that this method is:

- *Pertinent to a tunnel structure that is flexible relative to its surrounding medium*, such as all tunnels in rock and most tunnels in stiff soils. In this case it is reasonable to assume that the tunnel deforms according to its surrounding medium.

- *Not desirable for situations involving stiff structures buried in soft soil*, because under this condition, the calculated ground deformations may be too great (due to the soft nature of the soil) for the stiff structures to realistically accommodate. Once the calculated ground strain exceeds the allowable strain of the lining material, there is very little an engineer can do to improve his design.

For instance, if the effective shear wave velocity of the previous example is reduced to 350 ft/sec to reflect a much softer soil deposit, the tunnel lining will then be subjected to a combined maximum axial strain of 0.0052 in compression (see Design Example 2 in the next section). It is essentially unrealistic to provide an adequate concrete lining design resisting an axial strain of this amount. If the free-field deformation approach were used in this case, it appears that the only solution to this problem would be to provide needless flexible joints, forming a chainlink-like tunnel structure to accommodate the ground deformation.

In the next section, a design approach considering the tunnel-ground interaction effect is presented. This design approach, based on results from previous studies, may effectively alleviate the design difficulty discussed above.

3.5 Tunnel-Ground Interaction

When it is stiff in its longitudinal direction relative to its surrounding soils, the tunnel structure resists, rather than conforms to, the deformations imposed by the ground. Analysis of tunnel-ground interaction that considers both the tunnel stiffness and ground stiffness plays a key role in finding the tunnel response. With the computation capability of today's computers, this problem may be solved numerically using sophisticated computer codes.

For practical purposes, however, a simplified procedure is desirable and has been sought in previous studies (SFBARTD, 1960; Kuribayashi, et al, 1974; and St. John, et al,

1987). In general, the tunnel-ground system is simulated as an elastic beam on an elastic foundation, with the theory of wave propagating in an infinite, homogeneous, isotropic medium. When subjected to the axial and curvature deformations caused by the traveling waves in the ground, the tunnel will experience the following sectional forces (see Figure 6):

- Axial forces, Q, on the cross-section due to the axial deformation
- Bending moments, M, and shear forces, V, on the cross-section due to the curvature deformation

Simplified Interaction Equations

Maximum Axial Force: Q_{max}. Through theoretical derivations, the resulting maximum sectional axial forces caused by a shear wave with 45 degree angle of incidence can be obtained:

$$Q_{\max} = \frac{\frac{K_a L}{2\pi}}{1 + 2\left(\frac{K_a}{E_c A_c}\right)\left(\frac{L}{2\pi}\right)^2} D \qquad \text{(Eq. 3-1)}$$

Where L = wavelength of an ideal sinusoidal shear wave

K_a = longitudinal spring coefficient of medium (in force per unit deformation per unit length of tunnel)

D = free-field displacement response amplitude of an ideal sinusoidal shear wave

E_c = modulus of elasticity of tunnel lining

A_c = cross-section area of tunnel lining

The calculated maximum axial force, Q_{max}, shall not exceed an upper limit defined by the ultimate soil drag resistance in the longitudinal direction. This upper limit is expressed as:

$$Q_{\text{limit}} = \frac{fL}{4} \qquad \text{(Eq. 3-2)}$$

where f = ultimate friction force (per unit length of tunnel) between the tunnel and the surrounding medium

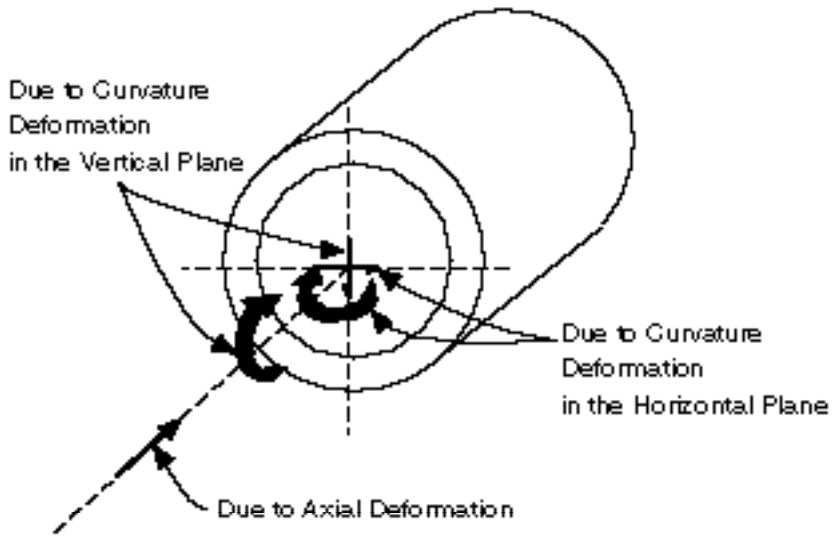

Figure 6.
Sectional Forces Due to Curvature and Axial Deformations
(Source: Owen and Scholl, 1981)

Maximum Bending Moment, M_{max}. The bending moment resulting from curvature deformations is maximized when a shear wave is traveling parallel to the tunnel axis (i.e., with an angle of incidence equal to zero). The mathematical expression of the maximum bending moment is:

$$M_{\max} = \frac{K_t \left(\frac{L}{2\pi}\right)^2}{1 + \frac{K_t}{E_c I_c}\left(\frac{L}{2\pi}\right)^4} D \qquad \text{(Eq. 3-3)}$$

where L, E_c and D are as defined in Equation 3-1

I_c = moment of inertia of the tunnel section

K_t = transverse spring coefficient of medium (in force per unit deformation per unit length of tunnel).

Maximum Shear Force, V_{max}. The maximum shear force corresponding to the maximum bending moment is derived as:

$$V_{\max} = \frac{\frac{K_t L}{2\pi}}{1 + \frac{K_t}{E_c I_c}\left(\frac{L}{2\pi}\right)^4} D = M_{\max} \frac{2\pi}{L} \qquad \text{(Eq. 3-4)}$$

where L, E_c, I_c, K_t and D are as defined in Equation 3-3.

Comments on the Interaction Equations

- The tunnel-ground interaction effect is explicitly accounted for in these formulations. The ground stiffness and the tunnel stiffness are represented by spring coefficients (K_a or K_t) and sectional modulus (E_cA_c or E_cI_c), respectively.
- The application of these equations is necessary only when tunnel structures are built in soft ground. For structures in rock or stiff soils, the evaluation based on the free-field ground deformation approach presented in Section 3.3 will, in general, be satisfactory.
- Equations 3-1, 3-3 and 3-4 are general mathematical forms. Other expressions of the maximum sectional forces exist in the literature. The differences are primarily due to the further maximization of the sectional forces with respect to the wavelength, L. For instance:

- In the JSCE (Japanese Society of Civil Engineers) *Specifications for Earthquake Resistant Design of Submerged Tunnels*, the values of wavelength that will maximize Equations 3-1, 3-3 and 3-4 are determined and substituted back into each respective equation to yield the maximum sectional forces.

- St. John and Zahran (1987) suggested a maximization scheme that is similar to the Japanese approach except that the spring coefficients (K_a or K_t) are assumed to be functions of wavelength, L, in the maximization process.

Both of these approaches assume that the free-field ground displacement response amplitude, D, is independent of the wavelength. This assumption sometimes may lead to very conservative results, as the ground displacement response amplitude generally decreases with the wavelength. It is, therefore, the author's view that Equations 3-1 through 3-4 presented in this section will provide a practical and adequate assessment, provided that the values (or the ranges of the values) of L, D, and K_t (or K_a) can be reasonably estimated.

A reasonable estimate of the wavelength can be obtained by

$$L = T \ C_s \qquad \text{(Eq. 3-5)}$$

where T is the predominant natural period of the shear wave traveling in the soil deposit in which the tunnel is built, and C_s is the shear wave propagation velocity within the soil deposit.

Often, T can also be represented by the natural period of the site. Dobry, Oweis and Urzua (1976) presented some procedures for estimating the natural period of a linear or equivalent linear model of a soil site.

- The ground displacement response amplitude, D, should be derived based on site-specific subsurface conditions by earthquake engineers. The displacement amplitude represents the spatial variations of ground motions along a horizontal alignment. Generally, the displacement amplitude increases as the wavelength, L, increases. For example, the displacement spectrum chart prepared by Housner (SFBARTD, 1960) for the SF BART project was expressed by $D = 4.9 \times 10^{-6} L^{1.4}$, where the units of D and L are in feet. This spectrum is intended for tunnel tubes in soft San Francisco Bay muds and was derived for a magnitude 8.2 earthquake on the San Andreas fault. The equation shows clearly that:

  - The displacement amplitude increases with the wavelength.

  - For any reasonably given wavelength, the corresponding ground displacement

amplitude is relatively small. Using the given wavelength and the corresponding displacement amplitude, the calculated free-field ground strains would be significantly smaller than those calculated using the simplified equations shown in Table 1. This suggests that it may be overly conservative to use the simplified equations to estimate the axial and curvature strains caused by seismic waves travelling in soils for tunnel design.

- With regard to the derivations of spring coefficients K_a and K_t, there is no consensus among design engineers. The derivations of these spring coefficients differ from those for the conventional beam on elastic foundation problems in that:

  -The spring coefficients should be representative of the dynamic modulus of the ground under seismic loads.

  -The derivations should consider the fact that loading felt by the surrounding soil (medium) is alternately positive and negative due to the assumed sinusoidal seismic wave.

  Limited information on this problem is available in the literature (SFBARTD 1960, St. John and Zahrah, 1987 and Owen and Scholl, 1981). For preliminary design, it appears that the expressions suggested by St. John and Zahrah (1987) should serve the purpose:

$$K_t = K_a = \frac{16\pi G_m(1 - \nu_m)}{(3 - 4\nu_m)} \frac{d}{L} \qquad \text{(Eq. 3-6)}$$

  where G_m = shear modulus of the medium (see Section 4.2 in Chapter 4)

  ν_m = Poisson's radio of the medium

  d = diameter (or equivalent diameter) of the tunnel

  L = wavelength

- A review of Equations 3-1, 3-3 and 3-4 reveals that increasing the stiffness of the structure (i.e., E_cA_c and E_cI_c), although it may increase the strength capacity of the structure, will not result in reduced forces. In fact, the structure may attract more forces as a result. Therefore, the designer should realize that strengthening of an overstressed section by increasing its sectional dimensions (e.g., lining thickness) may not always provide an efficient solution for seismic design of tunnel structures. Sometimes, a more flexible configuration with adequate reinforcements to provide sufficient ductility is a more desirable measure.

Design Example 2: A Linear Tunnel in Soft Ground

In this example, a tunnel lined with a cast-in-place circular concrete lining (e.g., a permanent second-pass support) is assumed to be built in a soft soil site. The geotechnical, structural and earthquake parameters are listed as follows:

Geotechnical Parameters:

- Effective shear wave velocity, C_S =350 ft/sec.
- Soil unit weight, γ_t =110 pcf =0.110 kcf.
- Soil Poisson's ratio, ν_m =0.5 (saturated soft clay).
- Soil deposit thickness over rigid bedrock, H =100 ft.

Structural Parameters:

- Lining thickness, t =1 ft.
- Lining diameter, d =20 ft.
- Lining moment of inertia, I_c = 0.5 x 3148 = 1574 ft^4
  (one half of the full section moment of inertia to account for concrete cracking and nonlinearity during the MDE).
- Lining cross section area, A_c =62.8 ft^2.
- Concrete Young's Modulus, E_c =3600 ksi =518400 ksf.
- Concrete yield strength, f_c =4000 psi.
- Allowable concrete compression strain under combined axial and bending compression, ε_{allow} = 0.003 (during the MDE)

Earthquake Parameters (for the MDE):

- Peak ground particle acceleration in soil, A_s =0.6 g.
- Peak ground particle velocity in soil, V_s =3.2 ft/sec.

First, try the simplified equation as used in Design Example 1. The combined maximum axial strain and curvature strain is calculated as:

$$\varepsilon_{max} = \pm\frac{V_s}{2C_s} \pm \frac{A_s R}{C_s^2}\cos^3\theta = \pm\frac{3.2}{2x350} \pm \frac{0.6x32.2x10}{(350)^2}\cos^3 45^\circ$$
$$= \pm 0.0046 \pm 0.0006 = \pm 0.0052$$

The calculated maximum compression strain exceeds the allowable compression strain of concrete (i.e., $\varepsilon_{max} > \varepsilon_{allow} = 0.003$).

Now use the tunnel-ground interaction procedure.

1. Estimate the predominant natural period of the soil deposit (Dobry, et al, 1976).

$$T = \frac{4H}{C_s} = \frac{4x100'}{350} = 1.14\,\text{sec.}$$

2. Estimate the idealized wavelength (Equation 3-5):

$$L = TxC_s = 4H$$
$$= 400\,ft$$

3. Estimate the shear modulus of soil:

$$G_m = \rho C_s^2 = \frac{0.110kcf}{32.2}\,x\,350^2 = 418.5\,ksf$$

4. Derive the equivalent spring coefficients of the soil (Equation 3-6):

$$K_a = K_t = \frac{16\pi G_m\,(1 - \eta_m)}{(3 - 4\eta_m)}\,\frac{d}{L}$$
$$= \frac{16\pi x418.5\,(1 - 0.5)}{(3 - 4x0.5)}\,x\frac{20}{400}$$
$$= 526\,kips/ft$$

5. Derive the ground displacement amplitude, D:

As discussed before, the ground displacement amplitude is generally a function of the wavelength, L. A reasonable estimate of the displacement amplitude must consider the site-specific subsurface conditions as well as the characteristics of the input ground motion. In this design example, however, the ground displacement amplitudes are calculated in such a manner that the ground strains as a result of these displacement amplitudes are comparable to the ground strains used in the calculations based on the simplified free-field equations. The purpose of this assumption is to allow a direct and clear evaluation of the effect of tunnel-ground interaction. Thus, by assuming a sinusoidal wave with a displacement amplitude D and a wavelength L, we can obtain:

For free-field axial strain:

$$\frac{V_s}{2C_s} = \frac{2\pi D}{L} \Rightarrow D = D_a = 0.291\,ft$$

For free-field bending curvature:

$$\frac{A_s}{C_s^2}\cos^3 45^\circ = \frac{4\pi^2 D}{L^2} \Rightarrow D = D_b = 0.226\,ft$$

6. Calculate the maximum axial force (Equation 3-1) and the corresponding axial strain of the tunnel lining:

$$Q_{\max} = \frac{\frac{K_a L}{2\pi}}{1 + 2\left(\frac{K_a}{E_c A_c}\right)\left(\frac{L}{2\pi}\right)^2} D_a$$

$$= \frac{\frac{526 \times 400}{2\pi}}{1 + 2\left(\frac{526}{518400 \times 62.8}\right)\left(\frac{400}{2\pi}\right)^2} \times 0.291$$

$$= 8619\,kips$$

$$\varepsilon_{axial} = \frac{Q_{\max}}{E_c A_c} = \frac{8619}{518400 \times 62.8} = 0.00026$$

7. Calculate the maximum bending moment (Equation 3-3) and the corresponding bending strain of the tunnel lining:

$$M_{\max} = \frac{K_t \left(\frac{L}{2\pi}\right)^2}{1 + \frac{K_t}{E_c I_c}\left(\frac{L}{2\pi}\right)^4} D_b$$

$$= \frac{526\left(\frac{400}{2\pi}\right)^2}{1 + \frac{526}{518400 \text{x} 1574}\left(\frac{400}{2\pi}\right)^4} \text{x} 0.226$$

$$= 41539\ k\ -\ ft$$

$$\varepsilon_{bending} = \frac{M_{\max} R}{E_c I_c}$$

$$= \frac{41539 \text{x} 10}{518400 \text{x} 1574}$$

$$= 0.00051$$

8. Compare the combined axial and bending compression strains to the allowable:

$$\varepsilon_{\max} = \varepsilon_{axial} + \varepsilon_{bending}$$
$$= 0.00026 + 0.00051$$
$$= 0.00077 < \varepsilon_{allow} = 0.003$$

9. Calculate the maximum shear force (Equation 3-4) due to the bending curvature:

$$V_{\max} = M_{\max} \text{x} \frac{2\pi}{L} = 41539 \text{x} \frac{2\pi}{400}$$
$$= 652 kips$$

10. Calculate the allowable shear strength of concrete during the MDE:

$$\phi V_c = 0.85 \times 2\sqrt{fc}\, A_{shear}$$

where ϕ = shear strength reduction factor (0.85)
f_c = yield strength of concrete (4000 psi)
A_{shear} = effective shear area = $A_c/2$

Note: Use of ϕ = 0.85 for earthquake design may be very conservative.

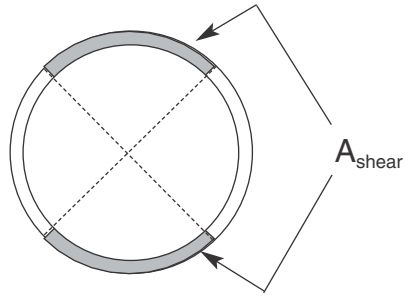

$$\phi V_c = 0.85 \times 2\sqrt{4000} \times \frac{62.8}{2} \times \frac{144}{1000}$$

$$= 486\ kips$$

11. Compare the induced maximum shear force with the allowable shear resistance:

$$V_{max} = 625\ kips > \phi V_c = 486\ kips$$

Although calculations indicate that the induced maximum shear force exceeds the available shear resistance provided by the plain concrete, this problem may not be of major concern in actual design because:

- The nominal reinforcements generally required for other purposes may provide additional shear resistance during earthquakes.
- The ground displacement amplitudes, D, used in this example are very conservative. Generally the spatial variations of ground displacements along a horizontal axis are much smaller than those used in this example, provided that there is no abrupt change in subsurface profiles.

3.6 Special Considerations

Through the design examples 1 and 2 presented above, it was demonstrated that under normal conditions the axial and curvature strains of the ground were not critical to the design of horizontally aligned linear tunnels. Special attention is required, however, in the following situations:

- Unstable ground, including ground that is susceptible to landslide and/or liquefaction
- Faulting, including tectonic uplift and subsidence
- Abrupt changes in structural stiffness or ground conditions

Unstable Ground

It is generally not feasible to design a tunnel lining of sufficient strength to resist large permanent ground deformations resulting from an unstable ground. Therefore, the proper design measures in dealing with this problem should consider the following:

- Ground stabilization (e.g., compaction, draining, reinforcement, grouting, and earth retaining systems)
- Removal and replacement of problem soils
- Reroute or deeper burial

Faulting

With regard to fault displacements, the best solution is to avoid any potential crossing of active faults. If this is not possible, the general design philosophy is to design a tunnel structure to accept and accommodate these fault displacements. For example, in the North Outfall Replacement Sewer (NORS, City of Los Angeles) project, the amount of fault displacement associated with an M=6.5 design earthquake on the Newport-Inglewood fault was estimated to be about 8 inches at the crossing. To accommodate this displacement, a design scheme using an oversized excavation and a compressible backpacking material was provided. The backpacking material was designed to withstand the static loads, yet be crushable under faulting movements to protect the pipe.

It is believed that the only transportation tunnel in the U.S. designed and constructed to take into consideration potential active fault displacements is the Berkeley Hills Tunnel, part of the San Francisco BART system. This horse-shoe-shaped tunnel was driven through the historically active creeping Hayward Fault with a one-foot oversized excavation. The purpose of the over-excavation was to provide adequate clearance for rail passage even when the tunnel was distorted by the creeping displacements. Thus rails in this section could be realigned and train services could be resumed quickly afterward.

The tunnel was lined with concrete encased ductile steel ribs on two-foot centers. The concrete encased steel rib lining is particularly suitable for this design because it provides sufficient ductility to accommodate the lining distortions with little strength degradation.

The two projects described above have several common design assumptions that allowed the special design to be feasible both technically and economically:

- The locations of the faults at crossings can be identified with acceptable uncertainty, limiting the lengths of the structures that require such special design.
- The design fault displacements are limited to be within one foot.

The cost associated with special design may become excessively high when significant uncertainty exists in defining the activities and locations of the fault crossings, or when the design fault displacements become large (e.g., five feet). Faced with these situations, designers as well as owners should re-evaluate and determine the performance goals of the structures based on a risk-cost balanced consideration, and design should be carried out accordingly.

Abrupt Changes in Structural Stiffness or Ground Conditions

These conditions include, but are not limited to, the following:

- When a regular tunnel section is connected to a station end wall or a rigid, massive structure such as a ventilation building
- At the junctions of tunnels
- When a tunnel traverses two distinct geological media with sharp contrast in stiffness
- When tunnels are locally restrained from movements by any means (i.e., “hard spots”)

Generally, the solutions to these interface problems are to provide either of the following:

- A movable joint, such as the one used at the connection between the Trans-Bay Tube and the ventilation building (Warshaw, 1968)
- A rigid connection with adequate strength and ductility

At these critical interfaces, structures are subjected to potential differential movements due to the difference in stiffness of two adjoining structures or geological media. Estimates of these differential movements generally require a dynamic analysis taking into account the soil-structure interaction effect (e.g., SFBARTD, 1991). There are cases where, with some assumptions, a simple free-field site response analysis will suffice. The calculated differential movements provide necessary data for further evaluations to determine whether special seismic joints are needed.

Once the differential movements are given, there are some simple procedures that may provide approximate solutions to this problem. For example, a linear tunnel entering a large station may experience a transverse differential deflection between the junction and the far field due to the large shear rigidity provided by the end wall of the station structure. If a conventional design using a rigid connection at the interface is proposed, additional bending and shearing stresses will develop near the interface. These stress concentrations can be evaluated by assuming a semi-infinite beam supported on an elastic foundation, with a fixed end at the connection. According to Yeh (1974) and Hetenyi (1976), the induced moment, M(x), and shear, V(x), due to the differential transverse deflection, δ, can be estimated as:

$$M(x) = \frac{K_t}{2\lambda^2}\delta e^{-\lambda x}(\sin \lambda x - \cos \lambda x) \qquad \text{(Eq. 3-7)}$$

$$V(x) = \frac{K_t}{\lambda}\delta e^{-\lambda x}\cos \lambda x \qquad \text{(Eq. 3-8)}$$

$$\lambda = \left(\frac{K_t}{4E_cI_c}\right)^{\frac{1}{4}}$$

where x = distance from the connection

I_c = moment of inertia of the tunnel cross section

E_c = Young's modulus of the tunnel lining

K_t = transverse spring coefficient of ground (in force per unit deformation per unit length of tunnel)

Based on Equations 3-7 and 3-8, the maximum bending moment and shear force occur at x=0 (i.e., at the connection). If it is concluded that an adequate design cannot be achieved by using the rigid connection scheme, then special seismic (movable) joints should be considered.

4.0 OVALING EFFECT ON CIRCULAR TUNNELS

4.0 OVALING EFFECT ON CIRCULAR TUNNELS

The primary purpose of this chapter is to provide methods for quantifying the seismic ovaling effect on circular tunnel linings. The conventionally used simplified free-field deformation method, discussed first, ignores the soil-structure interaction effects. Therefore its use, as demonstrated by two examples, is limited to certain conditions.

A refined method is then presented that is equally simple but capable of eliminating the drawbacks associated with the free-field deformation method. This refined method — built from a theory that is familiar to most mining/underground engineers — considers the soil-structure interaction effects. Based on this method, a series of design charts are developed to facilitate the design process. The results are further validated through numerical analyses.

4.1 Ovaling Effect

As defined in Chapter 3, ovaling of a circular tunnel lining is primarily caused by seismic waves propagating in planes perpendicular to the tunnel axis (see Figure 2). Usually, it is the vertically propagating shear waves that produce the most critical ovaling distortion of the lining. The results are cycles of additional stress concentrations with alternating compressive and tensile stresses in the tunnel lining. These dynamic stresses are superimposed on the existing static state of stress in the lining. Several critical modes may result (Owen and Scholl, 1981):

- Compressive dynamic stresses added to the compressive static stresses may exceed the compressive capacity of the lining locally.
- Tensile dynamic stresses subtracted from the compressive static stresses reduce the lining's moment capacity, and sometimes the resulting stresses may be tensile.

4.2 Free-Field Shear Deformations

As discussed in Chapter 3, the shear distortion of ground caused by vertically propagating shear waves is probably the most critical and predominant mode of seismic motions in many cases. It causes a circular tunnel to oval and a rectangular underground structure to rack (sideways motion), as shown in Figure 3. Analytical procedures by numerical methods are often required to arrive at a reasonable estimate of the free-field shear distortion, particularly for a soil site with variable stratigraphy. Many computer codes with variable degree of sophistication are available (e.g., SHAKE, 1972; FLUSH, 1975; and LINOS, 1991).

The most widely used approach is to simplify the site geology into a horizontally layered system and to derive a solution using one-dimensional wave propagation theory (Schnabel, Lysmer, and Seed, 1972). The resulting free-field shear distortion of the ground from this type of analysis can be expressed as a shear strain distribution or shear deformation profile versus depth. An example of the resulting free-field shear distortion for a soil site using the computer code SHAKE is presented in Figure 7.

Simplified Equation for Shear Deformations

For a deep tunnel located in relatively homogeneous soil or rock, the simplified procedure by Newmark (presented in Table 1) may also provide a reasonable estimate. Here, the maximum free-field shear strain, γ_{max}, can be expressed as:

$$\gamma_{max} = \frac{V_s}{C_s} \qquad \text{(Eq. 4-1)}$$

where V_s = peak particle velocity
C_s = effective shear wave propagation velocity

The values of C_s can be estimated from in-situ and laboratory tests. An equation relating the effective propagation velocity of shear waves to effective shear modulus, G_m, is expressed as:

$$C_s = \sqrt{\frac{G_m}{\rho}} \qquad \text{(Eq. 4-2)}$$

where ρ = mass density of the ground

It is worth noting that both the simplified procedure and the more refined SHAKE analysis require the parameters C_s or G_m as input. The propagation velocity and the shear modulus to be used should be compatible with the level of shear strains that may develop in the ground under design earthquake loading. This is particularly critical for soil sites due to the highly non-linear behavior of soils. The following data are available:

- Seed and Idriss (1970) provide an often used set of laboratory data for soils giving the effective shear wave velocity and effective shear modulus as a function of shear strain.

- Grant and Brown (1981) further supplemented the data sets with results from a series of field geophysical measurements and laboratory testing conducted for six soil sites.

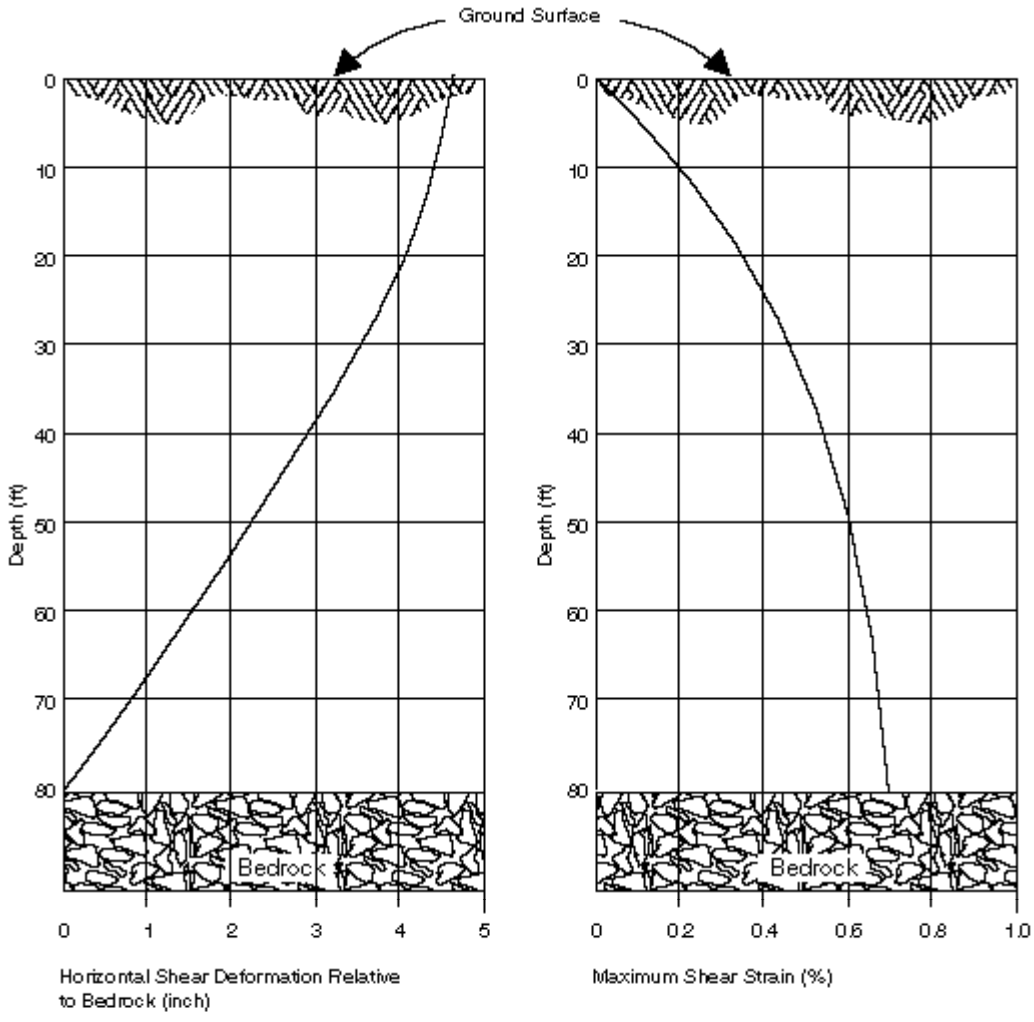

Figure 7.
Free-Field Shear Distortions of Ground Under Vertically Propagating Shear Waves

4.3 Lining Conforming to Free-Field Shear Deformations

When a circular lining is assumed to oval in accordance with the deformations imposed by the surrounding ground (e.g., shear), the lining's transverse sectional stiffness is completely ignored. This assumption is probably reasonable for most circular tunnels in rock and in stiff soils, because the lining stiffness against distortion is low compared with that of the surrounding medium. Depending on the definition of "ground deformation of surrounding medium," however, a design based on this assumption may be overly conservative in some cases and non-conservative in others. This will be discussed further as follows.

Shear distortion of the surrounding ground, for this discussion, can be defined in two ways. If the non-perforated ground in the free-field is used to derive the shear distortion surrounding the tunnel lining, the lining is to be designed to conform to the maximum diameter change, ΔD, shown in Figure 8. The diametric strain of the lining for this case can be derived as:

$$\frac{\Delta D}{D} = \pm \frac{\gamma_{max}}{2} \qquad \text{(Eq. 4-3)}$$

where D = the diameter of the tunnel
γ_{max} = the maximum free-field shear strain

On the other hand, if the ground deformation is derived by assuming the presence of a cavity due to tunnel excavation (Figure 9, for perforated ground), then the lining is to be designed according to the diametric strain expressed as:

$$\frac{\Delta D}{D} = \pm 2\gamma_{max}(1 - \nu_m) \qquad \text{(Eq. 4-4)}$$

where ν_m = the Poisson's Ratio of the medium

Equations 4-3 and 4-4 both assume the absence of the lining. In other words, tunnel-ground interaction is ignored.

Comparison between Equations 4-3 and 4-4 shows that the perforated ground deformation would yield a much greater distortion than the non-perforated, free-field ground deformation. For a typical ground medium, an engineer may encounter solutions provided by Equations 4-3 and 4-4 that differ by a ratio ranging from 2 to about 3. By intuition:

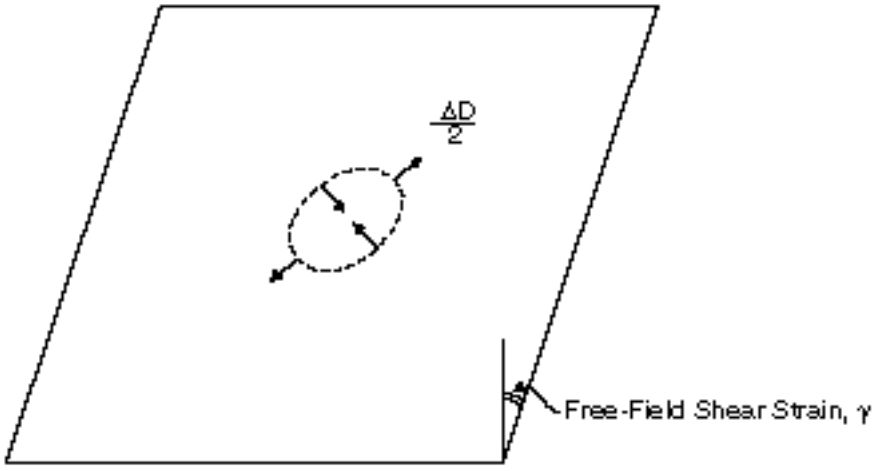

Figure 8.
Free-Field Shear Distortion of Ground (Non-Perforated Medium)

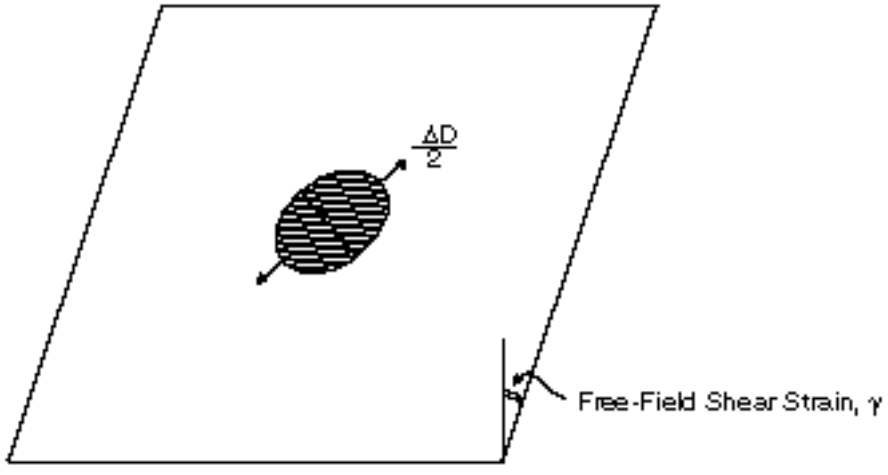

Figure 9.
Shear Distortion of Perforated Ground (Cavity in-Place)

- Equation 4-4, the perforated ground deformation, should serve well for a lining that has little stiffness (against distortion) in comparison to that of the medium.

- Equation 4-3, on the other hand, should provide a reasonable distortion criterion for a lining with a distortion stiffness equal to the surrounding medium.

It is logical to speculate further that a lining with a greater distortion stiffness than the surrounding medium should experience a lining distortion even less than that calculated by Equation 4-3. This latest case may occur when a tunnel is built in soft to very soft soils. The questions that may be raised are:

- *How important is the lining stiffness as it pertains to the engineering design?*

- *How should the lining stiffness be quantified relative to the ground?*

- *What solutions should an engineer use when the lining and ground conditions differ from those where Equations 4-3 and 4-4 are applicable?*

In the following sections (4.4 and 4.5), answers to these questions are presented.

4.4 Importance of Lining Stiffness

Compressibility and Flexibility Ratios

To quantify the relative stiffness between a circular lining and the medium, two ratios designated as the compressibility ratio, C, and the flexibility ratio, F (Hoeg, 1968, and Peck et al., 1972) are defined by the following equations:

$$Compressibility\ Ratio,\quad C = \frac{E_m\ (1 - v_1^2)\ R}{E_1 t\ (1 + v_m)\ (1 - 2v_m)} \qquad \text{(Eq. 4-5)}$$

$$Flexibility\ Ratio,\quad F = \frac{E_m\ (1 - v_1^2)\ R^3}{6E_1 I\ (1 + v_m)} \qquad \text{(Eq. 4-6)}$$

where E_m = modulus of elasticity of the medium
n_m = Poisson's Ratio of the medium
E_l = the modulus of elasticity of the tunnel lining
n_l = Poisson's Ratio of the tunnel lining

R = radius of the tunnel lining
t = thickness of the tunnel lining
I = moment of inertia of the tunnel lining (per unit width)

Of these two ratios, it is often suggested that the flexibility ratio is the more important because it is related to the ability of the lining to resist distortion imposed by the ground. As will be discussed later in this chapter, the compressibility ratio also has an effect on the lining thrust response.

The following examples on the seismic design for several tunnel-ground configurations are presented to investigate the adequacy of the simplified design approach presented in the previous section.

Example 1

The first illustrative example is a tunnel cross-section from the LA Metro project. The ground involved is an old alluvium deposit with an effective shear wave propagation velocity, C_s, equal to 1000 ft/sec. The peak shear wave particle velocity, V_s, according to the design criteria, is 3.4 ft/sec.

Using Equation 4-1, the maximum free-field shear strain, γ_{max} , is calculated to be 0.0034. The reinforced cast-in-place concrete lining properties and the soil properties are assumed and listed in the following table.

Lining Properties	**Soil Properties**
R = 9.5 feet	E_m = 7200 ksf
t = 8.0 inches	ν_m = 0.333
$E_l/(1-\nu_l^2)$ = 662400 ksf	
I = 0.0247 ft^4/ft	

Flexibility Ratio, F = 47
Compressibility Ratio, C = 0.35

Note that uncertainties exist in the estimates of many of the geological and structural parameters. For instance:

- The effective shear wave propagation velocity in the old alluvium may have an uncertainty of at least 20 percent.
- Uncertainty up to 40 percent may also be applied to the estimates of E_m.

- The moment of inertia, I, for a cracked lining section, or for a segmental lining with staggered joints in successive rings, may be considerably less than that for the typical cross section of a segment as used in this calculation example. (See Section 4.5 for a means of estimating the effective moment of inertia, I_e.)

It would be desirable, therefore, to define the ranges of the values considering these uncertainties in the actual design cases.

The LA Metro project has adopted Equation 4-4 as the criterion for ovaling of the running lines (SCRTD, 1984). Therefore, a maximum diametric strain, $\Delta D/D$, of 0.00453 is obtained. The maximum combined bending strain and thrust compression strain as a result of this diametric strain is calculated, with some simple assumptions based on ring theory, by using the following formulation:

$$\varepsilon_{total} = \frac{V_s}{C_s}\left[(1 - \nu_m)\left(\frac{t}{R}\right) + \frac{1}{2}\left(\frac{R}{t}\right)\left(\frac{E_m(1 - \nu_1^2)}{E_1(1 + \nu_m)}\right)\right] \qquad \text{(Eq. 4-7)}$$

$$= 0.00061$$

To verify the accuracy of the results, a numerical analysis using finite difference code is performed. No-slip interface between the lining and the surrounding ground is assumed in the analysis. A more detailed description of this modeling is presented in Section 4.5. Results from the finite difference analysis yield:

- A maximum diametric strain of 0.0038
- A combined maximum total compression strain in the lining of about 0.0006

The excellent agreement between the simplified approach using Equation 4-4 and the refined numerical analysis is explained by the flexibility ratio (F=47) of the ground-lining system. A flexibility ratio of this magnitude suggests that the lining should be flexible even when compared to ground with a cavity in it, and therefore should conform to the perforated ground deformation.

Example 2

In this example, the tunnel is assumed to be built in a very soft soil deposit. The cross-sectional properties of the lining and the surrounding ground are shown in the following table. Note that these properties are made in order to result in a flexibility ratio equal to 1.0.

Lining Properties	Soil Properties
R = 10 feet	E_m = 325 ksf
t = 12 inches	ν_m = 0.25
$E_l/(1-\nu_l^2)$ = 518400 ksf	
I = 0.0833 ft^4/ft	

Flexibility Ratio, F = 1.0
Compressibility Ratio, C = 0.01

It is further assumed that the free-field maximum shear strain, γ_{max} = 0.008, is obtained from one-dimensional site response analysis using SHAKE program. If Equation 4-4 is used, the maximum diametric strain, $\Delta D/D$, of the lining is calculated to be 0.012. With this diameter change, the lining will be subject to a maximum bending strain of approximately 0.0018 together with an almost negligible amount of thrust compression strain. This additional strain, when superimposed on the existing strain caused by the static load, may exceed the compression capacity of the concrete.

It is questionable, however, that designing the lining to conform to the perforated ground deformation (Equation 4-4) is adequate in this case. Flexibility ratio equal to 1.0 implies that the lining may just have enough stiffness to replace that of the soil being excavated. Ideally, the lining should distort in accordance with the free-field, non-perforated ground deformation (Equation 4-3). With this assumption, the maximum diametric strain according to Equation 4-3 is 0.004, a value only one-third of that calculated by Equation 4-4.

A computation by finite difference code is performed for comparison. The resulting maximum diametric strain is about 0.0037, which supports the suggestions made immediately above.

Summary and Conclusions

In conclusion, the simplified seismic design approach can serve its purpose, provided that good judgment is used during the design process. The ovaling effects on the lining, however, may in some cases be overestimated or underestimated, depending on the relative stiffness between the ground and the lining. The main reason for this drawback is the uncertainty of the tunnel-ground interaction.

This drawback, however, may be immaterial for most applications in the real world. For most circular tunnels encountered in practice, the flexibility ratio, F, is likely to be large enough (F>20) so that the tunnel-ground interaction effect can be ignored (Peck, 1972). In these cases, the distortions to be experienced by the lining can be reasonably assumed to be equal to those of the perforated ground.

This rule of thumb procedure may present some design problems in the real world too. These problems arise when a very stiff structure is surrounded by a very soft soil. A typical example would be to construct a very stiff immersed tube in a soft lake or river bed. In this case the flexibility ratio is very low, and the tunnel-ground interaction must be considered to achieve a more efficient design.

In the following section a refined procedure, equally simple, if not simpler, will be presented. This refined procedure considers the tunnel-ground interaction effect and provides a more accurate assessment of the seismic effect upon a circular lining.

4.5 Lining-Ground Interaction

Closed Form Solutions

Closed form solutions for estimating ground-structure interaction for circular tunnels have been proposed by many investigators. These solutions are commonly used for static design of tunnel lining. They are generally based on the assumptions that:

- The ground is an infinite, elastic, homogeneous, isotropic medium.
- The circular lining is generally an elastic, thin walled tube under plane strain conditions.

The models used in these previous studies vary in the following two major assumptions, the effects of which have been addressed by Mohraz et al. (1975) and Einstein et al. (1979):

- Full-slip or no-slip conditions exist along the interface between the ground and the lining.
- Loading conditions are to be simulated as external loading (overpressure loading) or excavation loading.

Most of the recent developments in these models fall into the category of excavation loading conditions, as they represent a more realistic simulation of actual tunnel excavation (Duddeck and Erdmann, 1982). To evaluate the effect of seismic loading, however, the solutions for external loading should be used. Peck, Hendron, and Mohraz (1972), based on the work by Burns and Richard (1964) and Hoeg (1968), proposed closed form solutions in terms of thrusts, bending moments and displacements under external loading conditions.

The expressions of these lining responses are functions of flexibility ratio and compressibility ratio as presented previously in Equations 4-5 and 4-6. The solutions also depend on the in-situ overburden pressure, $\gamma_t H$, and the at rest coefficient of earth pressure, K_o. To be adapted to the loading caused by seismic shear waves, it is necessary to replace the in-situ overburden pressure with free-field shear stress, τ, and assign K_o=–1, to simulate the simple shear condition in the field. The shear stress, τ, can be expressed as a function of shear strain, γ. With some mathematical manipulations, the resulting expressions for maximum thrust, T_{max}, bending moment, M_{max}, and diametric strain, $\Delta D/D$, can be presented in the following forms:

$$T_{\max} = \pm \frac{1}{6} K_1 \frac{E_m}{(1+\nu_m)} R\gamma_{\max} \qquad \text{(Eq. 4-8)}$$

$$M_{\max} = \pm \frac{1}{6} K_1 \frac{E_m}{(1+\nu_m)} R^2\gamma_{\max} \qquad \text{(Eq. 4-9)}$$

$$\frac{\Delta D}{D} = \pm \frac{1}{3} K_1 F \gamma_{\max} \qquad \text{(Eq. 4-10)}$$

where

$$K_1 = \frac{12(1-\nu_m)}{2F+5-6\nu_m} \qquad \text{(Eq. 4-11)}$$

where Em, ν_m = modulus of elasticity and Poisson's Ratio of medium
R = radius of the tunnel lining
γ_{max} = maximum free-field shear strain
F = flexibility ratio

K_1 is defined herein as lining response coefficient. The earthquake loading parameter is represented by the maximum shear strain, γ_{max}, which may be obtained through a simplified approach (such as Equation 4-1), or by performing a site-response analysis.

To ease the design process, Figures 10 and 11 show the lining response coefficient, K_1, as a function of flexibility ratio and Poisson's Ratio of the ground. It should be noted that the solutions provided here are based on the full-slip interface assumption.

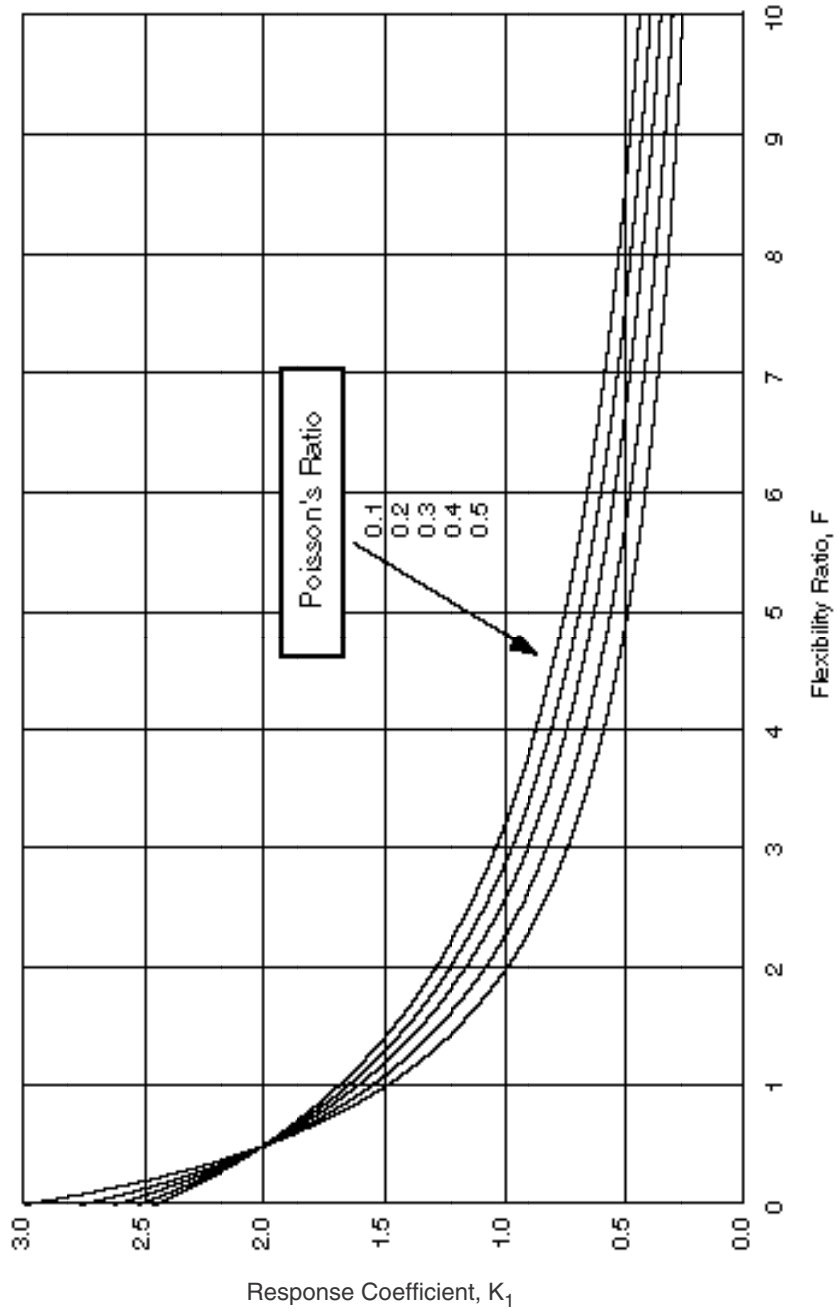

Figure 10.
Lining Response Coefficient, K_1
(Full-Slip Interface)

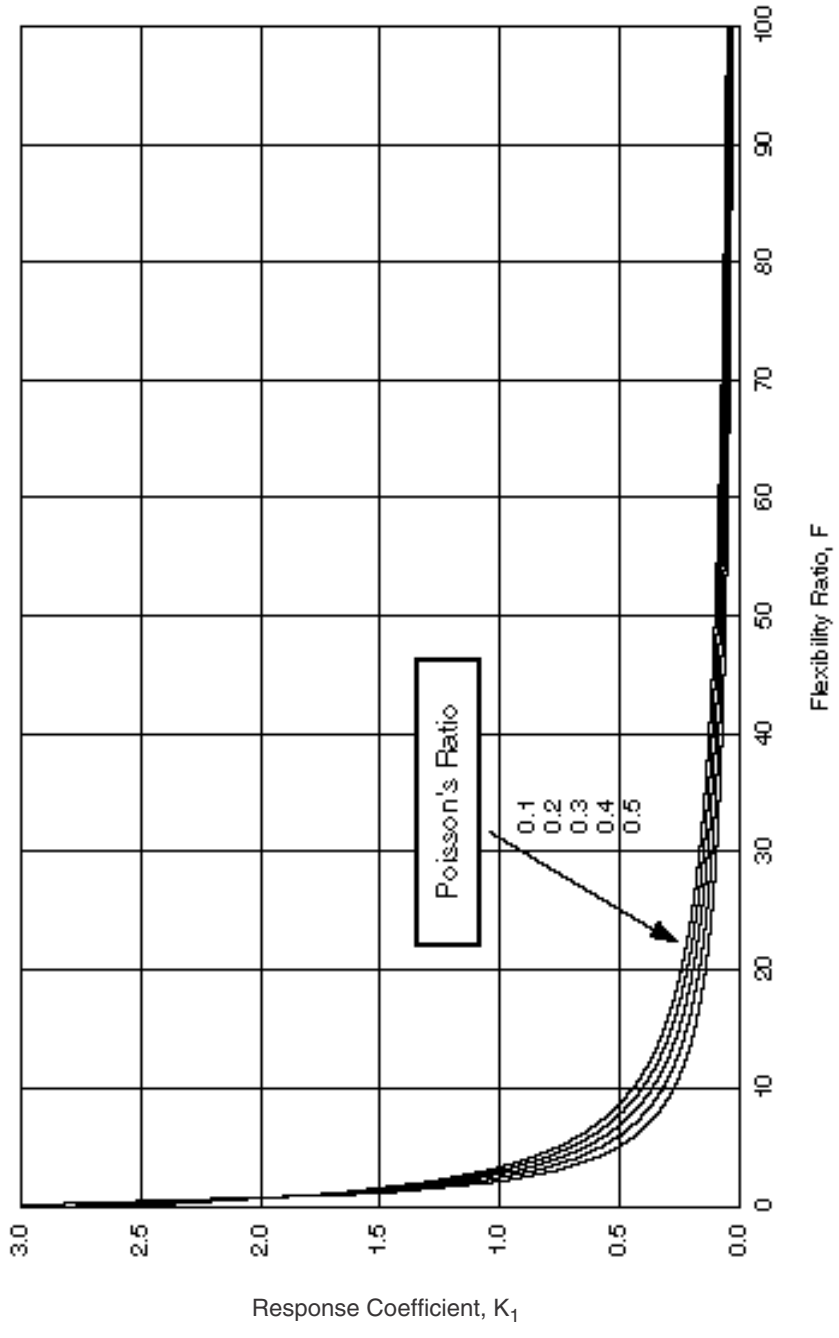

Figure 11.
Lining Response Coefficient, K_1
(Full-Slip Interface)

Comments on Closed Form Solutions

According to previous investigations, during an earthquake slip at interface is a possibility only for tunnels in soft soils, or when seismic loading intensity is severe. For most tunnels, the condition at the interface is between full-slip and no-slip. In computing the forces and deformations in the lining, it is prudent to investigate both cases and the more critical one should be used in design. The full-slip condition gives more conservative results in terms of maximum bending moment, M_{max} , and lining deflections D.

This conservatism is desirable to offset the potential underestimation (10 to 15 percent) of lining forces resulting from the use of equivalent static model in lieu of the dynamic loading condition (Mow and Pao, 1971). Therefore, the full-slip model is adopted for the present study in evaluating the moment and deflection response of a circular tunnel lining.

The maximum thrust, T_{max}, calculated by Equation 4-8, however, may be significantly underestimated under the seismic simple shear condition. The full-slip assumption along the interface is the cause. Therefore, it is recommended that the no-slip interface assumption be used in assessing the lining thrust response. The resulting expressions, after modifications based on Hoeg's work (Schwartz and Einstein, 1980), are:

$$T_{max} = \pm K_2 \tau_{max} R = \pm K_2 \frac{E_m}{2(1+\nu_m)} R\gamma_{max} \qquad \text{(Eq. 4-12)}$$

where the lining thrust response coefficient, K_2 , is defined as:

$$K_2 = 1 + \frac{F\left[(1-2\nu_m) - (1-2\nu_m)C\right] - \frac{1}{2}(1-2\nu_m)^2 + 2}{F\left[(3-2\nu_m) + (1-2\nu_m)C\right] + C\left(\frac{5}{12} - 8\nu_m + 6\nu_m^2\right) + 6 - 8\nu_m}$$

F = flexibility ratio as defined in Eq. 4-6
C = Compressibility ratio as defined in Eq. 4-5
E_m, ν_m = modulus of elasticity and Poisson's Ratio of medium
R = radius of the tunnel lining
τ_{max} = maximum free-field shear stress
γ_{max} = maximum free-field shear strain

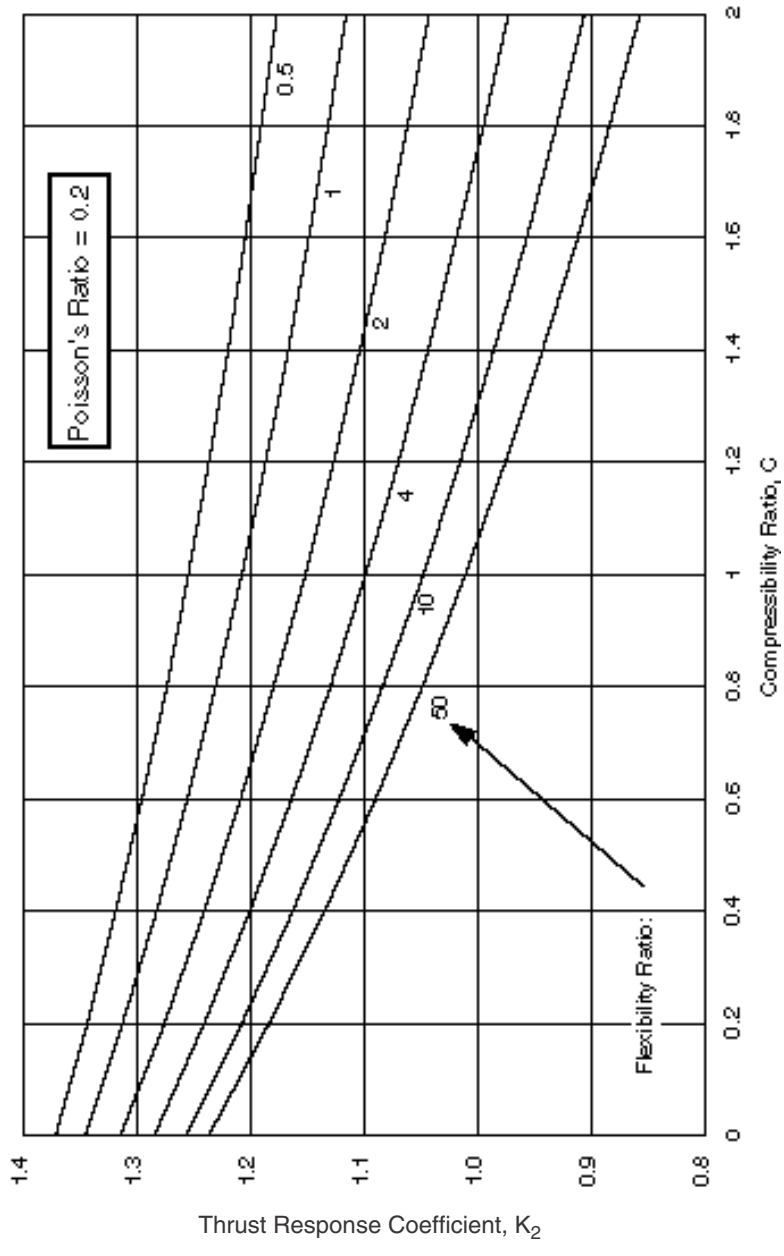

Figure 12.
Lining Response (Thrust) Coefficient, K_2
(No-Slip Interface)

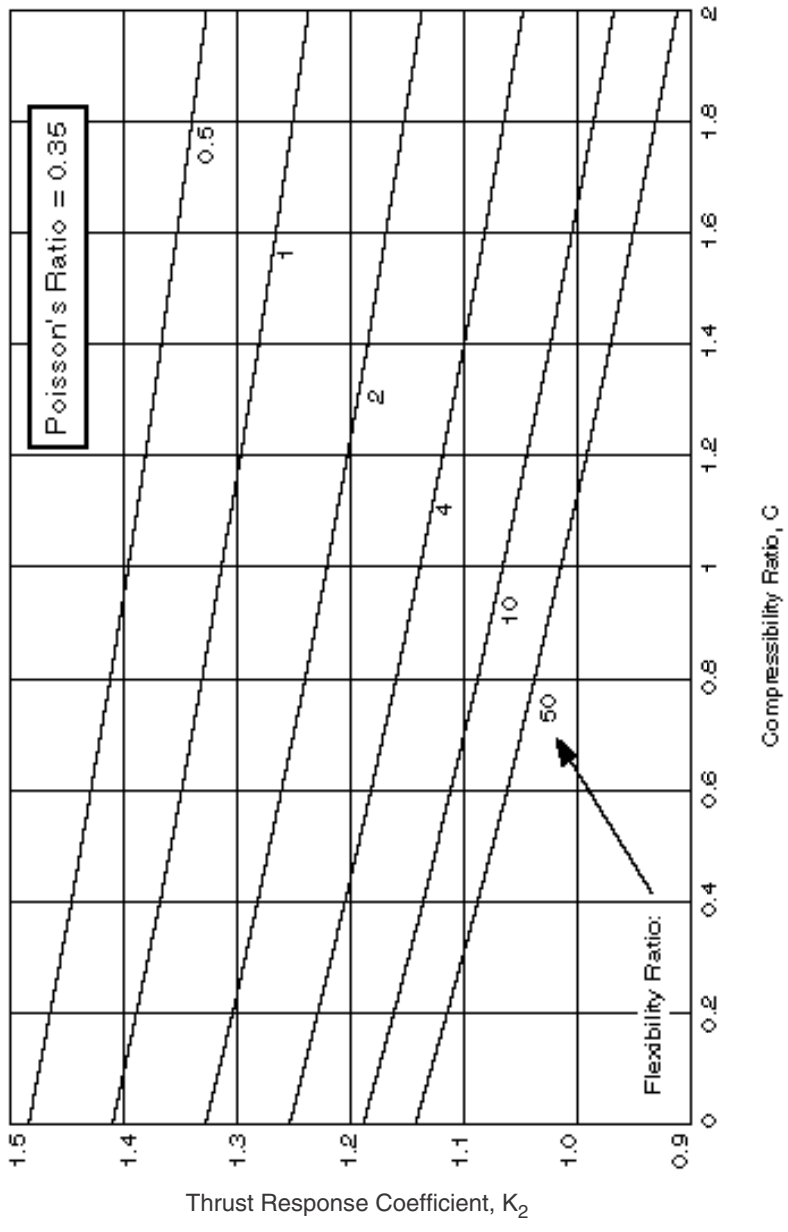

Figure 13.
Lining Response (Thrust) Coefficient, K_2
(No-Slip Interface)

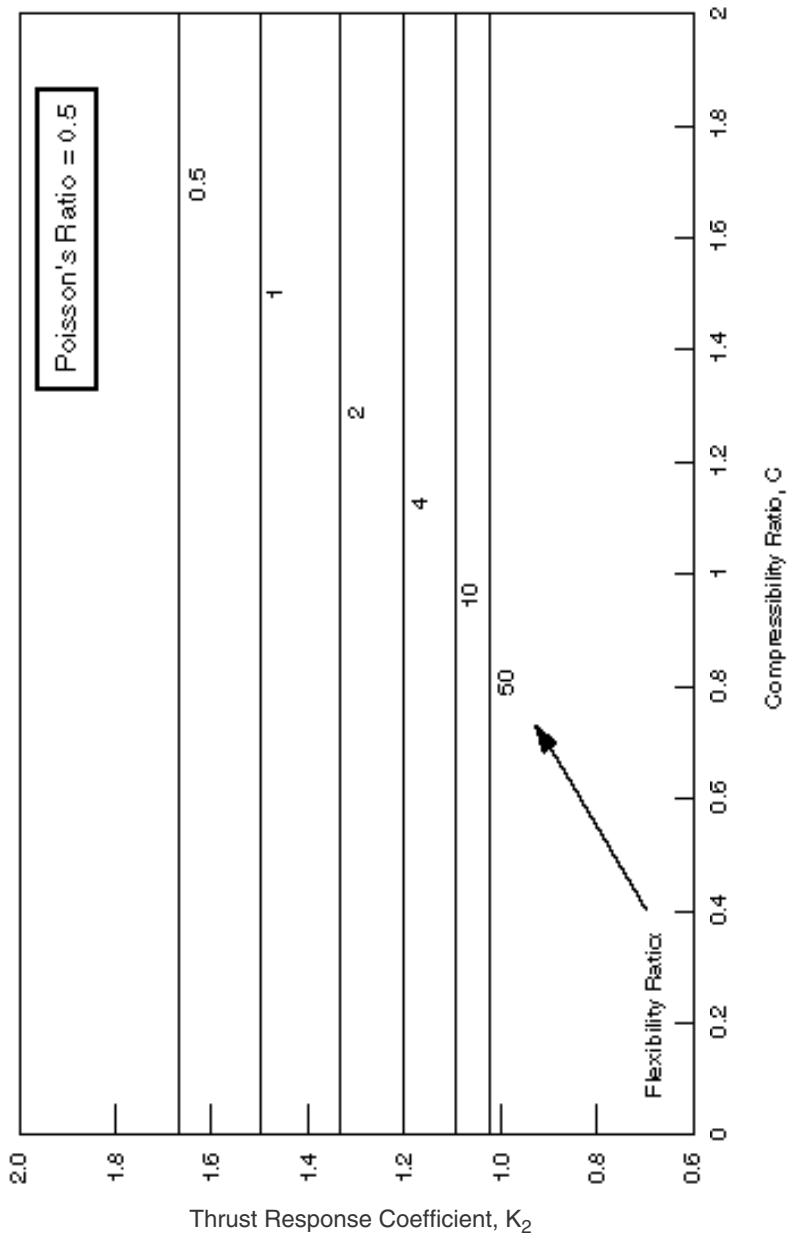

Figure 14.
Lining Response (Thrust) Coefficient, K_2
(No-Slip Interface)

A review of Equation 4-12 and the expression of K_2 suggests that lining thrust response is a function of compressibility ratio, flexibility ratio and Poisson's Ratio. Figures 12 through 14 graphically describe their interrelationships. As the plots show:

- The seismically induced thrusts increase with decreasing compressibility ratio and decreasing flexibility ratio when the Poisson's Ratio of the surrounding ground is less than 0.5.

- When the Poisson's Ratio approaches 0.5 (e.g., for saturated undrained clay), the lining's thrust response is essentially independent of the compressibility ratio.

Figures 12 through 14, along with data contained in Figures 10 and 11 provide a quick aid for designers. The theoretical solutions and the influence of interface assumptions will be further verified for their reasonableness by numerical analysis presented in the next section.

Another useful and important information, for illustration purpose, is to express the deformation ratio between the lining and the free-field as a function of flexibility ratio, F. This relationship can be obtained by dividing Equation 4-10 with Equation 4-3. The resulting expression is:

$$\frac{\Delta D_{lining}}{\Delta D_{free\ -\ field}} = \frac{2}{3} K_1 F \qquad \text{(Eq. 4-13)}$$

The normalized lining deflection is plotted and presented in Figures 15 and 16.

The results indicate that the lining tends to resist and therefore deforms less than the free-field when the flexibility ratio, F, is less than approximately 1. This situation may occur only when a stiff lining is built in soft to very soft soils. As the flexibility ratio increases, the lining deflects more than the free-field and may reach an upper limit as the flexibility ratio becomes infinitely large. This upper limit deflection is equal to the perforated ground deformations calculated by Equation 4-4, signaling a perfectly flexible lining situation. The relationship shown in Figures 15 and 16 supports and supplements the discussions presented in Examples 1 and 2 of Section 4.3.

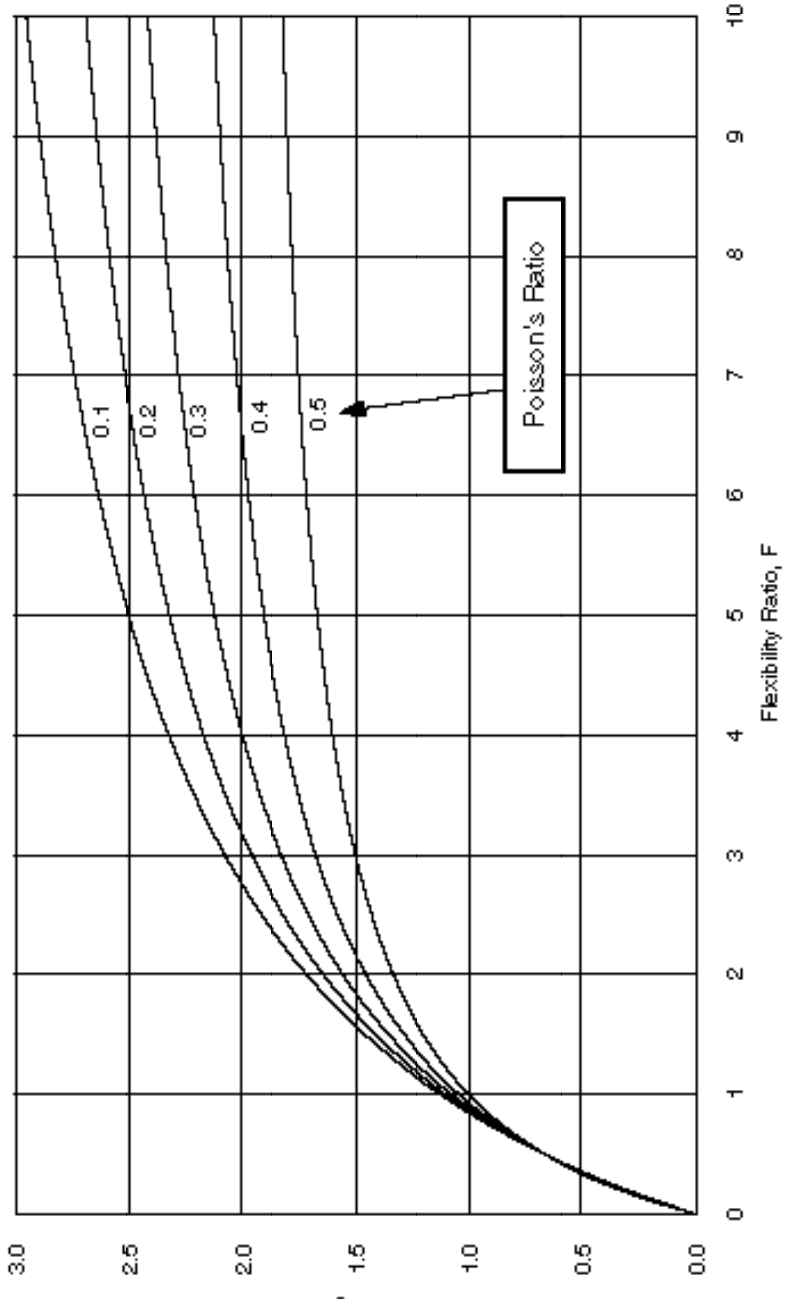

Figure 15.
Normalized Lining Deflection
(Full-Slip Interface)

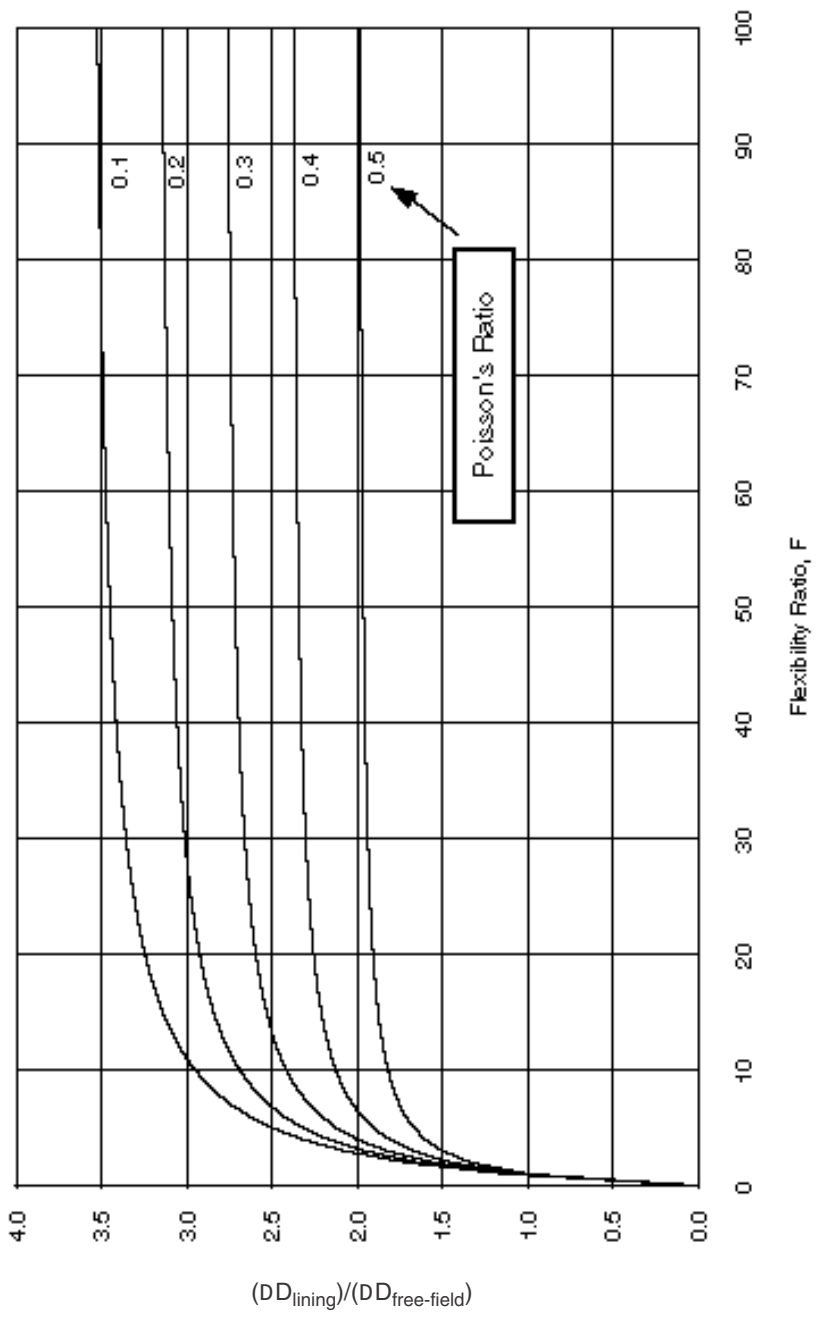

Figure 16.
Normalized Lining Deflection
(Full-Slip Interface)

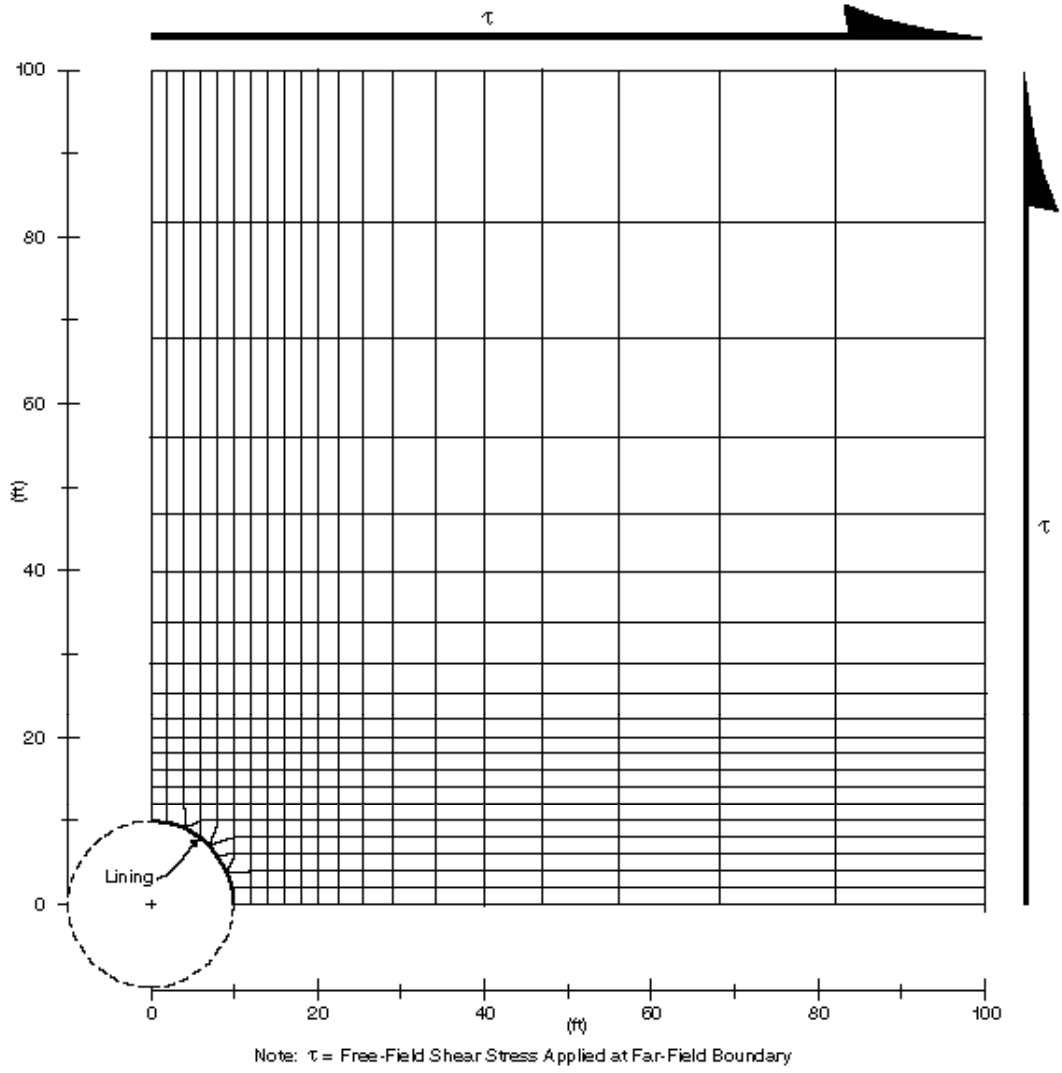

Figure 17.
Finite Difference Mesh
(Pure Shear Condition)

Numerical Analysis

A series of computer analyses using finite difference code (FLAC, 1989) is performed to verify the proposed procedure in the previous section. The mesh and the lining-ground system used in these analyses are shown in Figure 17. The assumptions made for these analyses include the following:

- Plane strain conditions are assumed.
- Seismic shear wave loading is simulated by pure shear conditions with shear stresses applied at far external boundaries.
- Taking advantage of the anti-symmetric loading conditions, only one quarter of the entire lining/ground system is analyzed. Rollers are provided at planes of anti-symmetry.
- Lining is modeled by a series of continuous flexural beam elements of linear elasticity.
- Ground (medium) is modeled as linear elastic material.
- No-slip condition along the lining-ground interface is assumed.

A total of 13 analyses are performed. In order to cover a wide range of possible effects of lining-ground interaction, the parameters for lining and ground are varied. Following is a list of the range of the variations:

Range of E_m = from 325 ksf to 72000 ksf
ν_m = 0.25 and 0.333
$E_l/(1-\nu_l^2)$ = 518400 ksf and 662400 ksf
Range of t = from 0.5 feet to 2.0 feet

The resulting flexibility ratios, F, and compressibility ratios, C, are tabulated in Table 2. To make the level of seismic loading within a reasonable range, the boundary shear stresses (τ_{max}) are made to result in the maximum free-field shear strains (γ_{max}) in the range between 0.001 and 0.008.

Results and Recommendations

Maximum Bending Moment, M_{max} . The resulting maximum bending moments are first calculated for each of the 13 cases by using the full-slip closed form solution, Equation 4-9. These values are then compared to those obtained from the no-slip finite difference analysis. A plot of comparison in terms of dimensionless bending moment between the two is shown in Figure 18. As expected, the full-slip interface assumption results in higher

Case No.	Flexibility Ratio, F	Compressibility Ratio, C	Poisson's Ratio of Medium, ν_m
1	2.22	0.022	0.25
2	47.2	0.35	0.333
3	1.0	0.01	0.25
4	0.75	0.009	0.25
5	0.46	0.0077	0.25
6	0.125	0.005	0.25
7	11.1	0.11	0.25
8	130.4	0.49	0.333
9	0.037	0.0033	0.25
10	163.0	2.45	0.333
11	20.4	1.22	0.333
12	∞	16200	0.333
13	326.0	4.9	0.333

Table 2.
Cases Analyzed by Finite Difference Modeling

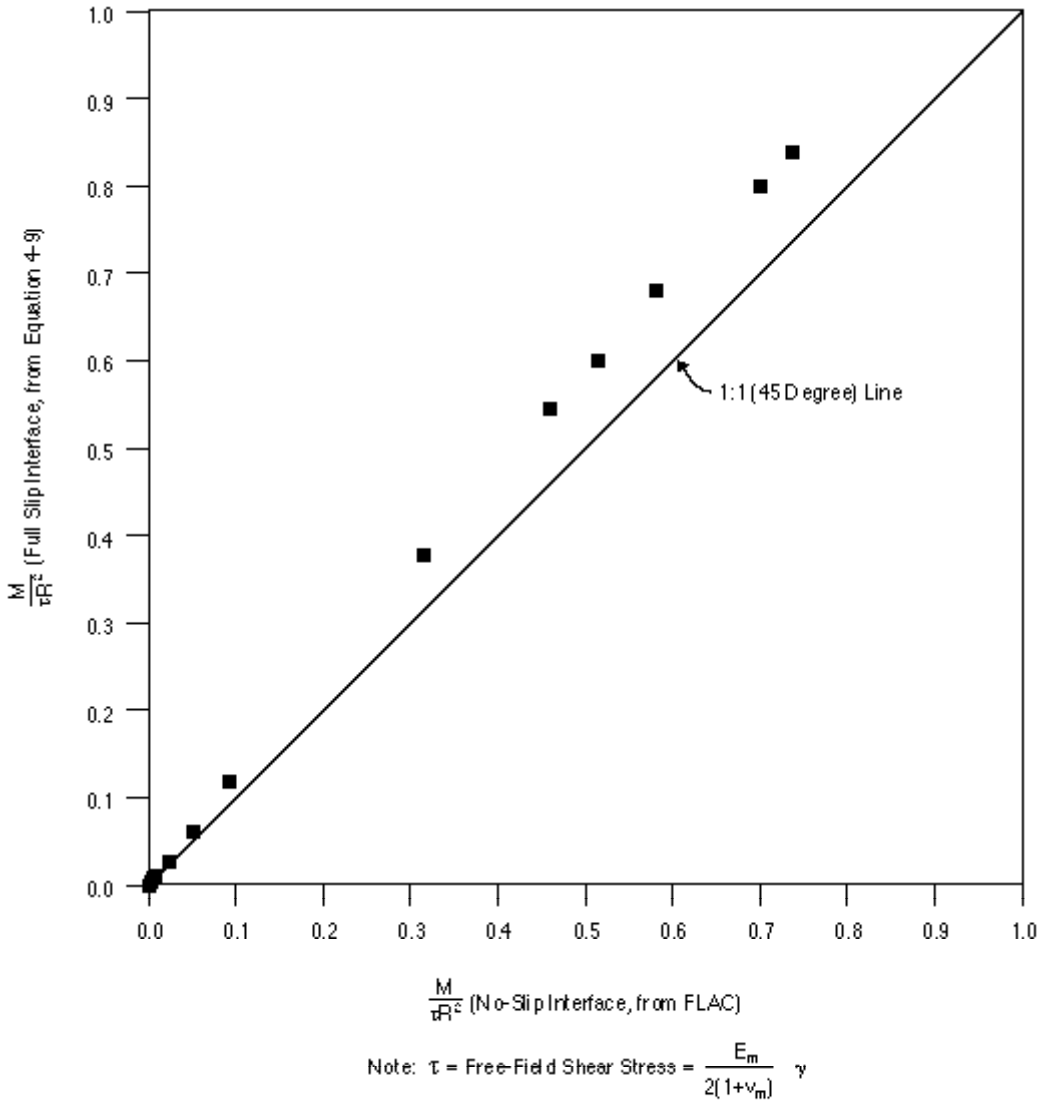

Figure 18.
Influence of Interface Condition on Bending Moment

maximum bending moment than the no-slip interface condition. The differences are within approximately 20 percent under seismic shear loading condition.

It should be realized, however, that these results are based on pseudo-static solutions that do not consider the potential dynamic amplification and stress concentrations at the tunnel excavation boundary (Mow and Pao, 1971). Previous studies suggest that a true dynamic solution would yield results that are 10 to 15 percent greater than an equivalent static solution, provided that the seismic wavelength is at least about 8 times greater than the width of the excavation (cavity).

Therefore, it is prudent to adopt the more conservative full-slip assumption for the calculation of bending moments. With this more conservative assumption, the effects of stress amplification need not be considered.

Maximum Lining Deflection, D D_{lining}. Figure 19 presents a plot of the maximum lining deflections from full-slip closed form solution versus those from no-slip finite difference analysis (noting that these lining deflections are normalized with respect to the free-field ground deflections). Similar to the discussion presented above, lining tends to oval (distort) more under the full-slip interface assumption. The differences, however, are very small.

The full-slip assumption (Equation 4-10 or Equation 4-13) is recommended for calculating the lining distortion. The effects of stress amplification need not be considered when the conservative full-slip assumption is adopted.

It is interesting to note from the plot that almost no difference exists between the two assumptions for Case No. 12. This can be explained by the fact that a nearly “perfectly flexible” lining is used and little lining-ground interaction is involved in the Case No.12 analysis.

Maximum Lining Thrust, T_{max}. For comparison, the maximum lining thrusts are calculated using closed form solutions for both assumptions (Equations 4-8 and 4-12). The results, along with those from the finite difference analysis, are tabulated in Table 3. The table shows excellent agreement on the thrust response between the numerical finite difference analysis and the closed form solution for the no-slip condition. It also verified that the full-slip assumption will lead to significant underestimation of the lining thrust under seismic shear condition.

Therefore, it is recommended that Equation 4-12 be used for thrust calculation. To account for the dynamic stress amplification due to the opening, it is further recommended that thrusts calculated from Equation 4-12 be multiplied by a factor of 1.15 for design purpose.

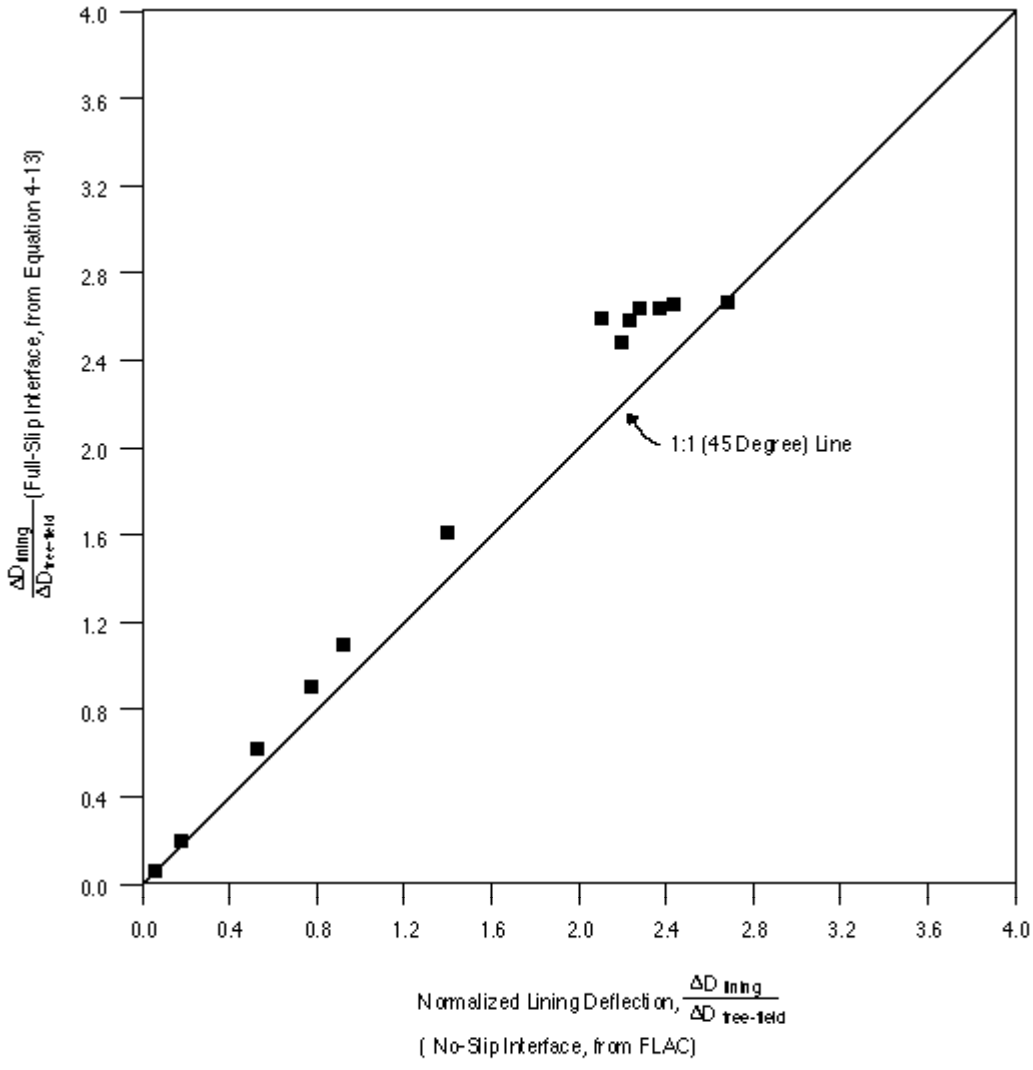

Figure 19.
Influence of Interface Condition on Lining Deflection

Case No.	FLAC Analysis	Closed Form Solution	Closed Form Solution
	T/πR (No-Slip)	T/πR (Full-Slip)	T/πR (No-Slip)
1	1.33	0.378	1.31
2	1.117	0.027	1.102
3	1.385	0.545	1.364
4	1.4	0.80	1.38
5	1.43	0.88	1.41
6	1.477	0.80	1.45
7	1.222	0.117	1.21
8	1.085	0.010	1.073
9	1.495	0.84	1.462
10	0.852	0.008	0.852
11	1.0	0.061	1.007
12	= 0	= 0	= 0
13	0.573	0.004	0.575

$$\tau = \frac{c_m}{2(1+\nu_m)}$$

Table 3.
Influence of Interface Conditions on Thrust

Lining Stiffness, I. The results presented above are based on the assumption that the lining is a monolithic and continuous circular ring with intact, elastic properties. Many circular tunnels are constructed with bolted or unbolted segmental lining. Besides, a concrete lining subjected to bending and thrust often cracks and behaves in a nonlinear fashion. Therefore, in applying the results presented herewith, the effective (or, equivalent) stiffness of the lining will have to be estimated first. Some simple and approximate methods accounting for the effect of joints on lining stiffness can be found in the literature:

- Monsees and Hansmire (1992) suggested the use of an effective lining stiffness that is one-half of the stiffness for the full lining section.

- Analytical studies by Paul, et al., (1983) suggested that the effective stiffness be from 30 to 95 percent of the intact, full-section lining.

- Muir Wood (1975) and Lyons (1978) examined the effects of joints and showed that for a lining with n segments, the effective stiffness of the ring was:

$$I_e = I_j + \left(\frac{4}{n}\right)^2 I \qquad \text{(Eq. 4-14)}$$

where $I_e < I$ and $n > 4$
I =lining stiffness of the intact, full-section
I_j = effective stiffness of lining at joint
I_e = effective stiffness of lining

5.0 RACKING EFFECT ON RECTANGULAR TUNNELS

5.0 RACKING EFFECT ON RECTANGULAR TUNNELS

This chapter first addresses some of the conventional methods used in seismic racking design of cut-and-cover tunnels and the limitations associated with these methods. To provide a more rational design approach to overcoming these limitations, an extensive parametric study was conducted using dynamic finite-element soil-structure interaction analyses.

The purpose of these complex and time consuming analyses was not to show the elegance of the mathematical computations. Neither are these complex analyses recommended for a regular tunnel design job. Rather, they were used to generate sets of data that can readily be incorporated into conventional design procedures. At the end of this chapter, a recommended procedure using simplified frame analysis models is presented for practical design purposes.

5.1 General

Shallow depth transportation tunnels are often of rectangular shape and are often built using the cut-and-cover method. Usually the tunnel is designed as a rigid frame box structure. From the seismic design standpoint, these box structures have some characteristics that are different from those of the mined circular tunnels, besides the geometrical aspects. The implications of three of these characteristics for seismic design are discussed below.

First, cut-and-cover tunnels are generally built at shallow depths in soils where seismic ground deformations and the shaking intensity tend to be greater than at deeper locations, due to the lower stiffness of the soils and the site amplification effect. As discussed in Chapter 2, past tunnel performance data suggest that tunnels built with shallow soil overburden cover tend to be more vulnerable to earthquakes than deep ones.

Second, the dimensions of box type tunnels are in general greater than those of circular tunnels. The box frame does not transmit the static loads as efficiently as the circular lining, resulting in much thicker walls and slabs for the box frame. As a result, a rectangular tunnel structure is usually stiffer than a circular tunnel lining in the transverse direction and less tolerant to distortion. This characteristic, along with the potential large seismic ground deformations that are typical for shallow soil deposits, makes the soil-structure interaction effect particularly important for the seismic design of cut-and-cover rectangular tunnels, including those built with sunken tube method.

Third, typically soil is backfilled above the structure and possibly between the in-situ medium and the structure. Often, the backfill soil may consist of compacted material having different properties than the in-situ soil. The properties of the backfill soil as well as the in-situ medium should be properly accounted for in the design and analysis.

5.2 Racking Effect

During earthquakes a rectangular box structure in soil or in rock will experience transverse racking deformations (sideways motion) due to the shear distortions of the ground, in a manner similar to the ovaling of a circular tunnel discussed in Chapter 4. The racking effect on the structure is similar to that of an unbalanced loading condition.

The external forces the structure is subjected to are in the form of shear stresses and normal pressures all around the exterior surfaces of the box. The magnitude and distribution of these external forces are complex and difficult to assess. The end results, however, are cycles of additional internal forces and stresses with alternating direction in the structure members. These dynamic forces and stresses are superimposed on the existing static state of stress in the structure members. For rigid frame box structures, the most critical mode of potential damage due to the racking effect is the distress at the top and bottom joints.

Damages to shallow buried cut-and-cover structures, including regular tunnel sections, were reported during the earthquakes of 1906 San Francisco and 1971 San Fernando (Owen and Scholl, 1981). The damages included:

- Concrete spalling and longitudinal cracks along the walls
- Failure at the top and bottom wall joints
- Failure of longitudinal construction joints

For structures with no moment resistance — such as the unreinforced brick arch in one of the cases during the 1906 San Francisco earthquake — total collapse is a possibility.

The methods used in current design practice to counteract the seismic effects on rectangular tunnel linings are described in the following two sections (5.3 and 5.4).

5.3 Dynamic Earth Pressure Methods

Mononobe-Okabe Method

Dynamic earth pressure methods have been suggested for the evaluation of underground box structures by some engineers. The most popular theory for determining the increase in lateral earth pressure due to seismic effect is the Mononobe-Okabe theory described, for example, by Seed and Whitman (1970), recognized by Japanese Society of Civil Engineers for earthquake resistant design of submerged tunnels (1975), and recommended in several other documents (Converse Consultants, 1983; EBMUD, 1973). Using this method, the dynamic earth pressure is assumed to be caused by the inertial force of the surrounding soils and is calculated by relating the dynamic pressure to a determined seismic coefficient and the soil properties.

Originally developed for aboveground earth retaining walls, the Mononobe-Okabe method assumes that the wall structure would move and/or tilt sufficiently so that a yielding active earth wedge could form behind the wall. For a buried rectangular structural frame, the ground and the structure would move together, making it unlikely that a yielding active wedge could form. Therefore, its applicability in the seismic design of underground structures has been the subject of controversy.

The obvious applicable situation is limited to the typical “boat section” (i.e., U-section) type of underground construction, where the structure configuration resembles that of conventional retaining walls. Another situation where the use of the Mononobe-Okabe method may also be adequate is when the structure is located at a very shallow depth. Experience from PB’s recent underground transportation projects has indicated that the Mononobe-Okabe earth pressure, when considered as an unbalanced load, may cause a rectangular tunnel structure to rack at an amount that is greater than the deformation of the surrounding ground. This unrealistic result tends to be amplified as the depth of burial increases. This amplification is primarily due to the inertial force of the thick soil cover, which acts as a surcharge and, according to the Mononobe-Okabe method, has to be considered. In spite of this drawback, the method has been shown to serve as a reasonable safety measure against dynamic earth thrust for tunnels buried at shallow depths (e.g., in the Los Angeles Metro Project).

Wood Method

Another theoretical form of dynamic earth pressure was derived by Wood (1973). By assuming infinite rigidity of the wall and the foundation, Wood derived a total dynamic

thrust that is approximately 1.5 to 2.0 times the thrust calculated by the Mononobe-Okabe method. Model experiments by Yong (1985) confirmed these theoretical results. This method is possibly adequate for a volume structure (e.g., a basement) resting on a very stiff/hard medium (such as rock) and rigidly braced across (e.g., by transverse shear wall diaphragms). A possible application of this method in a cut-and-cover tunnel construction is at the end walls of a subway station, where the end walls act as rigid shear wall diaphragms and prevent the structure from making sideways movements during earthquakes. For regular rectangular cross-sections under plane strain condition, the Wood theory, like the Mononobe-Okabe method, would lead to unrealistic results and is not recommended for use in typical tunnel sections with significant soil cover thickness.

Implications for Design

It is logical to postulate that the presence of a rectangular frame structure in the ground will induce dynamic earth pressures acting upon the structure. This earth pressure loading, however, is in a form of complex distributions of shear stresses as well as normal pressures along the exterior surfaces of the roof, the walls and the invert. To quantify these external earth loads accurately requires a rigorous dynamic soil-structure analysis.

Realizing that the overall effect of this complex external earth loading is to cause the structure to rack, engineers find it more realistic to approach the problem by specifying the loading in terms of deformations. The structure design goal, therefore, is to ensure that the structure can adequately absorb the imposed racking deformation (i.e., the deformation method), rather than using a criterion of resisting a specified dynamic earth pressure (i.e., the force method). The focus of the remaining sections of this chapter, therefore, is on the method based on seismic racking deformations.

5.4 Free-Field Racking Deformation Method

Conventionally, a rectangular tunnel structure is designed by assuming that the amount of racking imposed on the structure is equal to the free-field shear distortions of the surrounding medium. The racking stiffness of the structure is ignored with this assumption. In Section 4.2 (Chapter 4), the commonly used approach to estimating the free-field shear distortions of the medium was discussed. Using the free-field racking deformation method, Figure 20 shows a typical free-field soil deformation profile and the resulting differential distortion to be used for the design of a buried rectangular structure.

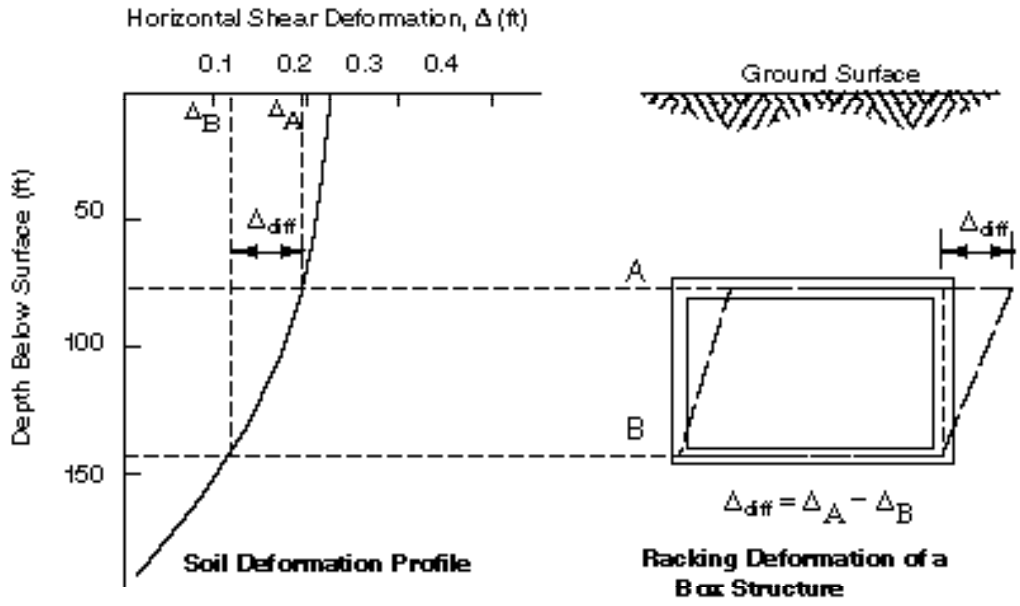

Figure 20.
Typical Free-Field Racking Deformation Imposed on a Buried Rectangular Frame

(Source: St. John and Zahrah, 1987)

San Francisco BART

In his pioneering development of the seismic design criteria for the San Francisco BART subway stations, Kuesel (1969) presented this approach and developed project-specific soil distortion profiles for design purpose. The elastic and plastic distortion limits of the reinforced concrete box structure were studied and compared to the design free-field soil distortions. For the BART project, Kuesel concluded that:

- The structure would have sufficient capacity to absorb the imposed free-field soil distortions elastically in most cases, and that no special provisions need be made for seismic effects.

- When the imposed shear distortions caused plastic rotation of joints, such joints should be designed with special structural details.

The soil deformation profiles and some of the assumptions used by Kuesel at that time are applicable only for the SFBART project. The design philosophy and the general approach proposed are still valid, however, even when viewed more than two decades later.

Los Angeles Metro

In setting forth the seismic design criteria for the LA Metro project, Monsees and Merritt (1991), also adopted the free-field deformation method for the racking evaluation of rectangular frame structures. They specified that joints being strained into plastic hinges should be allowed under the Maximum Design Earthquake (MDE) provided that no plastic hinge combinations were formed that could lead to a potential collapse mechanism. The acceptable and unacceptable hinging conditions specified in the LA Metro project are described in Figure 21.

Flexibility vs. Stiffness

In contrast to the static design, where the loads are well defined and the analysis is based on a “force method,” the seismic effect based on the “deformation method” is highly dependent on the structural details. The seismic forces induced in structural members decrease as the structure’s flexibility increases. Therefore, from the seismic design standpoint it is desirable to make the structure flexible rather than to stiffen it. In

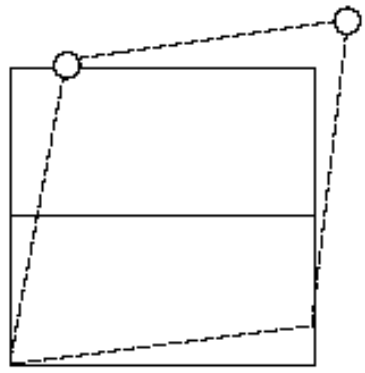

A. Acceptable Condition – Two Plastic Hinges

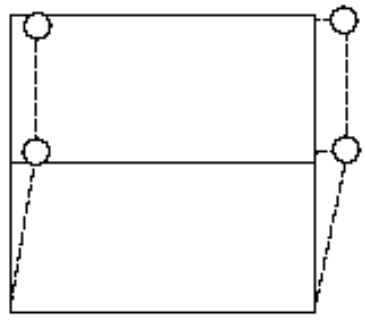

B. Acceptable Condition – Four Plastic Hinges

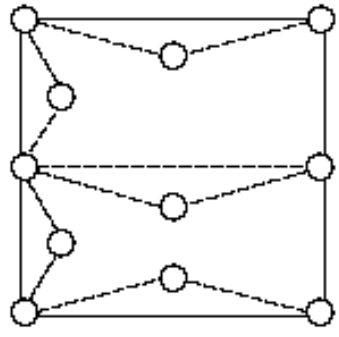

C. Unacceptable Condition – Three Plastic Hinges in any Member

Figure 21.
Structure Stability for Buried Rectangular Frames

(Source: Monsees and Merritt, 1991)

general, flexibility can be achieved by using ductile reinforcement at critical joints. In contrast, increasing the thickness of the members makes the structure less flexible. The special structural details suggested by Kuesel and the plastic-hinge design specified by Monsees and Merritt are in fact based on this philosophy.

Another design concept that can increase the flexibility of the cut-and-cover box structure is to specify pinned connections at walls/slabs joints. This design detail becomes attractive when cofferdam retaining structures are used as permanent walls because pinned connections are less difficult to build than fixed connections in this case.

Applicability of the Free-Field Racking Method

The free-field deformation method serves as a simple and effective design tool when the seismically induced ground distortion is small, for example when the shaking intensity is low or the ground is very stiff. Given these conditions, most practical structural configurations can easily absorb the ground distortion without being distressed. The method is also a realistic one when the structure, compared to its surrounding medium, is flexible.

Cases arise, however, when this simple procedure leads to overly conservative design for box structures. These situations generally occur in soft soils. Seismically induced free-field ground distortions are generally large in soft soils, particularly when they are subjected to amplification effects. Ironically, rectangular box structures in soft soils are generally designed with stiff configurations to resist the static loads, making them less tolerant to racking distortions. Imposing free-field deformations on a structure in this situation is likely to result in unnecessary conservatism, as the stiff structure may actually deform less than the soft ground. An example to demonstrate the effect of structure stiffness on racking deformation is given below.

Examples

Soil Parameters. In this example a simplified subsurface profile is used in the free-field deformation analysis and the soil-structure interaction analysis. Figure 22 shows the soil stratigraphy of this profile. Shear wave velocities are used to represent the stiffness of the soil layers overlying the bedrock. For parametric study purposes, the analysis is performed for two cases with the silty clay layer being represented by a shear wave velocity of:

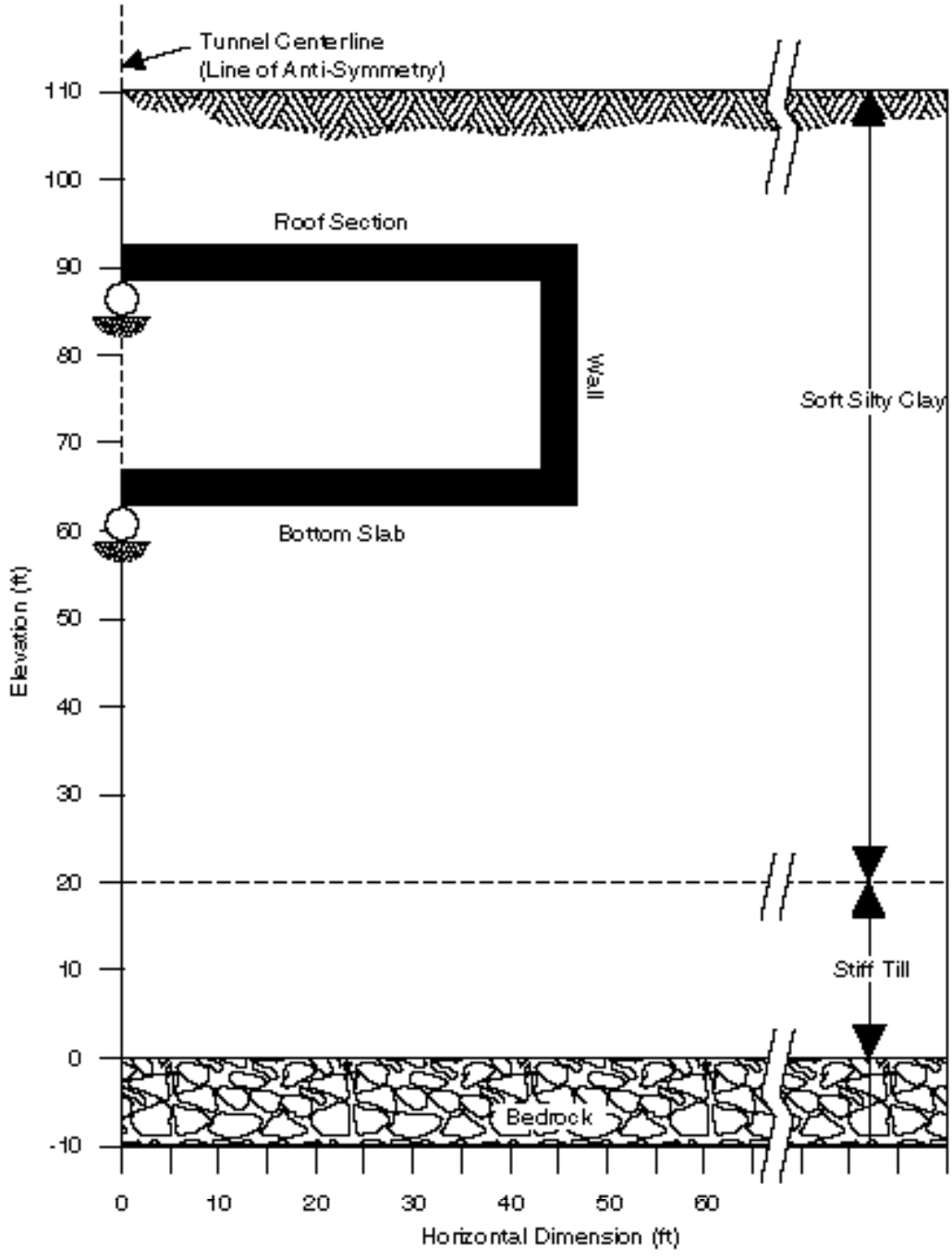

Figure 22.
Soil-Structure System Analyzed in Example

- 254 ft/sec for case I
- 415 ft/sec for case II

These shear wave velocities are assumed to be compatible with the shear strains the soil experiences during the design earthquake. Assuming a unit weight of 115 pcf for the silty clay, the corresponding shear moduli are:

- G = 230 ksf for case I
- G = 615 ksf for case II

Figure 23 shows the shear wave velocity profiles used in the analysis.

Structure Properties. A reinforced one-barrel concrete box structure with the following properties is assumed:

Structure Member	Elastic* Modulus(ksi)	Moment of Inertia(ft^4/ft)	Thickness (ft)	Length (ft)
Side Wall	3640	42.7	8.0	26
Base Slab	3640	51.2	8.5	90
Roof Slab	3640	51.2	8.5	90

* Plane Strain Elastic Modulus

The structure members are modeled as rigid continuous beam elements under a two-dimensional plane strain condition.

Analytical Model. Earthquake excitation is represented by a vertically propagating shear wave accelerogram originated from the rigid bedrock. The relative geometric relationship between the soil and the tunnel structure is described in Figure 22.

To assess the effect of soil-structure interaction the analysis is conducted using the dynamic finite element program FLUSH (1975). Under horizontal earthquake excitation the seismic loading condition is anti-symmetrical. Therefore, only one half of the soil-structure system need be analyzed, by imposing horizontal rollers along the vertical axis of anti-symmetry (see Figure 21). A more detailed description of the time-history finite element analysis including the input ground motions and the structural modeling will be given in Section 5.5.

Results. Figure 24 shows results based on free-field analysis, ignoring the presence of structure and the opening. The free-field differential deformations between the projected

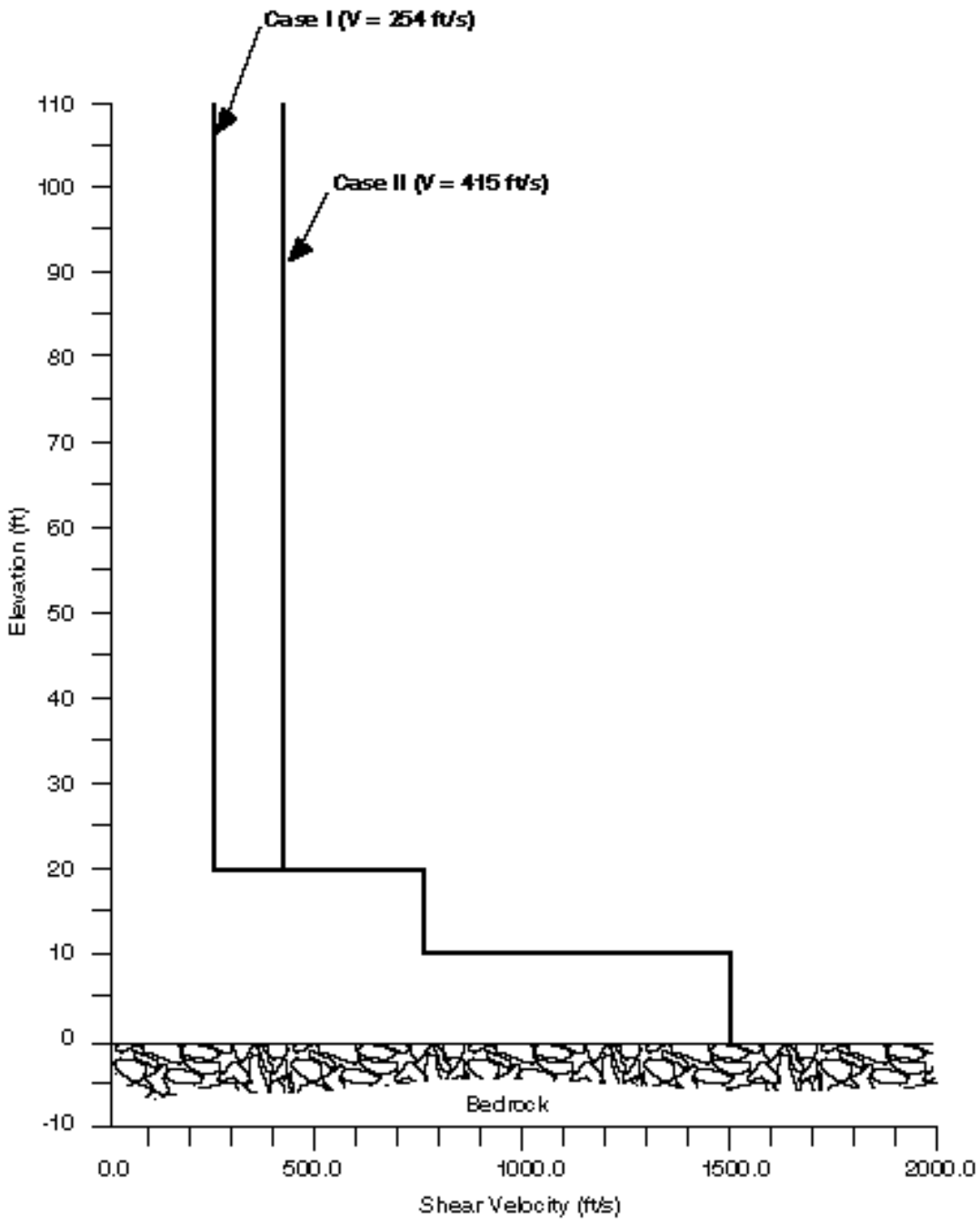

Figure 23.
Subsurface Shear Velocity Profiles

locations of roof and invert are approximately 0.26 inch and 0.17 inch for case I and case II respectively. When both soil and structure are included in the analysis, the calculated racking distortions (between the roof and the invert) were only about 13 percent and 32 percent of the free-field deformations for case I and case II, respectively (see Figures 25 and 26).

Conclusions. The results of the analysis lead to the following conclusions:

- It may be very conservative to design a rectangular tunnel structure to accommodate all the shear deformations in the free-field, particularly when the structure is stiff and the surrounding ground is soft. This finding coincides with results from several previous studies (Hwang and Lysmer, 1981; and TARTS, 1989).

- As the relative stiffness between the soil and the structure decreases (e.g., from case II to case I), the actual structure racking deformation would also decrease, when expressed as a percentage of the free-field deformation. This suggests that the soil-structure interaction effect on the racking of a rectangular tunnel should be:

  -Similar to that on the ovaling of a circular tunnel (Chapter 4)

  -A function of the relative stiffness between the ground and the structure

A series of analyses performed to define this relationship and their results are presented and discussed next.

5.5 Tunnel-Ground Interaction Analysis

Although closed-form solutions accounting for soil-structure interaction, such as those presented in Chapter 4, are available for deep circular lined tunnels, they are not available for rectangular tunnels due primarily to the highly variable geometrical characteristics typically associated with rectangular tunnels. Conditions become even more complex because most of the rectangular tunnels are built using the cut-and-cover method at shallow depths, where seismically induced ground distortions and stresses change significantly with depth.

It is desirable, therefore, that a simple and practical procedure be developed for use by design engineers that accounts for the soil-structure interaction effect. To that end, a series of dynamic soil-structure interaction finite element analyses were performed in this study. The results from these complex analyses were then transformed so that they could be adapted easily to simple analytical tools used currently in design practice.

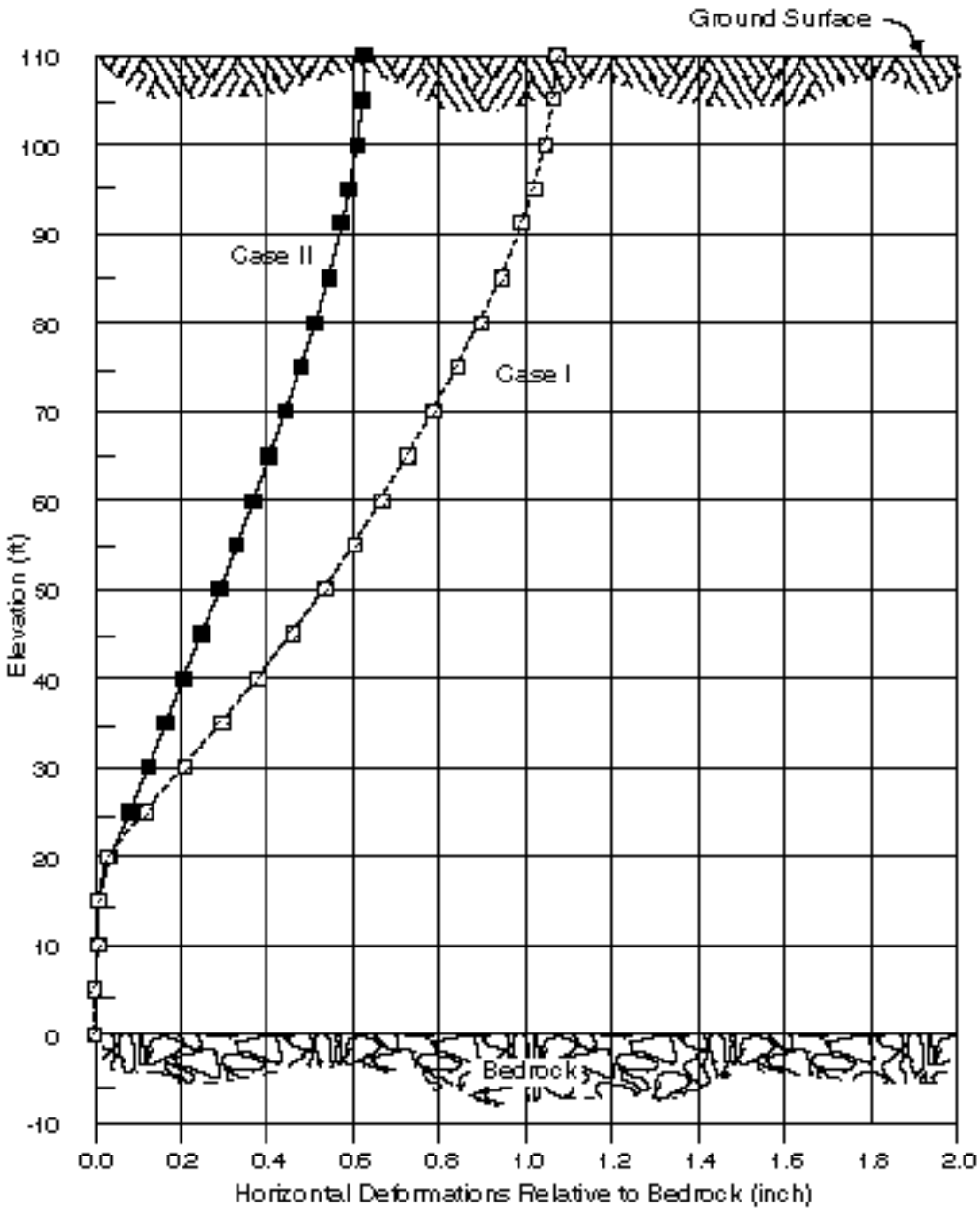

Figure 24.
Free-Field Shear Deformation
(from Free-Field Site Response Analysis, SHAKE)

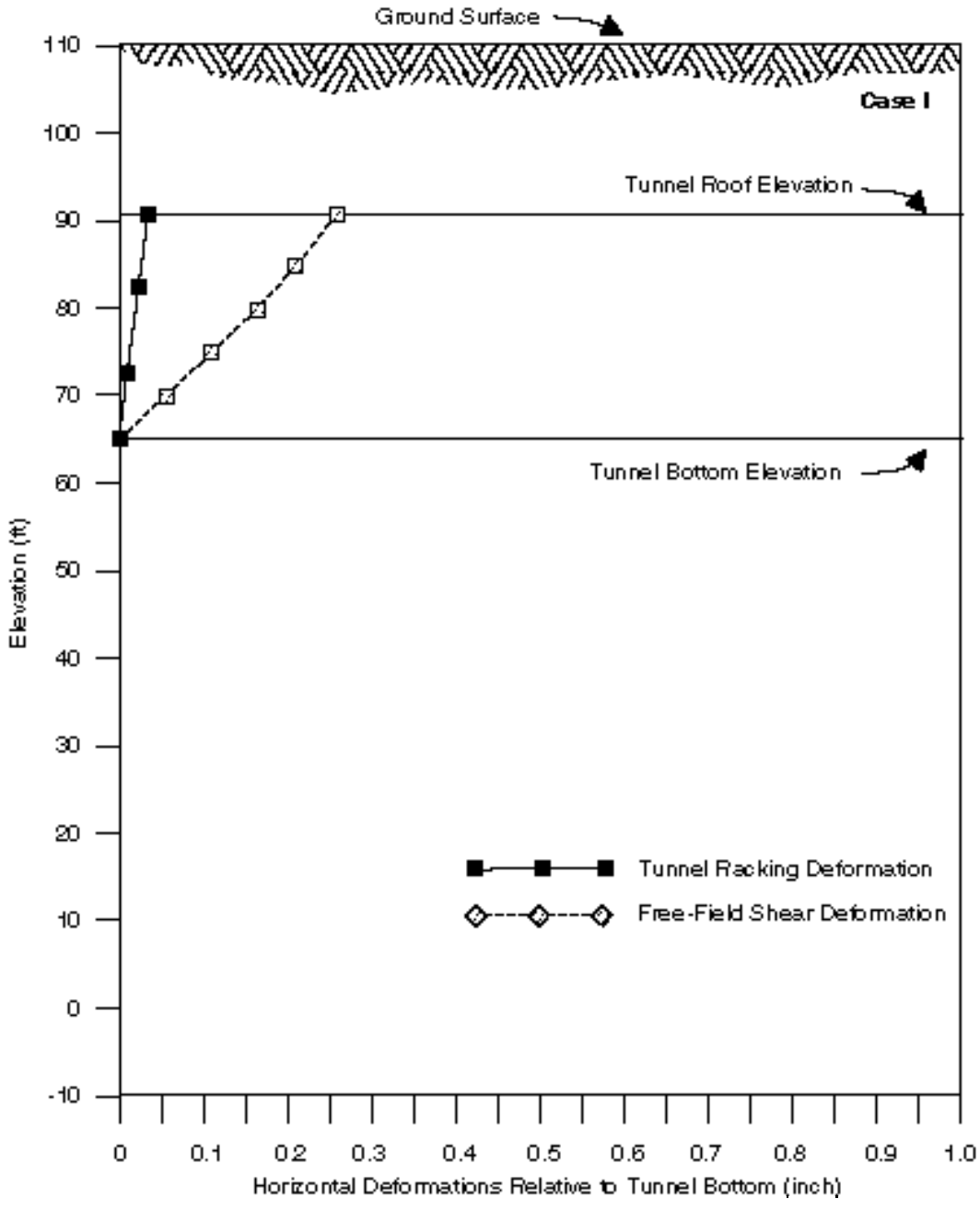

Figure 25.
Structure Deformations vs. Free-Field Deformations, Case I (from Soil/Structure Interaction Analysis, FLUSH)

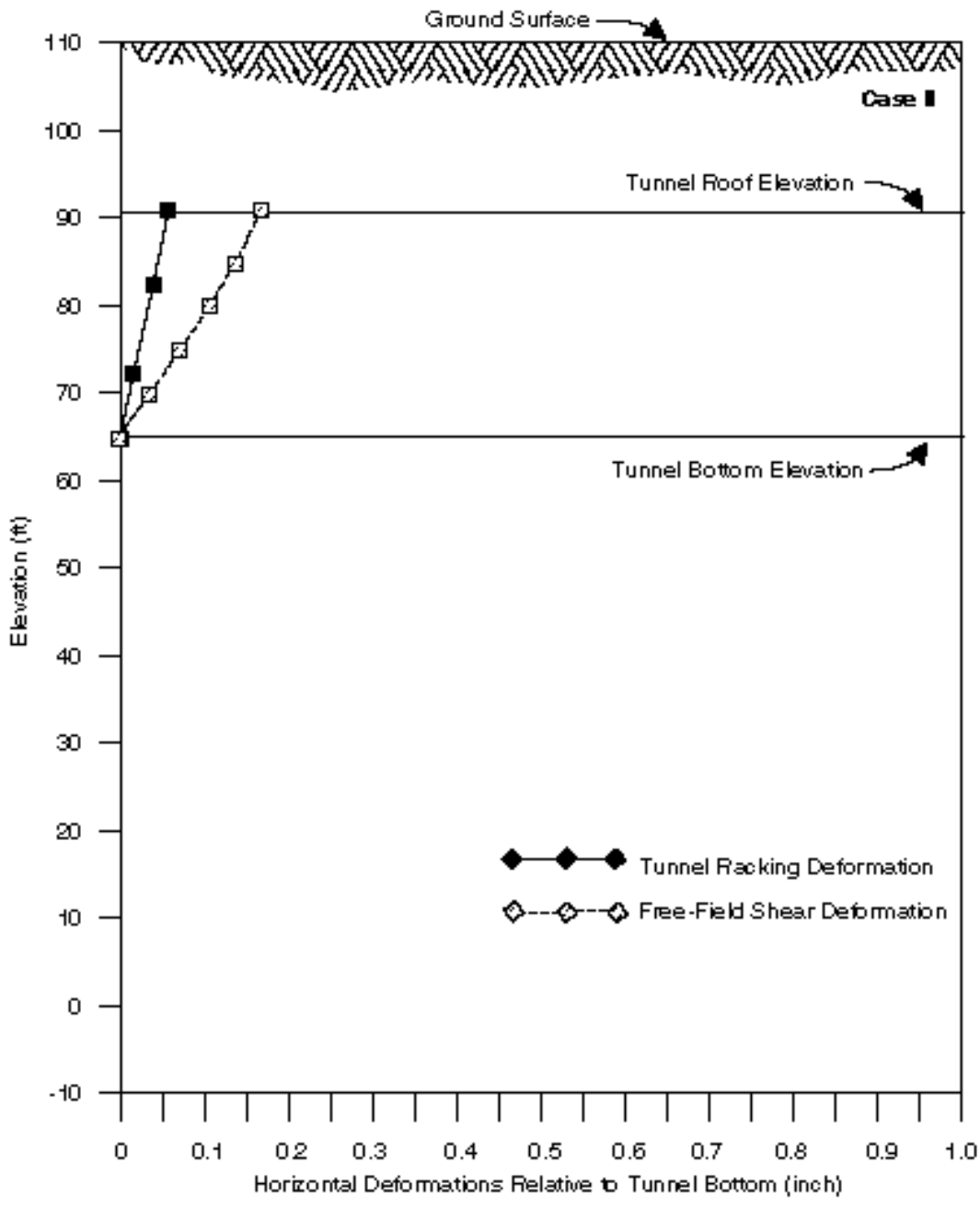

Figure 26.
Structure Deformations vs. Free-Field Deformations, Case II (from Soil/Structure Interaction Analysis, FLUSH)

Factors Contributing to the Soil-Structure Interaction Effect

Many factors contribute to the soil-structure interaction effect. In this study, the main factors that may potentially affect the dynamic racking response of rectangular tunnel structures are investigated. These factors are:

- Relative Stiffness between Soil and Structure. Based on results derived for circular tunnels (see Chapter 4), it is anticipated that the relative stiffness between soil and structure is the dominating factor governing the soil/structure interaction. Therefore, a series of analyses using ground profiles with varying properties and structures with varying racking stiffness was conducted for parametric study purpose. A special case where a tunnel structure is resting directly on stiff foundation materials (e.g., rock) was also investigated.

- Structure Geometry. Five different types of rectangular structure geometry were studied, including one-barrel, one-over-one two-barrel, and one-by-one twin-barrel tunnel structures.

- Input Earthquake Motions. Two distinctly different time-history accelerograms were used as input earthquake excitations.

- Tunnel Embedment Depth. Most cut-and-cover tunnels are built at shallow depths. To study the effect of the depth factor, analyses were performed with varying soil cover thickness.

A total number of 36 dynamic finite element analyses were carried out to account for the variables discussed above.

Method of Analysis

Computer Program. The dynamic finite element analyses were performed using the computer code FLUSH (1975), a two-dimensional, plane strain, finite element program in frequency domain. Besides calculating the internal forces in the structure members, FLUSH analysis:

- Produces data in the form of maximum relative movements between any two locations within the soil/structure system being analyzed

- Allows a simultaneous free-field response analysis and compares the relative movement between any two locations in the soil/structure system and in the free field

These features are ideal for this study because design of the tunnel structures is based on the "deformation method." A detailed description of this program can be found in Lysmer, et al. (1975).

Soil-Structure Model. Figure 27 shows the typical soil-structure finite element model used. The assumptions related to the model were as follows:

- The structure members are modeled by continuous flexural beam elements of linear elasticity. Structural frames with rigid connections are considered.
- A rigid base underlies the soil (medium) deposit.
- The soil overburden generally consists of a soft layer overlying a stiffer layer. Except for 7 cases where the top of the stiffer layer is raised to the invert elevation (to study the effect of stiff foundation), all cases assume the stiffer layer is below the base of the structure by a vertical distance of at least one time the full height of the structure. Materials of both layers are linearly elastic.
- No-slip condition along the soil/structure interface is assumed.
- Taking advantage of the anti-symmetric loading condition, only one half the entire soil/structure system is analyzed. Horizontal rollers are provided at planes of anti-symmetry.
- To minimize the boundary effect on the geometric dissipation of seismic energy, an energy absorbing boundary is placed at the far side of the mesh (i.e., transmitting boundary).

Earthquake Accelerograms. The two digitized ground motion accelerograms employed in the analyses (see Figures 28A and 28B) were generated synthetically from the two sets of design response spectra presented in Figure 29. The following should be noted:

- The "W. EQ" spectra and the corresponding accelerogram represent the rock outcrop ground motions that are typical in the western states of the United States. They were obtained from the San Francisco BART extension project.
- The "N.E. EQ" spectra and the corresponding accelerogram represent rock outcrop earthquake motions in the northeastern part of the country. They are taken from the Seismic Design Criteria of Underground Structures for the Boston Central Artery and Third Harbor Tunnel project (1990).
- Horizontal earthquake accelerograms are input at the rigid base to simulate the vertically propagating shear waves.

As Figures 28A and 28B show, earthquake motions of these two types have very different frequency characteristics, with the “N.E. EQ” motions displaying significantly increased high frequency components. The purpose of using two sets of design response spectra instead of one was to evaluate the effect of ground motion characteristics on soil/structure interaction.

Note that these design spectra were developed for motions expected at rock outcrop (ground surface). For motions to be used as rigid base input in the FLUSH analysis, a suitable modification of ground motion characteristics should be made. This was achieved in this study by using the one-dimensional site response analysis program SHAKE based on wave propagation theory. Details of this de-convolution process can be found in Schnabel, et al.(1972).

Flexibility Ratio for Rectangular Tunnels

Figure 30 shows the five different types of structure configurations that were analyzed. Note that although the configurations were limited to five types, the racking stiffness of each structure type was varied further (for parametric studies) by varying the properties of the structure members (e.g., EI and EA values). Similarly, the stiffness of the surrounding soil, as represented by shear modulus, was also varied in such a manner that the resulting relative stiffness between the soil medium and the structure covered a range that was of interest. This relative stiffness, as represented by the Flexibility Ratio, F, will be defined in detail in the following paragraphs.

The flexibility ratio for a rectangular tunnel, just as for a circular tunnel, is a measure of the flexural stiffness of the medium relative to that of the tunnel structure. Under a seismic simple shear condition, this relative stiffness may be translated into the shear stiffness of the medium relative to the lateral racking stiffness of the rectangular frame structure.

General Cases. Consider a rectangular soil element in a soil column under simple shear condition (see Figure 31). Assume the soil element has a width, L, and a height, H, that are equal to the corresponding dimensions of the rectangular tunnel. When subjected to the simple shear stress, τ, the shear strain (or angular distortion, γ) of the soil element is given by:

$$\gamma = \frac{\Delta}{H} = \frac{\tau}{G} \qquad \text{(Eq. 5-1)}$$

where G = shear modulus of soil
Δ = shear deflection over tunnel height, H

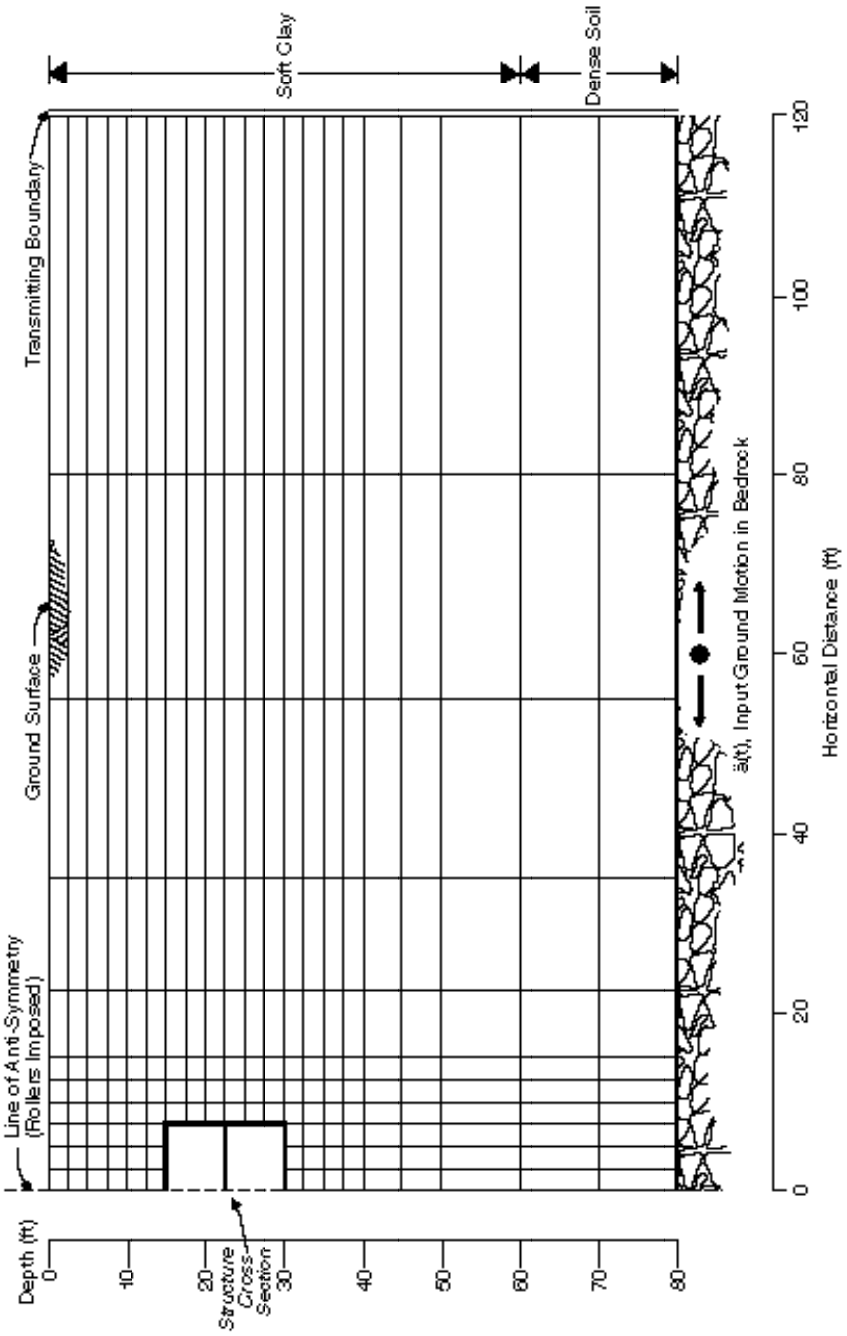

Figure 27.
Typical Finite Element Model
(from Structure Type 2)

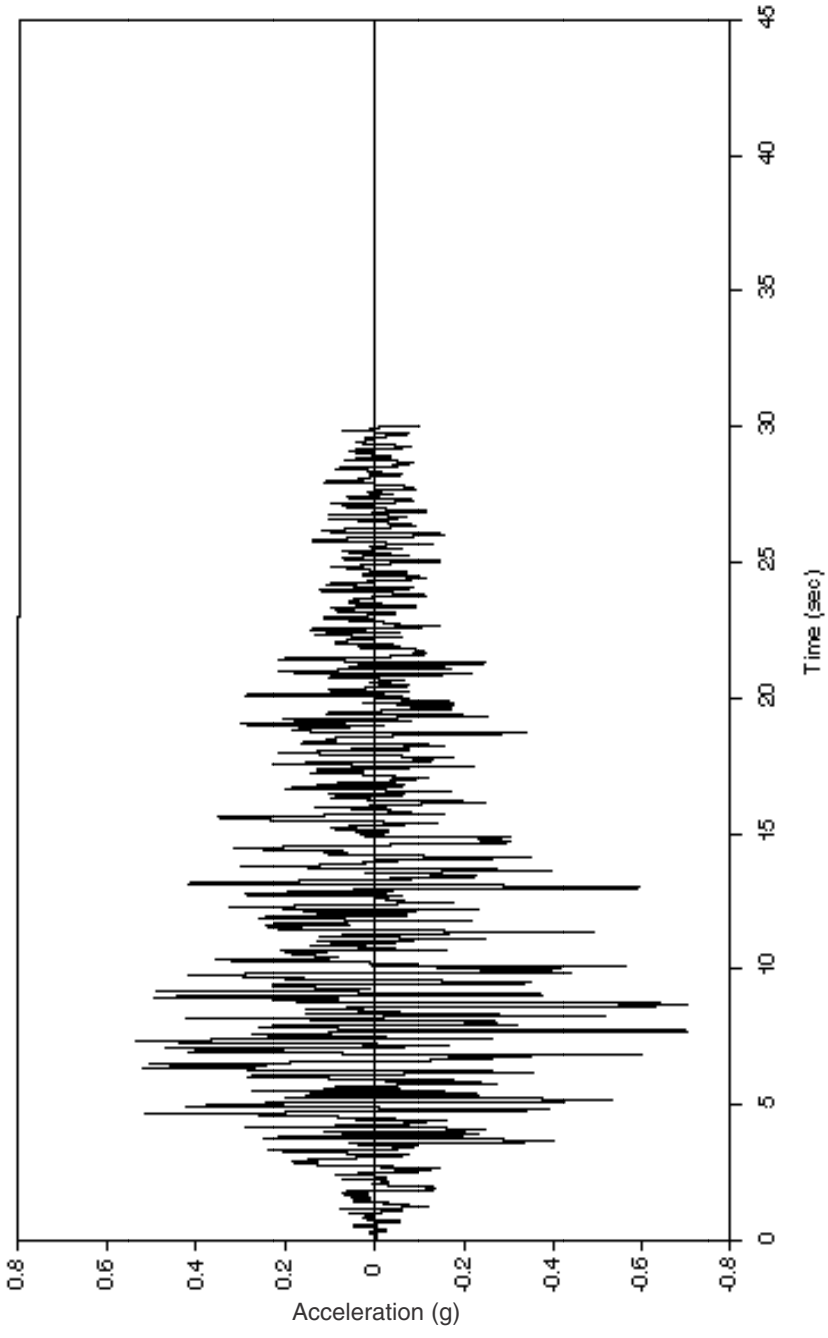

Figure 28A.
West Coast Earthquake Accelerogram (on Rock)

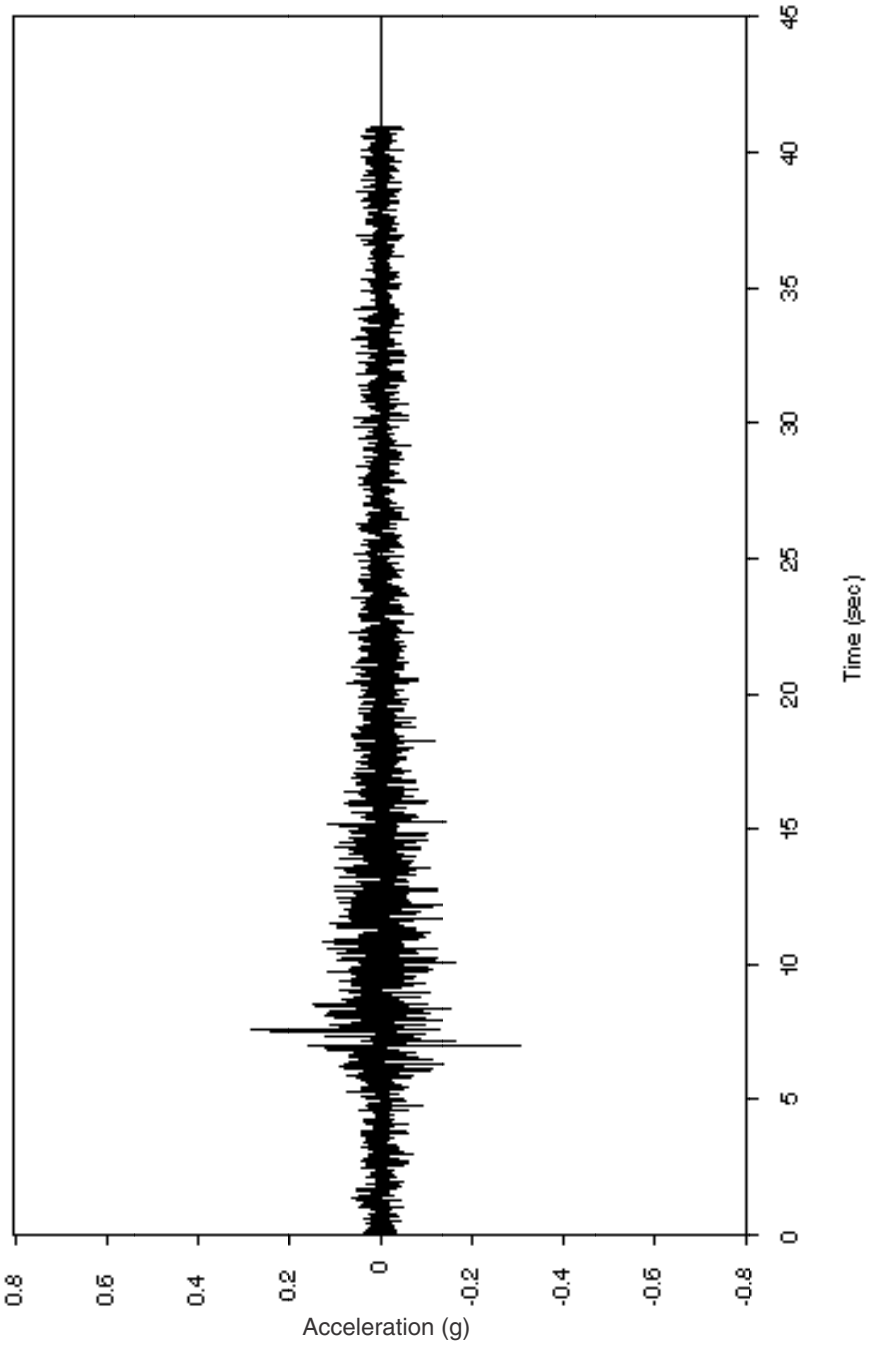

Figure 28B.
Northeast Earthquake Accelerogram
(on Rock)

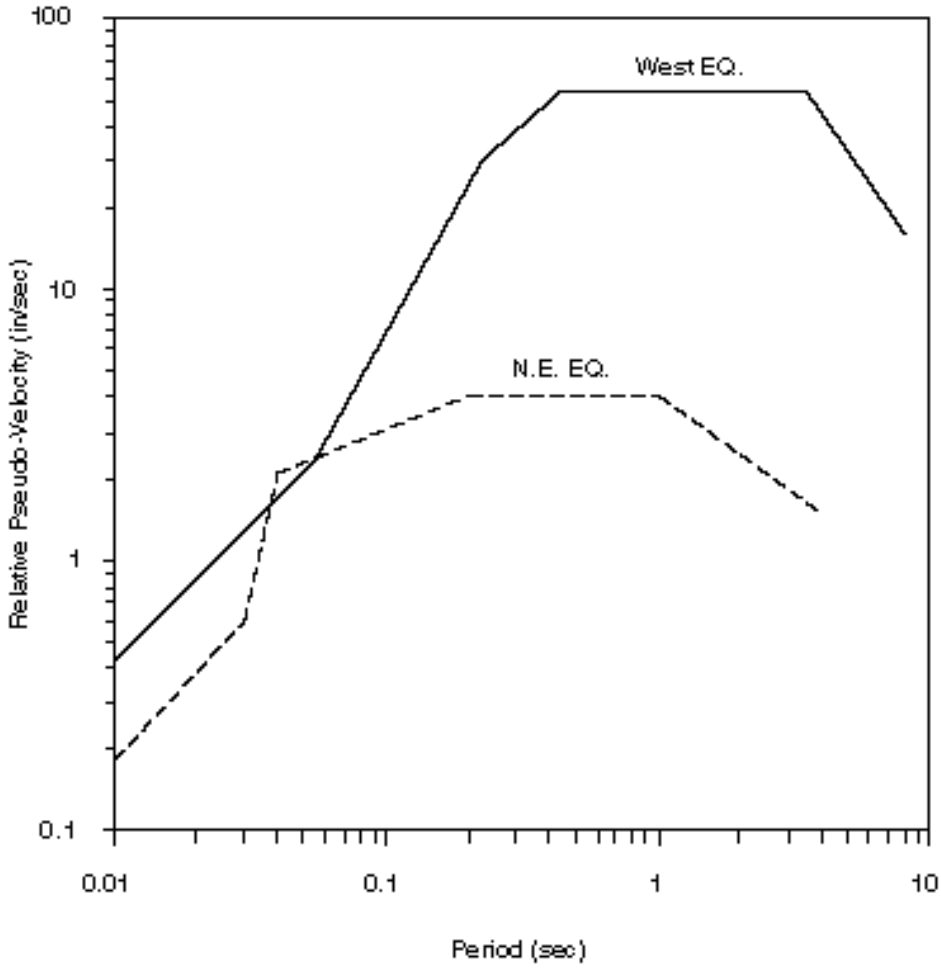

Figure 29.
Design Response Spectra
(West Coast Earthquake vs. Northeast Earthquake)

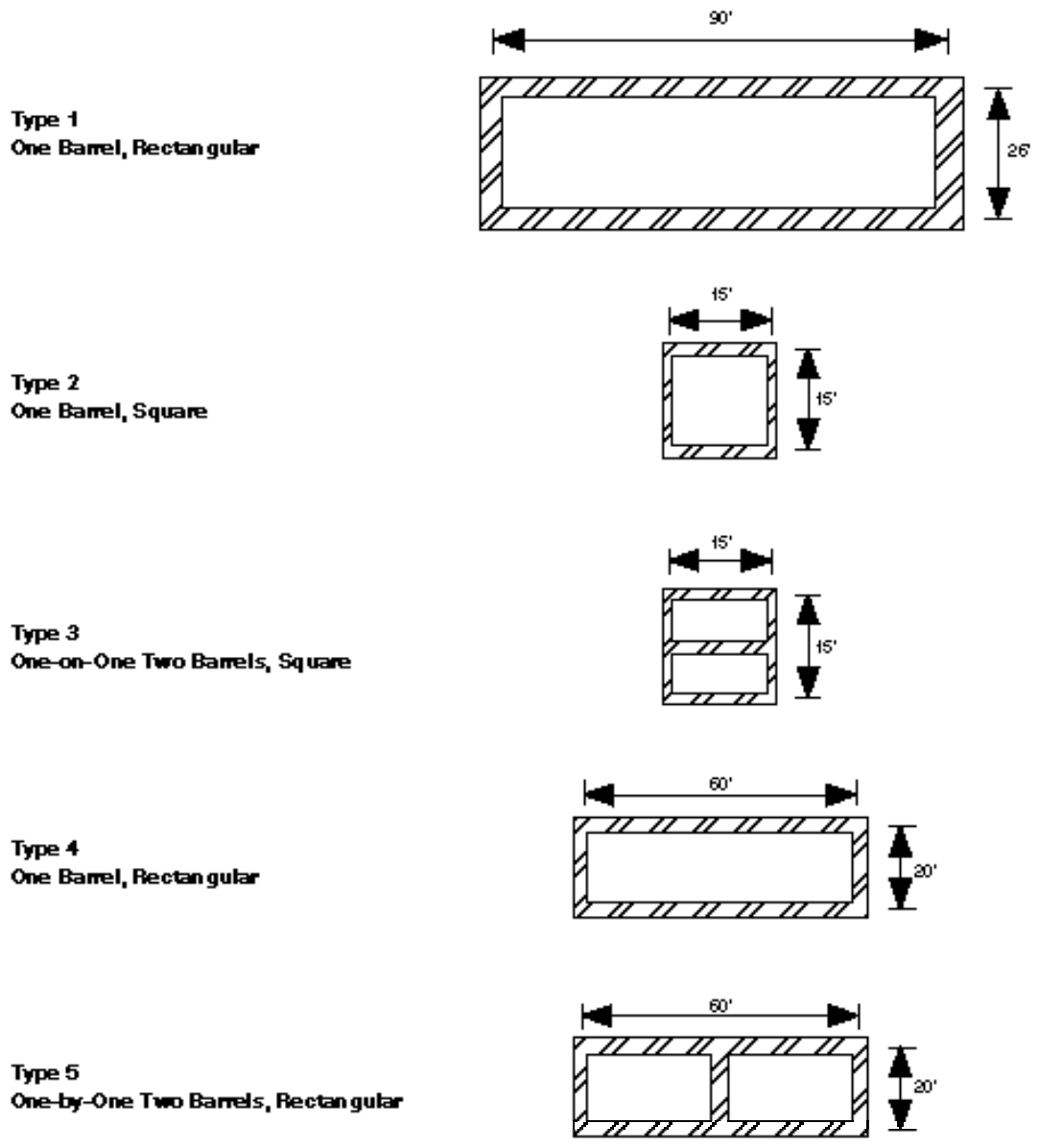

Figure 30.
Types of Structure Geometry Used in the Study

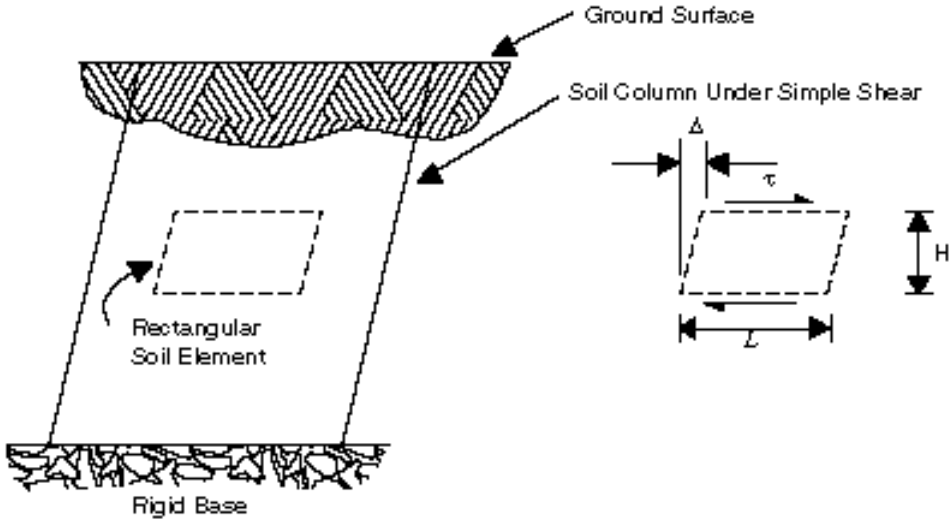

A. Flexural (Shear) Distortion of Free-Field Soil Medium

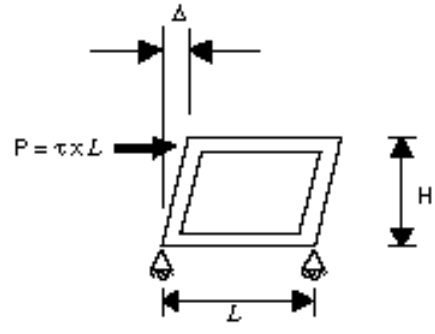

B. Flexural (Racking) Distortion of a Rectangular Frame

Figure 31.
Relative Stiffness Between Soil and a Rectangular Frame (from Soil/Structure Interaction Analysis, FLUSH)

The shear (or flexural) stiffness of the soil element is taken as the ratio of the shear stress to the corresponding angular distortion as expressed by:

$$\frac{\tau}{\gamma} = \frac{\tau}{\Delta / H} = G \qquad \text{(Eq. 5-2)}$$

When the rectangular frame structure is subjected to the same shear stress, τ, the stress can be converted into a concentrated force, P, by multiplying the shear stress by the width of the structure ($P = \tau L$). The resulting expression for the angular distortion of the structure becomes:

$$\gamma = \frac{\Delta}{H} = \frac{P}{HS_1} = \frac{\tau L}{HS_1} \qquad \text{(Eq. 5-3)}$$

where S_1 = the force required to cause an unit racking deflection of the structure

The flexural (or, racking) stiffness of the structure is, therefore, given by:

$$\frac{\tau}{\gamma} = \frac{\tau}{\Delta / H} = \frac{S_1 H}{L} \qquad \text{(Eq. 5-4)}$$

The flexibility ratio, F, is obtained by dividing Equation 5-2 by Equation 5-4. The resulting expression is:

$$F = \frac{GL}{S_1 H} \qquad \text{(Eq. 5-5)}$$

In the expression above, the unit racking stiffness, S_1, is simply the reciprocal of lateral racking deflection, $S_1 = 1/\Delta_1$ caused by a unit concentrated force (i.e., p=1 in Figure 32A). For a rectangular frame with arbitrary configuration, the flexibility ratio can be determined by performing a simple frame analysis using conventional frame analysis programs such as STAAD-III (see Figure 32A). Additional effort required to perform this type of analysis should be minimal as most of the computer input is readily established for static design.

Special Case 1. For some of the simple one-barrel frames (Figure 32B), it is possible to derive the flexibility ratio without resorting to computer analysis. The expression of F

developed for a one-barrel frame with equal moment of inertia, I_L, for roof and invert slabs and equal moment of inertia, I_H, for side walls is given by:

$$F = \frac{G}{24}\left(\frac{H^2 L}{EI_H} + \frac{HL^2}{EI_L}\right) \qquad \text{(Eq. 5-6)}$$

where E = plane strain elastic modulus of frame
G = shear modulus of soil
I_L, I_H = moments of inertia per unit width for slabs and walls, respectively

Note that the expressions by Equation 5-6 and Equation 5-7 that follow are valid only for homogeneous, continuous frames with rigid connections. Reinforced framed concrete structures are examples of this type of construction.

Special Case 2. The flexibility ratio derived for a one-barrel frame with roof slab moment of inertia, I_R, invert slab moment of inertia, I_I, and side wall moment of inertia, I_W , is expressed as:

$$F = \frac{G}{12}\left(\frac{HL^2}{EI_R}\right)\Upsilon \qquad \text{(Eq. 5-7)}$$

where

$$\Upsilon = \frac{(1+a_2)(a_1+3a_2)^2 + (a_1+a_2)(3a_2+1)^2}{(1+a_1+6a_2)^2}$$

$$a_1 = \left(\frac{I_R}{I_I}\right) \quad \text{and} \quad a_2 = \left(\frac{I_R}{I_W}\right)\frac{H}{L}$$

E = plane strain elastic modulus of frame
G = shear modulus of soil
I_R, I_I, I_W = moments of inertia per unit width

Implications of Flexibility Ratios. The derivation of the flexibility ratio presented in this section is consistent with that for the circular tunnels. The theoretical implications are:

- A flexibility ratio of 1.0 implies equal stiffness between the structure and the ground. Thus, the structure should theoretically distort the same magnitude as estimated for the ground in the free-field.

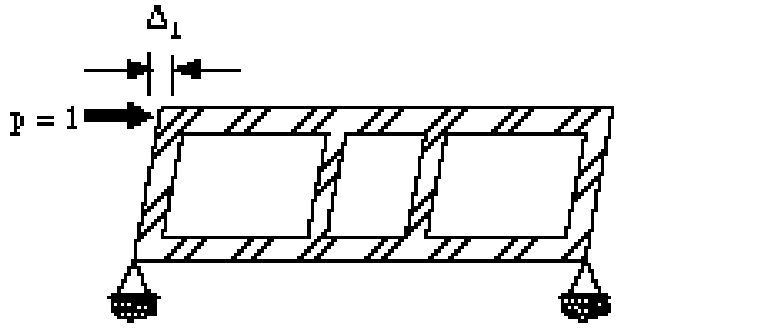

A. Structure Geometries Other than Single Barrel

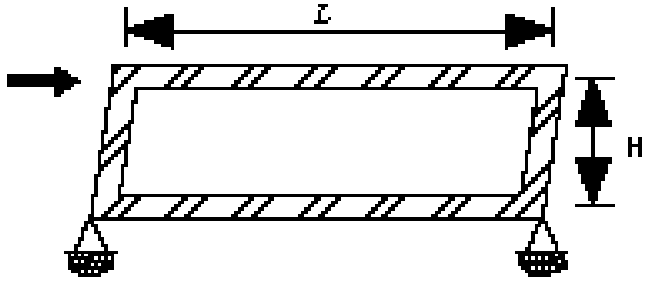

B. Single Barrel Structure

Figure 32.
Determination of Racking Stiffness
(from Soil/Structure Interaction Analysis, FLUSH)

- For flexibility ratios less than 1.0, the structure is considered stiff relative to the free-field and should distort less.

- An infinitely large flexibility ratio represents a perfectly flexible structure. At this state, the deformed shape of the structure should be identical to that of a perforated ground. The size and shape of the perforation, of course, should match the structure.

Results of Analysis

Analyses were first performed for 25 cases of soil/structure systems with varying combinations of soil profile, structure configuration, input ground motion type and flexibility ratio. Table 4 lists the details of the combinations for all 25 cases. Note that:

- The backfilled overburden thickness (soil cover) used in these analyses was limited to a range between 15 and 22.5 feet.

- The soil medium surrounding the embedded structure was assumed to be homogeneous, except for Cases 10, 14 and 15 where a soil profile with linearly increasing shear modulus with depth was assumed. An average soil shear modulus taken at the mid-height of the structure was used to represent the soil stiffness and to calculate the flexibility ratio for these three cases.

For each of the 25 cases, a free-field site response analysis (i.e., with no structure and no opening in ground) was first performed, followed subsequently by a corresponding soil/structure interaction analysis. The free-field site response analysis calculated the free-field shear deformation of the ground, $\gamma_{free\text{-}field}$, at the depth where the structure was to be placed, specifically, the differential shear distortion between the projected locations of the roof and the invert. The corresponding soil/structure interaction analysis then calculates the actual racking distortion, γ_s, of the structure.

Racking Coefficient. A racking coefficient, R, defined as the normalized structure racking distortion with respect to the free-field ground distortion is given as:

$$R = \frac{\gamma_s}{\gamma_{free\text{-}field}} = \frac{\left(\frac{\Delta_s}{H}\right)}{\left(\frac{\Delta_{free\text{-}field}}{H}\right)} = \frac{\Delta_s}{\Delta_{free\text{-}field}} \qquad \text{(Eq. 5-8)}$$

Case No.	Structure Type	Soil Cover (in feet)	Soil Shear Modulus, G (in ksf)	Flexibility Ratio, F	Input Ground Motion	Racking Coefficient, R
1	1	20.0	230.0	0.101	N.E.	0.133
2	1	20.0	615.0	0.271	N.E.	0.323
3	1	20.0	1500.0	0.661	N.E.	0.733
4	1	20.0	1500.0	1.313	N.E.	1.170
5	1	20.0	1500.0	1.000	N.E.	0.957
6	1	20.0	1500.0	3107.000	N.E.	2.420
7	2	15.0	230.0	0.463	N.E.	0.549
8	2	22.5	230.0	0.463	W.	0.565
9	2	15.0	230.0	0.463	W.	0.537
10	2	15.0	*232.3	0.458	W.	0.562
11	2	15.0	230.0	0.000	W.	0.000
12	2	15.0	1500.0	3.000	W.	1.550
13	2	15.0	1500.0	3100.000	W.	2.800
14	2	15.0	*232.3	0.187	W.	0.271
15	2	15.0	*232.3	0.766	W.	0.789
16	2	15.0	920.0	1.840	W.	1.260
17	2	15.0	500.0	1.000	W.	0.900
18	2	15.0	1500.0	6.600	W.	1.930
19	2	15.0	1500.0	1.000	W.	0.930
20	3	15.0	230.0	0.215	N.E.	0.287
21	3	15.0	230.0	0.215	W.	0.280
22	4	20.0	348.0	0.309	W.	0.445
23	4	20.0	348.0	0.309	N.E.	0.448
24	5	20.0	348.0	0.258	N.E.	0.351
25	5	20.0	348.0	0.142	N.E.	0.195

* Average Shear Moduli

Table 4.
Cases Analyzed by Dynamic Finite Element Modeling

where γ_s = angular distortion of the structure
Δ_s = lateral racking deformation of the structure
$\gamma_{free\text{-}field}$ = shear distortion/strain of the free-field
$\Delta_{free\text{-}field}$ = lateral shear deformation of the free-field

The racking coefficients, R, obtained from the analyses are presented in the last column of Table 4 for all 25 cases.

Note that the total structural deformation obtained from the finite element analyses contains a rigid body rotational movement, which causes no distortion to the cross-section of the structure. Therefore, this portion of the movement is excluded in the calculation of the structure racking deformation.

Effect of Relative Stiffness. As expected, results of the analyses indicate that the relative stiffness between the soil medium and the structure has the most significant influence on the structure response. This is demonstrated in Figure 33, where the structure racking coefficients, R, are plotted against the flexibility ratios, F.

- *When the flexibility ratio approaches zero*, representing a perfectly rigid structure, the structure does not rack regardless of the distortion of the ground in the free-field. The normalized structure distortion (i.e., R) increases with the increasing flexibility ratio. At F=1, the structure is considered to have the same stiffness as the ground and therefore is subjected to a racking distortion that is comparable in magnitude to the ground distortion in the free field (i.e., $R \approx 1$).

- *With a flexibility ratio greater than 1.0*, the structure becomes flexible relative to the ground and the racking distortion will be magnified in comparison to the shear distortion experienced by the ground in the free field. This latter phenomenon is not caused by the effect of dynamic amplification. Rather, it is primarily attributable to the fact that the ground surrounding the structure has a cavity in it (i.e., a perforated ground). A perforated ground, compared to the non-perforated ground in the free field, has a lower stiffness in resisting shear distortion and thus will distort more than will the non-perforated ground.

An interesting presentation of these data for rectangular structures is shown in Figures 34 and 35, where the closed-form solutions obtained for the normalized circular lining deflections (Figure 15 in Chapter 4) are superimposed. Note that the definitions of flexibility ratio, F, are different.

- *For circular tunnels*, Equation 4-6 is used.

- *For rectangular tunnels*, Equation 5-5, 5-6 or 5-7, as appropriate, is used.

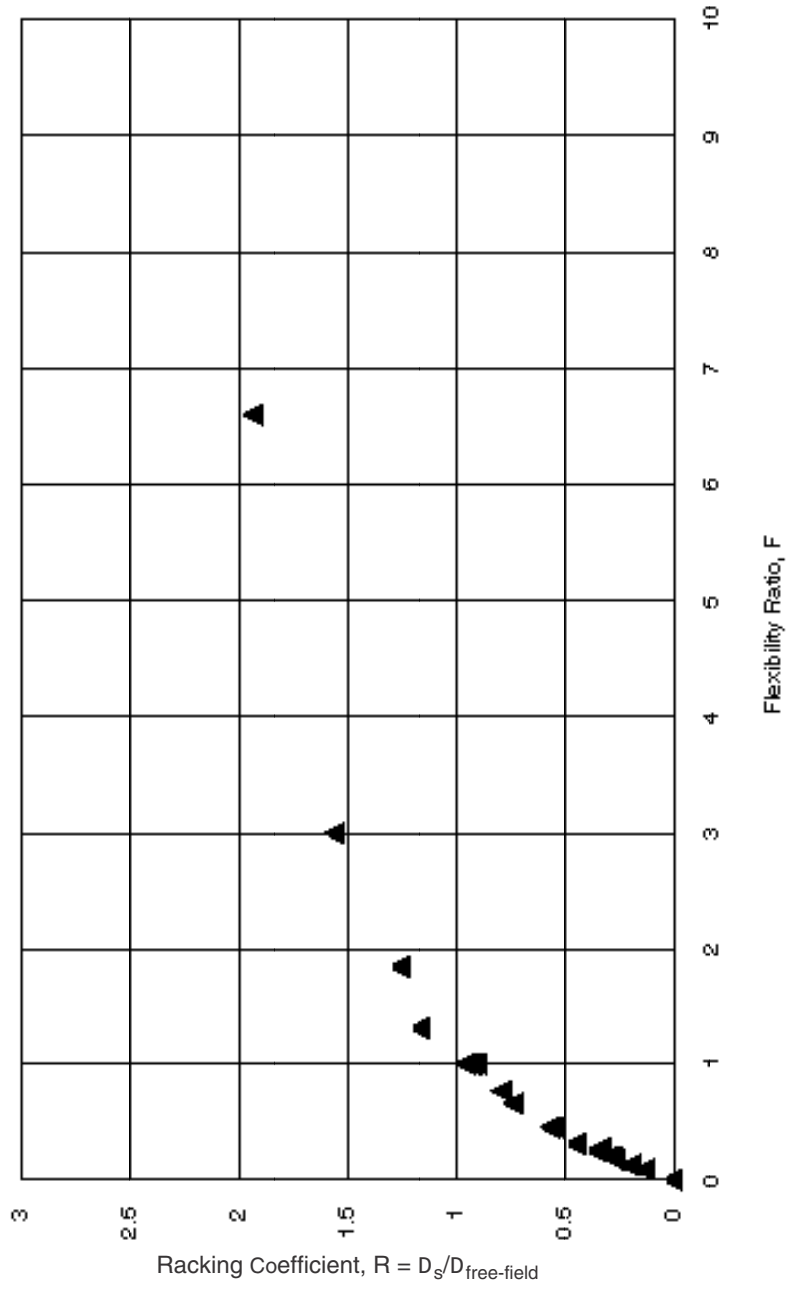

Figure 33.
Normalized Racking Deflections
(for Cases 1 through 25)

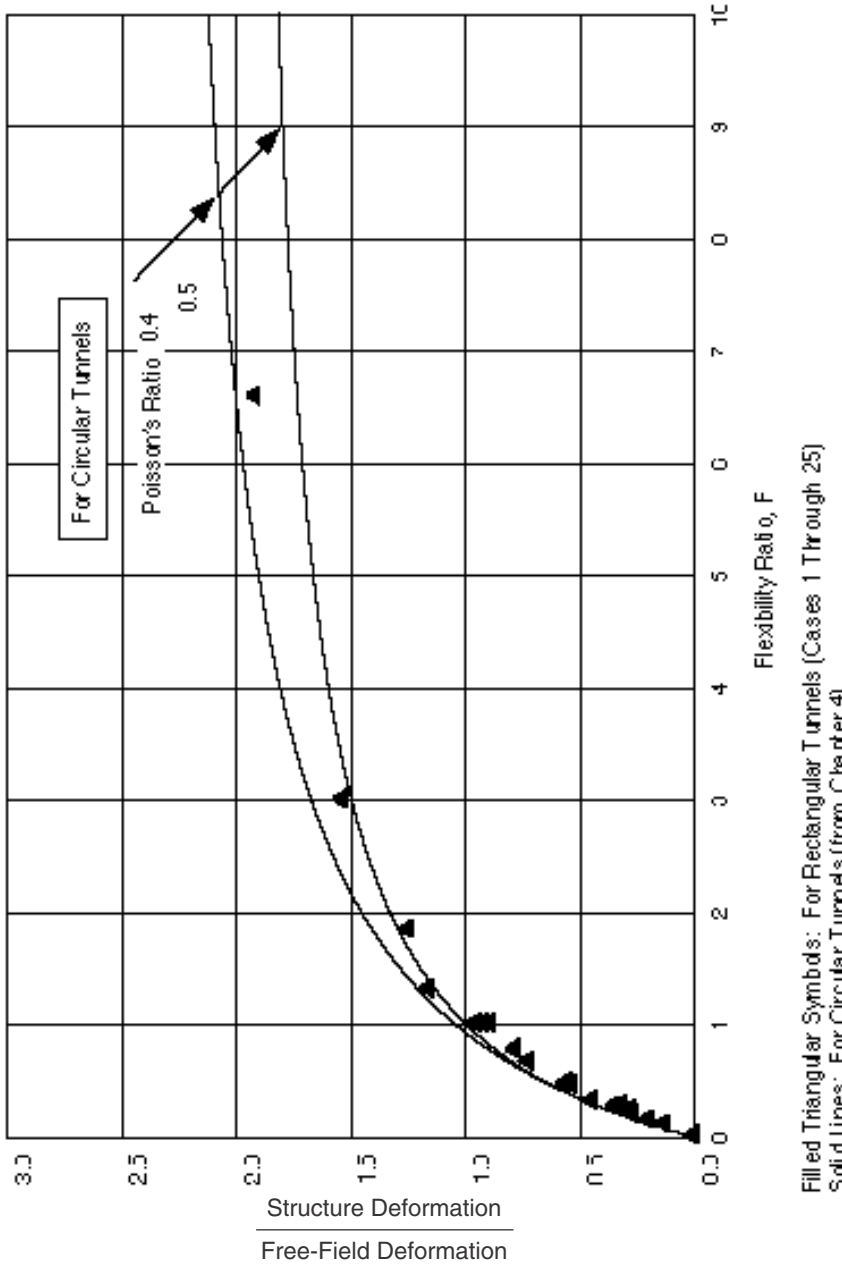

Figure 34.
Normalized Structure Deflections

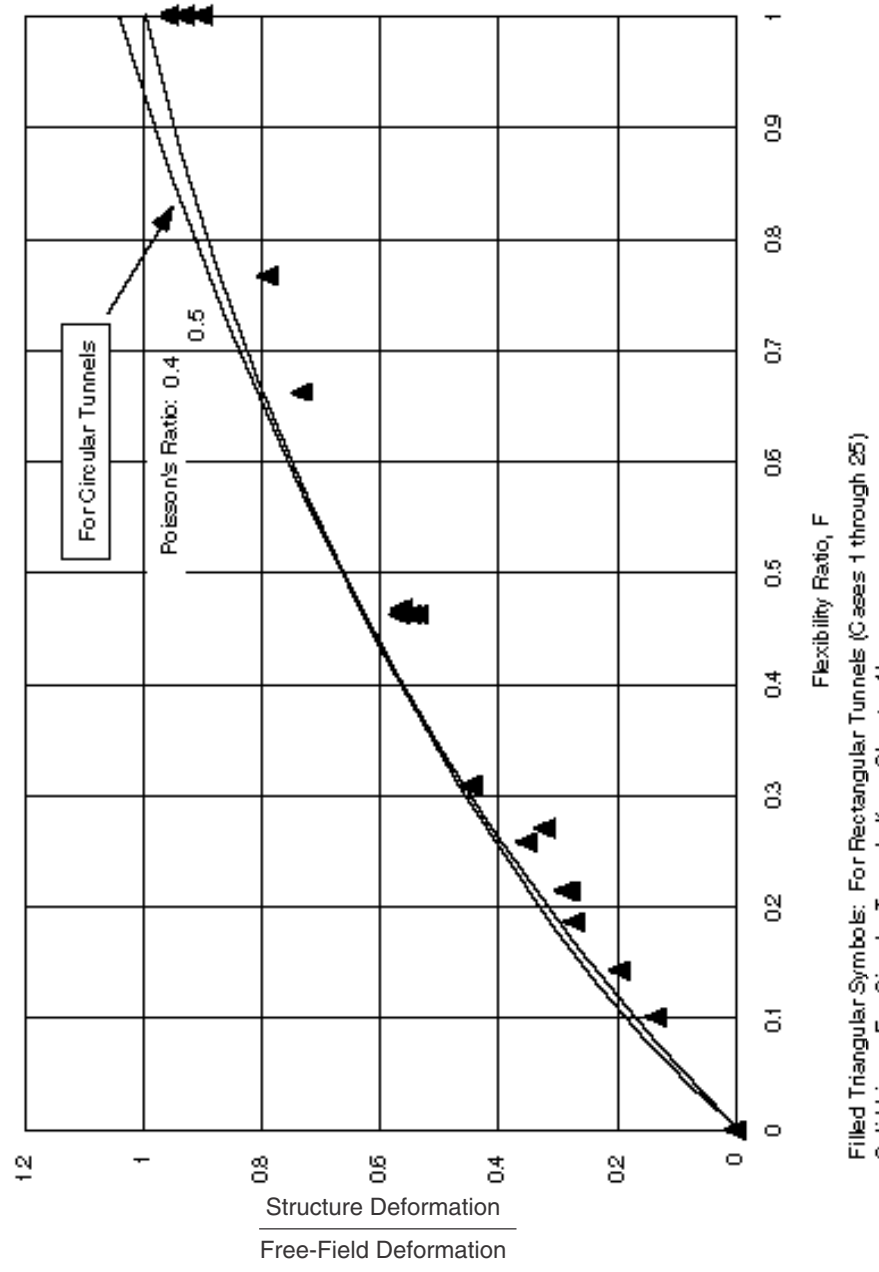

Figure 35.
Normalized Structure Deflections

Because the Poisson's Ratios of the soil used in all the rectangular cases are between 0.4 and 0.48, for comparison, the data for circular tunnels are shown only for Poisson's Ratios of 0.4 and 0.5. The figures show excellent consistency in distortion response between the two distinctly different types of tunnel configurations. Generally speaking, for a given flexibility ratio the normalized distortion of a rectangular tunnel tends to be less than that of a circular tunnel by approximately 10 percent.

The results presented above lead to the following conclusions:

- The conventional seismic design practice for rectangular tunnels (see Section 5.4) is too conservative for cases involving stiff structures in soft soils (specifically, when $F<1.0$).

- Designing a rectangular tunnel according to the free-field deformation method leads to an underestimation of the tunnel response when the flexibility ratio, F, becomes greater than 1.0. From a structural standpoint, fortunately, this may not be of major concern in most cases because $F>1.0$ may imply the medium (soil/rock) is very stiff, and therefore the free-field deformation can be expected to be small. $F>1.0$ may also imply the structure is very flexible so that the structure can, in general, absorb greater distortions without being distressed.

- From a practical standpoint, the data presented in Figures 34 and 35 can be used for design purposes. The normalized deflection curves derived for circular tunnels (Figures 15 and 16) may serve as upper-bound estimates for tunnels with rectangular shapes. Note that Figures 15 and 16 are based on Equation 4-13 in Chapter 4.

Effect of Structure Geometry. The effect of structure geometry was studied by using five different types of box structure configurations (Figure 30) in the 25 cases of analyses listed in Table 4. The results presented in Figure 33, however, clearly demonstrate that:

- The normalized racking deformations are relatively insensitive to the structure geometry.

- The soil/structure interaction is mainly a function of the relative stiffness between the soil and the structure, regardless of the variations of structure types.

Effect of Ground Motion Characteristics. The effect of ground motion characteristics on the normalized racking deformations is negligible. Consider the comparisons of the following pairs of analyses listed in Table 4:

- Cases 7 and 9 for structure type 2

- Cases 20 and 21 for structure type 3

- Cases 22 and 23 for structure type 4

In each pair of analyses, the parameters characterizing the soil/structure system are identical except for the input ground motions (i.e., the northeastern versus the western earthquakes). The seismically induced racking distortions of the structures are much greater under the assumed western design earthquake than the northeastern design earthquake. However, for the three comparisons made in this study, the normalized racking response with respect to the free-field, R, is very little affected by the type of ground motions used in the analysis. For instance, the calculated racking response coefficients show negligible difference (R=0.445 vs.R=0.448) between cases 22 and 23.

Effect of Embedment Depth. To determine the effect of shallow embedment depth on the normalized racking response, finite-element analyses were performed using Type 2 structure as an example. Here, the burial depths of the structure were varied. Table 5 presents the cases that were analyzed for this purpose. Note that flexibility ratio, F, remained the same for all cases. The normalized racking distortions from these analyses versus the dimensionless depth of burial, h/H, are presented in Figure 36.

Based on the results, it appears that:

- *The normalized racking distortion, R, is relatively independent of the depth of burial for h/H>1.5* (i.e., soil cover thickness equal to structure height). At this burial depth the structure can be considered to respond as a deeply buried structure.
- *For cases where the depth of embedment is less than 1.5, the normalized racking distortion decreases as the depth of burial decreases*, implying that design based on data presented in Figures 34 and 35 is on the safe side for tunnels with little to no soil cover.

Effect of Stiffer Foundation. The results of analyses discussed thus far are primarily for cases involving structures entirely surrounded by relatively homogeneous soil medium, including soil profiles with linearly increasing stiffness. A frequently encountered situation for cut-and-cover tunnels is when structures are built directly on the top of geological strata (e.g., rock) that are much stiffer than the overlying soft soils.

To investigate the effect of stiffer foundation, seven analyses were performed with varying foundation material properties as well as varying overlying soil properties. Table 6 lists the various parameters used in each of these analyses. The flexibility ratios shown in Table 6 are based on the overlying soil modulus only. The stiffness of the more competent foundation material is not taken into account. The calculated racking distortions, as normalized by the free-field shear deformations, are presented as a function of the flexibility ratio in Figure 37.

Case No.	Structure Type	Soil Cover (in feet)	Soil Shear Modulus, G (in ksf)	Flexibility Ratio, F	Racking Coefficient, R
8	2	22.5	230.0	0.463	0.565
9	2	15.0	230.0	0.463	0.537
33	2	7.5	230.0	0.463	0.488
34	2	0.0	230.0	0.463	0.438
35	2	31.5	230.0	0.463	0.589
36	2	40.0	230.0	0.463	0.564

Table 5.
Cases Analyzed to Study the Effect of Burial Depth

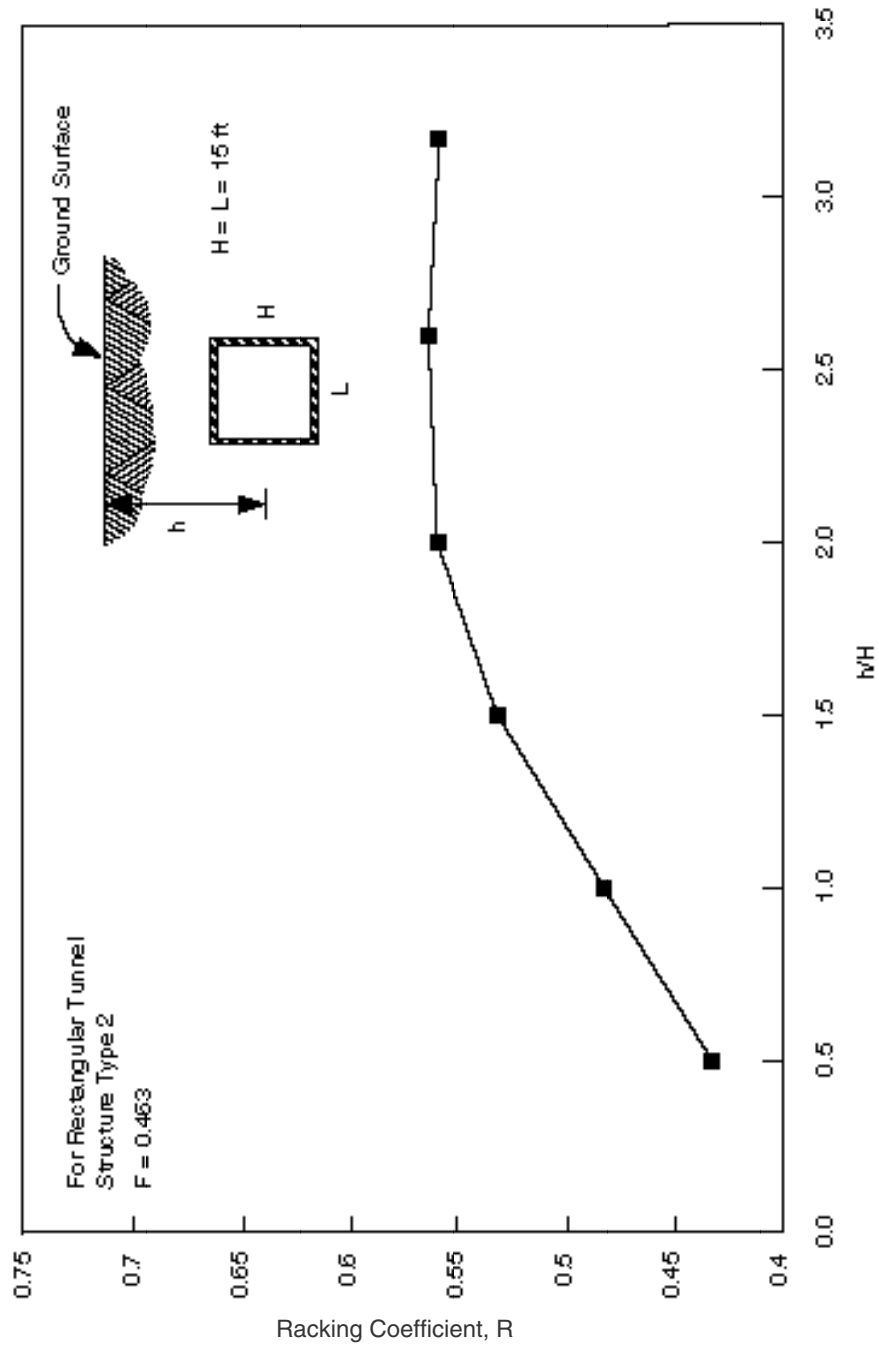

Figure 36.
Effect of Embedment Depth on Racking Response Coefficient, R

In comparison with the results shown in Figure 35 it may be concluded that in general, the presence of a stiffer foundation would result in some, but not significant, increase in the normalized racking distortion of the structure.

It should be noted, however, that:

- Although the magnitude of this increase is not significant when expressed in a "normalized" form, the actual impact to the structure may be significantly greater due to the increased free-field deformations.
- Normally, amplification of shear strains is expected near the zone of interface between two geological media with sharp contrast in stiffness.
- Care should be taken, therefore, in estimating the free-field shear deformations in a soft soil layer immediately overlying a stiff foundation (e.g., rock).

5.6 Recommended Procedure: Simplified Frame Analysis Models

In Section 5.5 the soil-structure interaction effect has been quantified through a series of dynamic finite-element analyses. Exercises of such complex analyses are not always necessary. For practical design purposes, a simplified procedure considering the interaction effect is desirable.

Therefore, a simple, rational and practical way of solving this problem is presented in this section, based on the data from soil-structure analyses presented in Section 5.5 . By following this procedure, an engineer equipped with a conventional frame analysis program (such as STAAD-III) can easily derive the solution for his design task.

Step-by-Step Design Procedure

The simplified frame analysis models shown in Figure 38 are proposed. A step-by-step description of this procedure is given below:

(a) Characterize the subsurface conditions at the site and determine the soil/rock properties based on results from field and laboratory investigations.

Case No.	Structure Type	Soil Cover in Feet	Soil Shear Modulus, G (in ksf)	Foundation Material Shear Modulus G, (in ksf)	Flexibility Ratio, F	Racking Coefficient, R
26	1	20.0	1500.0	80000.0	0.661	0.808
27	2	15.0	230.0	19320.0	0.463	0.695
28	2	15.0	500.0	19320.0	1.000	0.933
29	4	20.0	348.0	8700.0	0.309	1.465
30	4	20.0	348.0	8700.0	0.604	0.670
31	5	20.0	348.0	8700.0	0.258	0.415
32	5	20.0	348.0	8700.0	0.142	0.262

Note: In calculating the Flexibility Ratio, F, the ground stiffness was represented by soil shear modulus only. Stiffness of the foundation material was not considered.

Table 6.
Cases Analyzed to Study the Effect of Stiff Foundation

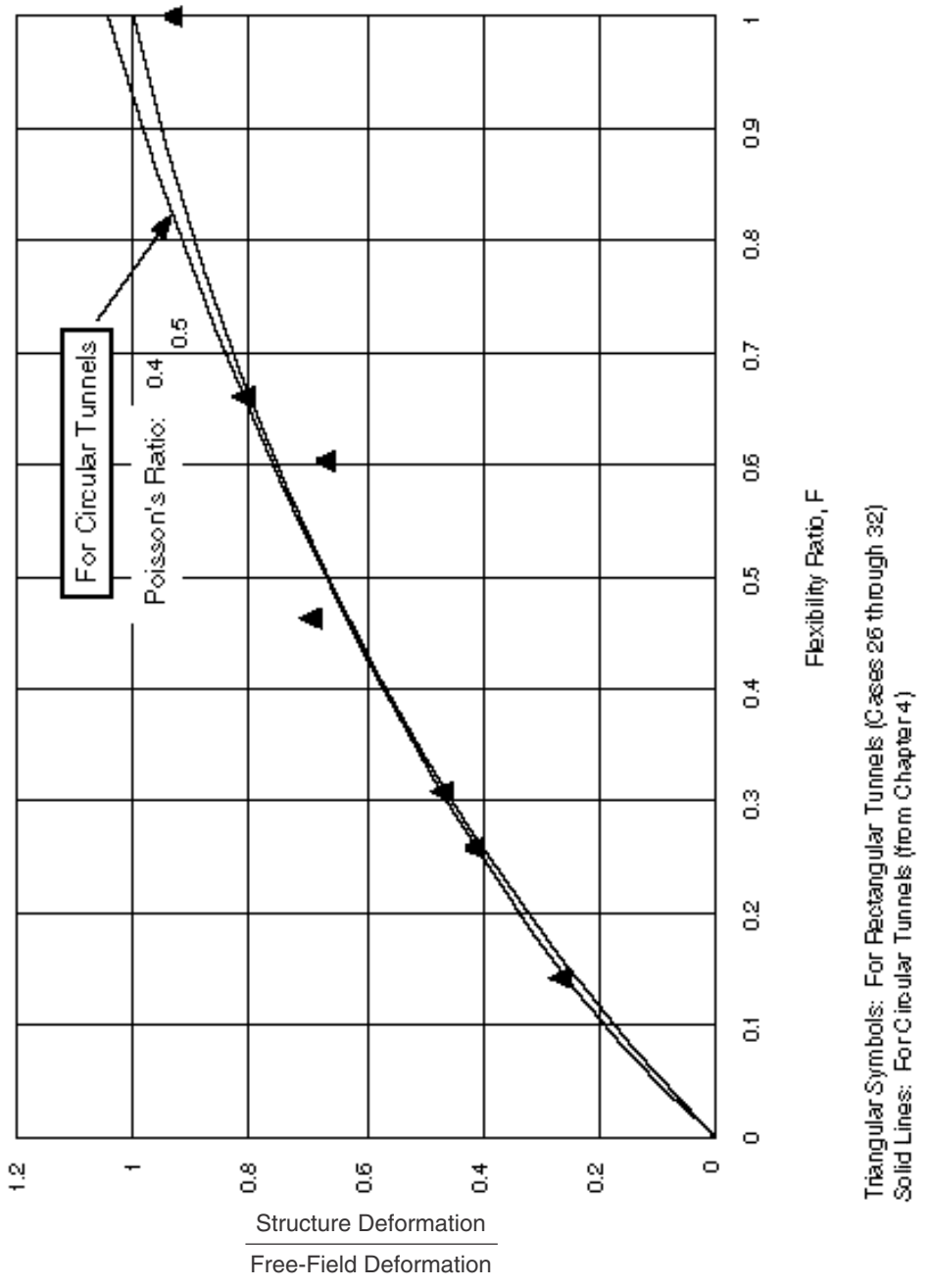

Figure 37.
Normalized Structure Deflections

(b) Derive earthquake design parameters. As a minimum, these parameters should include peak ground accelerations, velocities, displacements, design response spectra, and possibly the time-history accelerograms for both Maximum Design Earthquake (MDE) and Operating Design Earthquake (ODE). This work should be carried out by earthquake engineers with assistance from geotechnical engineers and seismologists.

(c) Conduct a preliminary design of the structure. Size and proportion members of the structure based on the loading criteria under static loading conditions. Normally, applicable design codes for buildings and bridges should be used, recognizing that the structure is surrounded by geological materials rather than a freestanding configuration.

(d) Based on the soil/rock properties from step (a) and the design earthquake parameters from step (b), estimate the free-field shear strains/deformations of the ground at the depth that is of interest. Generally:

- For a deep tunnel in a relatively homogeneous medium the simplified Newmark method, as presented by Equations 4-1 and 4-2, may be used.
- For shallow tunnels, for tunnels in stratified soil sites, or for tunnels sitting on stiff foundation medium, a simple one-dimensional site response analysis (e.g., SHAKE) is desirable.

The end results of this step provide the free-field deformation data, $\Delta_{\text{free-field}}$, as depicted in Figure 38.

(e) Determine the relative stiffness (i.e., the flexibility ratio, F) between the free-field medium and the structure using the properties established for the structure and the medium in steps (a) and (c) respectively. Equation 5-5, 5-6 or 5-7, as appropriate, may be used to calculate the flexibility ratio for a rectangular structure.

(f) Determine the racking coefficient, R, based on the flexibility ratio obtained from step (e), using the data presented in Figures 34 and 35, or Figure 37 as applicable.

(g) Calculate the actual racking deformation of the structure, Δ_s, using the values of $\Delta_{\text{free-field}}$ and R from steps (d) and (f) as follows:

$$\Delta_s = R \quad \Delta_{free-field} \qquad \text{(Eq. 5-9)}$$

(h) Impose the seismically induced racking deformation, Δ_s, upon the structure in simple frame analyses as depicted in Figures 38A and 38B.

- *Pseudo-Concentrated Force Model for Deep Tunnels* (Figure 38A). For deeply buried rectangular structures, the primary cause of the racking of the structure generally is attributable to the shear force developed at the exterior surface of the roof. Thus, a simplified pseudo-concentrated force model provides a reasonable means to simulate the racking effects on a deep rectangular tunnel. Using a conventional frame analysis program, this may be achieved by applying a horizontal support movement or an equivalent concentrated force at the roof level.

- *Pseudo-Triangular Pressure Distribution Model for Shallow Tunnels* (Figure 38B). For shallow rectangular tunnels, the shear force developed at the soil/roof interface will decrease as the soil cover (i.e., soil overburden) decreases. The predominant external force that causes the structure to rack may gradually shift from the shear force at the soil/roof interface to the normal earth pressures developed along the side walls. Therefore, for shallow tunnels, the racking deformation, D_s, should be imposed by applying some form of pressure distribution along the walls instead of a concentrated force. The triangular pressure distribution is recommended for this purpose.

Generally, for a given racking deformation, D_s, the triangular pressure distribution model (Figure 38B) provides a more critical evaluation of the moment capacity of rectangular structure at its bottom joints (e.g., at the invert-wall connections) than the concentrated force model (Figure 38A). On the other hand, the concentrated force model gives a more critical moment response at the roof-wall joints than the triangular pressure distribution model.

For design, it is prudent to employ both models in the frame analyses. The more critical results should govern to account for the complex distributions of shear stresses as well as normal earth pressures along the exterior surfaces of the structures.

(i) Add the racking-induced internal member forces, obtained from step (h), to the forces due to other loading components by using the loading combination criteria specified for the project. The loading criteria presented in Chapter 2 (Equations 2-1 through 2-4) are recommended for this purpose.

(j) If the results from step (i) show that the structure has adequate strength capacity according to the loading combination criteria (for both MDE and ODE), the design is considered satisfactory and no further provisions under the seismic conditions are required. Otherwise, proceed to step (k) below.

(k) If the flexural strength of the structure is found to be exceeded from the step (i) analysis, the structural members' rotational ductility should be checked. Special design provisions using practical detailing procedures should be implemented if inelastic

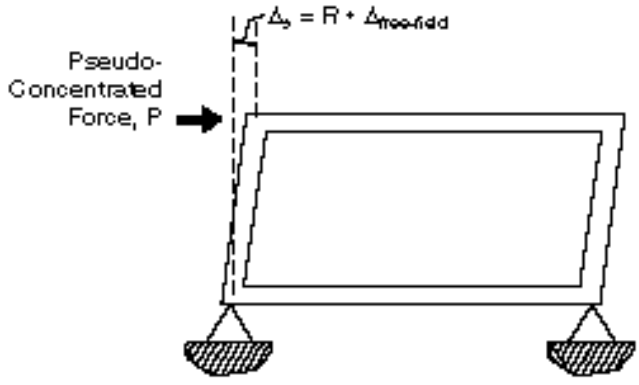

A. Pseudo-Concentrated Force for Deep Tunnels

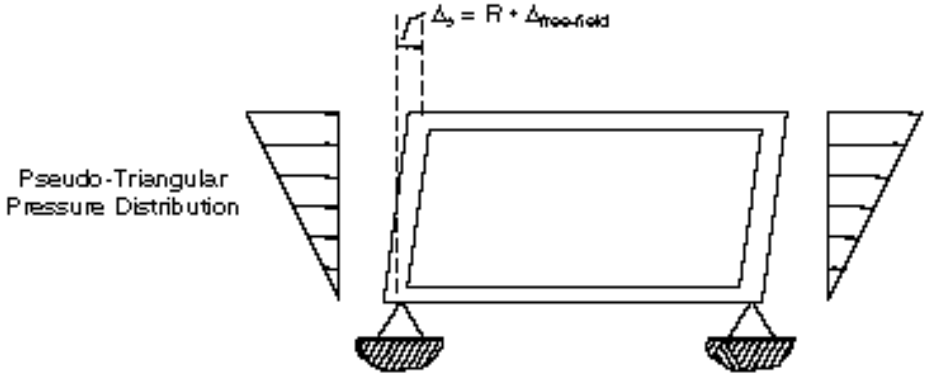

B. Pseudo-Triangular Pressure Distribution for Shallow Tunnels

Figure 38.
Simplified Frame Analysis Models

deformations result. Section 2.4 in Chapter 2 includes a detailed discussion on the strength and ductility requirements for both MDE and ODE loading combinations.

(l) The structure, including its members and the overall configurations, should be redesigned if:

- The strength and ductility requirements based on step (k) evaluation could not be met, and/or
- The resulting inelastic deformations from step (k) evaluation exceed the allowables (which depend on the performance goals of the structure)

In this case, repeat the procedure from step (e) to step (l), using the properties of the redesigned structure section until all criteria are met.

Verification of the Simplified Frame Model

The simplified frame models according to Equation 5-8 and Figures 38A and 38B were performed for Cases 1 through 5 (see Table 4) to verify the models' validity. The bending moments induced at the exterior joints of the one-barrel rectangular framed structure (simplified analyses) were compared to those calculated by the dynamic finite-element soil/structure interaction analyses (rigorous analyses). The comparisons are presented, using the concentrated force model, in Figures 39 and 40 for bending moments at the roof-wall connections and the invert-wall connections, respectively. Similar comparisons made for the triangular pressure distribution model are shown in Figures 41 and 42.

As Figures 39 and 40 show, the simplified frame analyses using the concentrated force model provide a reasonable approximation of the structure response under the complex effect of the soil/structure interaction. One of the cases, however, indicates an underestimation of the moment response at the bottom joints (i.e., invert-wall connections) by about fifteen percent (Figure 40). When the triangular-pressure distribution model is used, the simplified frame analyses yield satisfactory results in terms of bending moments at the bottom joints (Figure 42). The triangular-pressure distribution model, however, is not recommended for evaluation at the roof-wall connections, as it tends to underestimate the bending moment response at these upper joints (Figure 41).

Through the comparisons made above, and considering the uncertainty and the many variables involved in the seismological and geological aspects, the proposed simplified

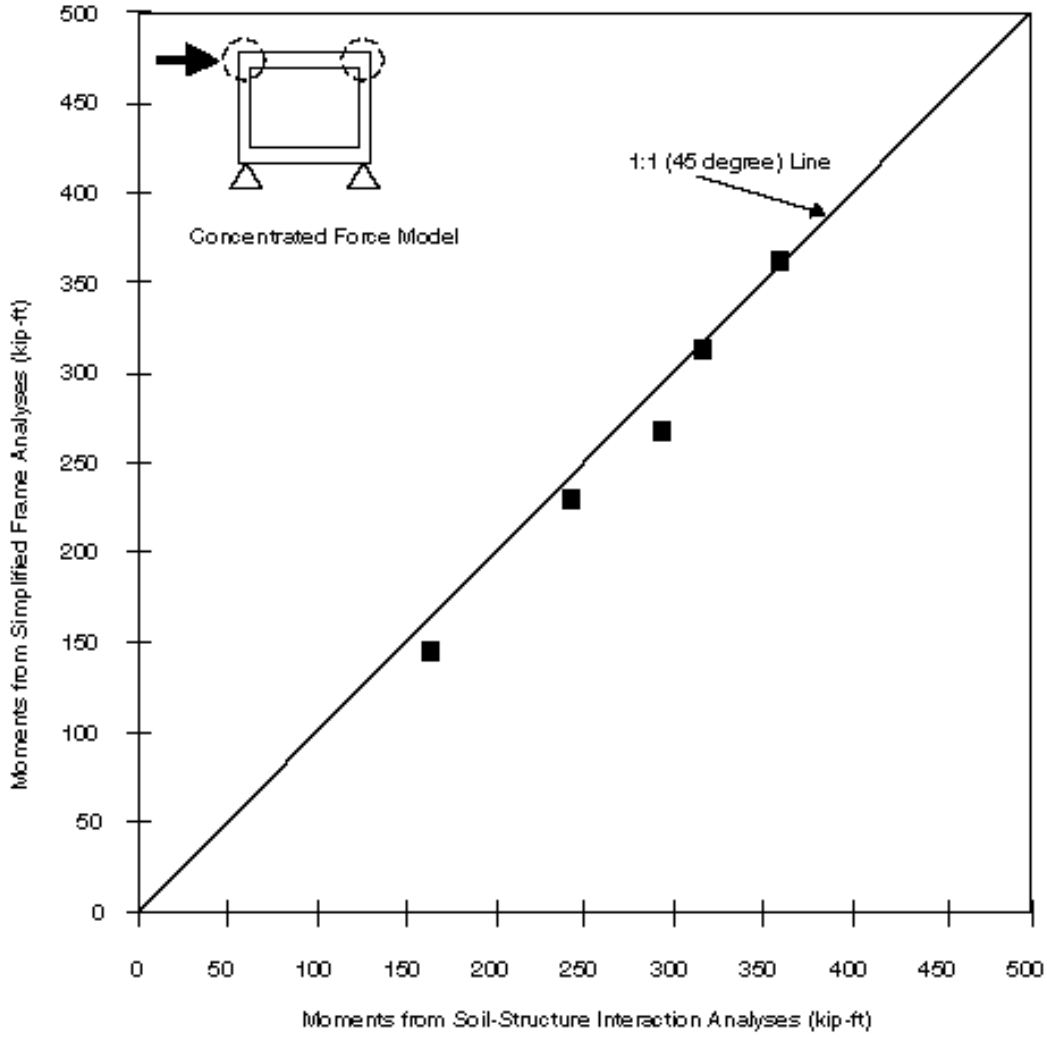

Figure 39.
Moments at Roof-Wall Connections
Concentrated Force Model
(for Cases 1 through 5)

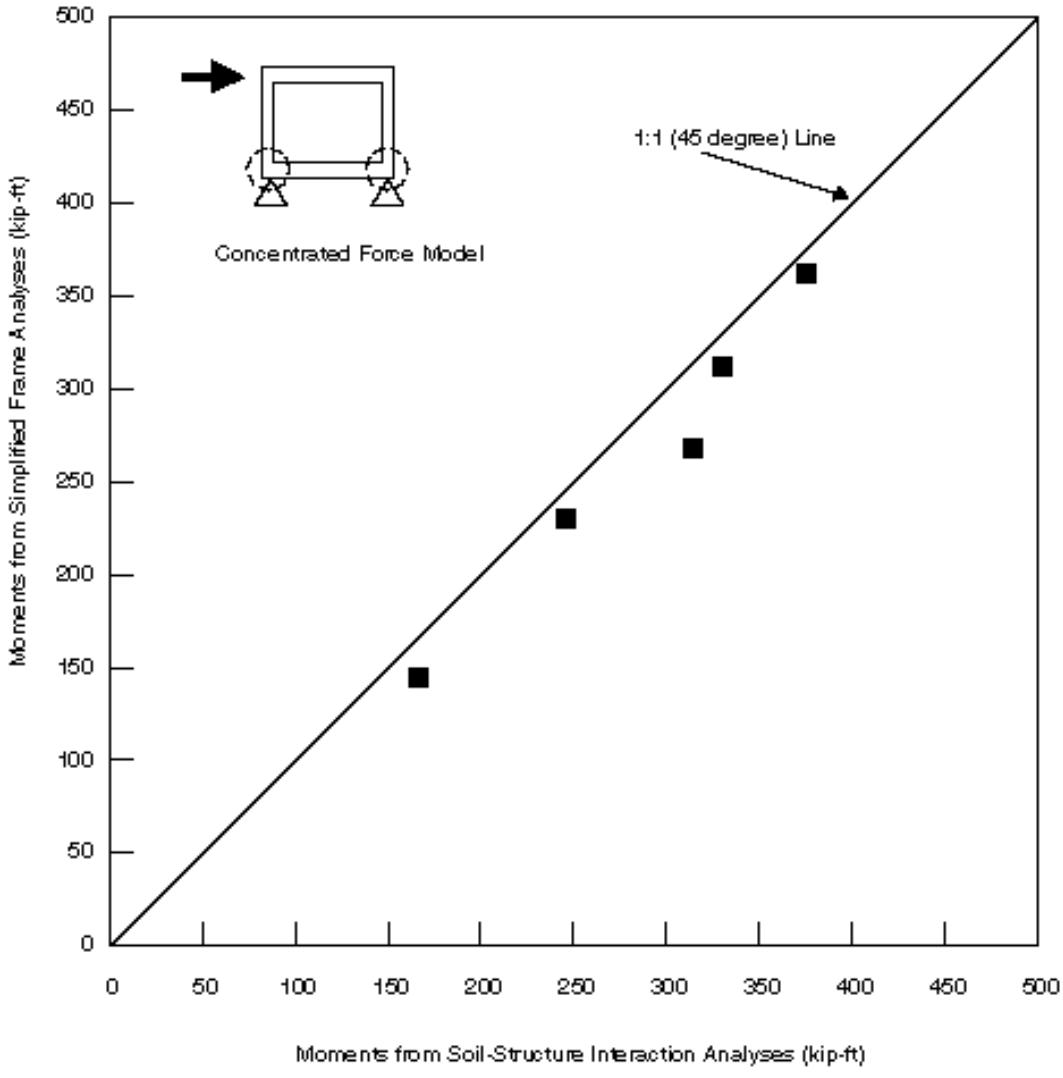

Figure 40.
Moments at Invert-Wall Connections
Concentrated Force Model
(for Cases 1 through 5)

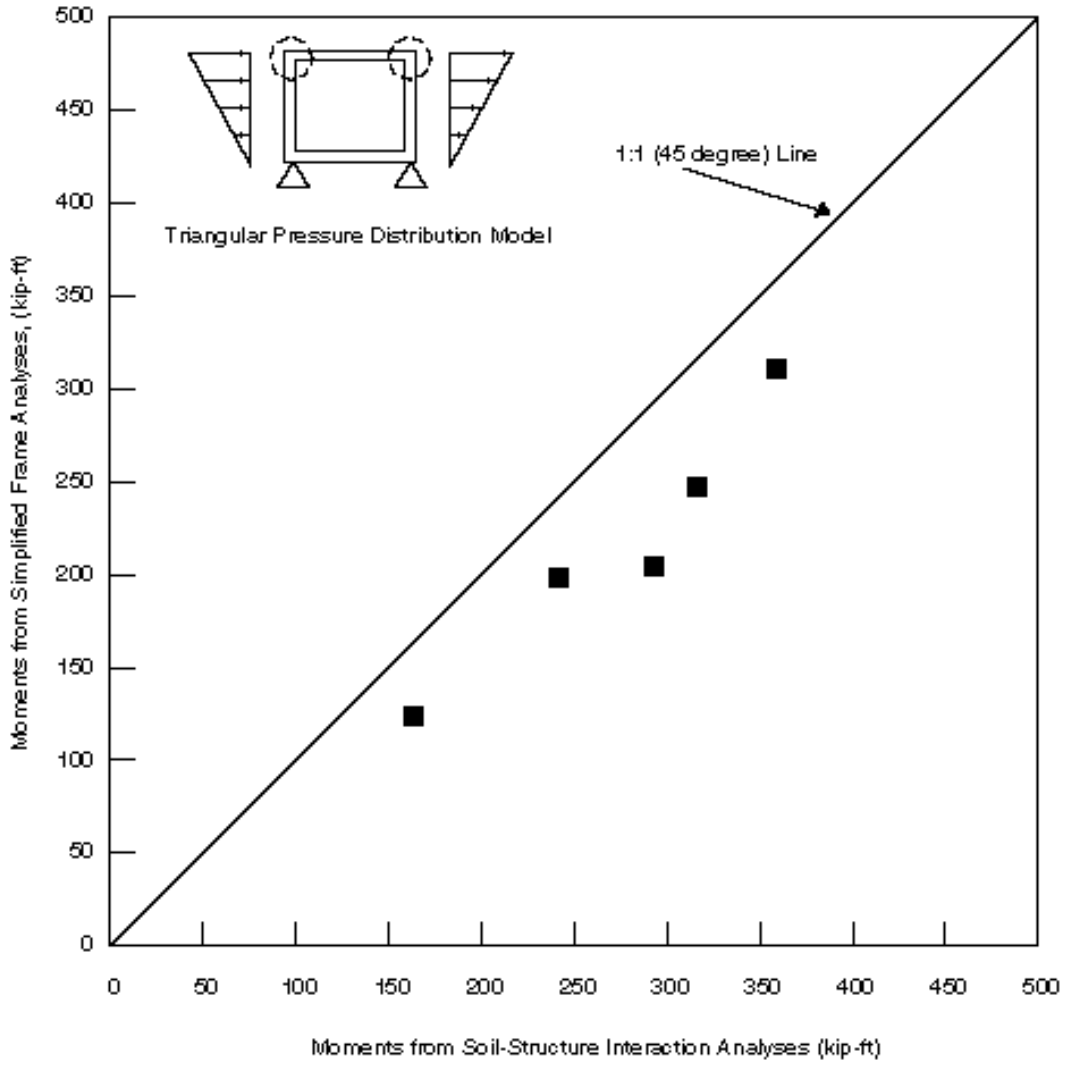

Figure 41.
Moments at Roof-Wall Connections
Triangular Pressure Distribution Model
(for Cases 1 through 5)

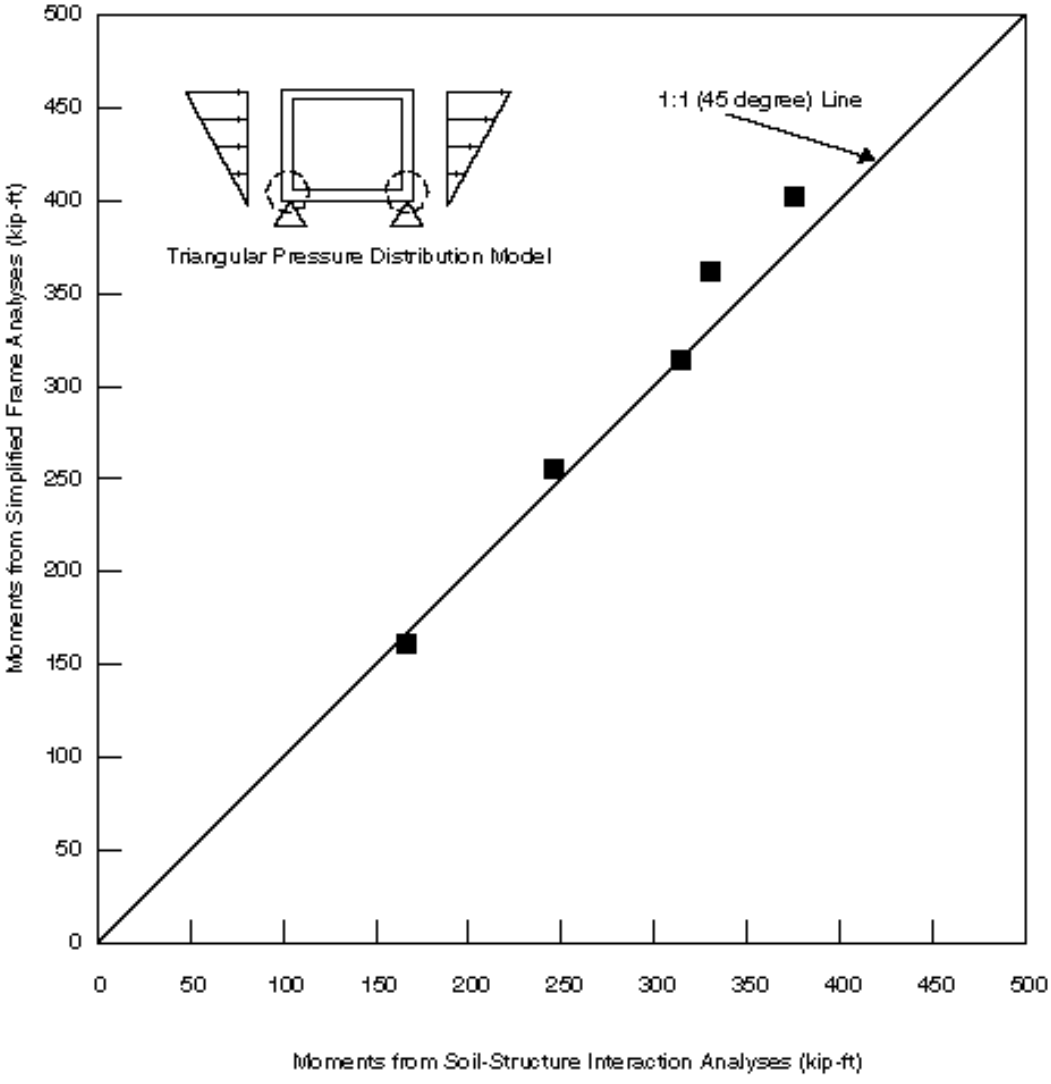

Figure 42.
Moments at Invert-Wall Connections
Triangular Pressure Distribution Model
(for Cases 1 through 5)

frame analysis models shown in Figures 38A and 38B are considered to comprise an adequate and reasonable design approach to the complex problem.

5.7 Summary of Racking Design Approaches

In summary, four different approaches to analyzing the seismic racking effect on two-dimensional cut-and-cover tunnel section have been presented in this chapter. Table 7 summarizes the advantages, disadvantages and applicability of these four approaches.

Based on the comparisons made in Table 7, it can be concluded that:

- The simplified frame analysis procedure recommended in Section 5.6 should be used in most cases.
- The complex soil-structure interaction finite-element analysis is warranted only when highly variable ground conditions exist at the site and other methods using conservative assumptions would yield results that are too conservative.
- The dynamic earth pressure methods (e.g., the Mononobe-Okabe method) should be used to double check the structure's capacity for tunnels with small soil burial and with soil-structure characteristics similar to those of aboveground retaining structures (e.g., a depressed U-section).

Approaches	Advantages	Disadvantages	Applicability
Dynamic Earth Pressure Methods (Section 5.3)	• Used with reasonable results in the past • Require minimal parameters and computation effort • Serve as additional safety measures against seismic loading	• Lack of rigorous theoretical basis • Resulting in excessive racking deformations for tunnels with significant burial • Use limited to certain types of ground properties	• For tunnels with minimal soil cover thickness
Free-Field Racking Deformation Method (Section 5.4)	• Conservative for tunnel structure stiffer than ground • Comparatively easy to formulate • Used with reasonable results in the past	• Non-conservative for tunnel structure more flexible than ground • Overly conservative for tunnel structures significantly stiffer than ground • Less precision with highly variable ground conditions	• For tunnel structures with equal stiffness to ground
Soil-Structure Interaction Finite-Element Analysis (Section 5.5)	• Best representation of soil-structure system • Best accuracy in determining structure response • Capable of solving problems with complicated tunnel geometry and ground conditions	• Requires complex and time consuming computer analysis • Uncertainty of design seismic input parameters may be several times of the uncertainty of the analysis	• All conditions
Simplified Frame Analysis Model (Section 5.6)	• Good approximation of soil-structure interaction • Comparatively easy to formulate • Reasonable accuracy in determining structure response	• Less precision with highly variable ground conditions	• All conditions except for complicated subsurface ground profiles

Table 7.
Seismic Racking Design Approaches

6.0 SUMMARY

6.0 SUMMARY

A rational and consistent methodology for seismic design of lined transportation tunnels was developed in this study which was mainly focused on the interaction between the ground and the buried structures during earthquakes. Although transportation tunnels were emphasized, the methods and results presented here would also be largely applicable to other underground facilities with similar characteristics, such as water tunnels, large diameter pipelines, culverts, and tunnels and shafts for nuclear waste repositories (Richardson, St. John and Schmidt, 1989).

Vulnerability of Tunnel Structures

Tunnel structures have fared more favorably than surface structures in past earthquakes. Some severe damages — including collapse — have been reported for tunnel structures, however, during earthquakes. Most of the heavier damages occurred when:

- The peak ground acceleration was greater than 0.5 g
- The earthquake magnitude was greater than 7.0
- The epicentral distance was within 25 km.
- The tunnel was embedded in weak soil
- The tunnel lining was lacking in moment resisting capacity
- The tunnel was embedded in or across an unstable ground including a ruptured fault plane

Seismic Design Philosophy

State-of-the-art design criteria are recommended for transportation tunnel design for the following two levels of seismic events:

- The small probability event, Maximum Design Earthquake (MDE), is aimed at public life safety.

- The more frequently occurring event, Operating Design Earthquake (ODE), is intended for continued operation of the facility, and thus economy.

Loading combination criteria consistent with current seismic design practice were established in this study for both the MDE and the ODE.

The proper seismic design of a tunnel structure should consider the structural requirements in terms of ductility, strength, and flexibility.

Running Line Tunnel Design

Seismic effects of ground shaking on a linear running tunnel can be represented by two types of deformations/strains: axial and curvature. The following procedures currently used in quantifying the axial and curvature deformations/strains were reviewed:

- The simplified free-field method (Table 1 equations), which allows simple and quick evaluations of structure response but suffers the following drawbacks:

  - By ignoring the stiffness of the structure, this method is not suitable for cases involving stiff structures embedded in soft soils.

  - The ground strains calculated by simplified free-field equations (see Table 1) are generally conservative and may be overly so for horizontally propagating waves travelling in soft soils.

- The tunnel-ground interaction procedure (beam on elastic foundation), which provides a more realistic evaluation of the tunnel response when used in conjunction with a properly developed ground displacement spectrum.

Through several design examples presented in Chapter 3, it was demonstrated that under normal conditions the axial and curvature strains of the ground were not critical to the design of horizontally or nearly horizontally aligned linear tunnels. Special attention should be given, however, to cases where high stress concentrations may develop as follows (Section 3.6):

- When tunnels traverse two distinctly divided geological media with sharp contrast in stiffness

- When abrupt changes in tunnel cross sectional stiffness are present, such as at the connections to other structures or at the junctions with other tunnels

- When the ground ruptures across the tunnel alignments (e.g., fault displacements)

- When tunnels are embedded in unstable ground (e.g., landslides and liquefiable sites)
- When tunnels are locally restrained from movements by any means (i.e., “hard spots”)

Ovaling Effect on Circular Tunnels

Ovaling of a circular tunnel lining is caused primarily by seismic waves propagating in planes perpendicular to the tunnel axis. Usually, the vertically propagating shear waves produce the most critical ovaling distortion of the lining.

The conventional simplified free-field shear deformation method was first reviewed, through the use of several design examples in this study, for its applicability and limitations. Then a more precise, equally simple method of analysis was developed to assist the design. This method takes into account the soil-lining interaction effects and provides closed form solutions (Equations 4-9 through 4-13) to the problems.

Numerical finite difference analyses using the computer program FLAC were performed to validate the proposed method of analysis. A series of design charts (Figures 10 through 16) was developed to facilitate the engineering design work.

Racking Effect on Rectangular Tunnels

The racking effect on a cut-and-cover rectangular tunnel is similar to the ovaling effect on a mined circular tunnel. The rectangular box structure will experience transverse sideways deformations when subjected to an incoming shear wave travelling perpendicularly to the tunnel axis. The most vulnerable part of the rectangular frame structure, therefore, is at its joints.

Conventional approaches to seismic design of cut-and-cover boxes consist of:

- The dynamic earth pressure method (Section 5.3), originally developed for aboveground retaining structures. Its applications in the seismic design of underground structures are limited only to those built with very small backfill cover, and those with structural characteristics that resemble the characteristics of aboveground retaining structures (e.g., a depressed U-section).
- The free-field shear deformation method (Section 5.4), which assumes that the racking deformation of a tunnel conforms to the shear deformation of the soil in the free-field.

Use of this method will lead to a conservative design when a stiff structure is embedded in a soft soil deposit. On the other hand, when the tunnel structure is flexible relative to the surrounding ground, this method may also underestimate the seismic racking response of the structure.

A proper design procedure that can avoid the drawbacks discussed above must consider the soil-structure interaction effect. For this purpose, an in-depth study using dynamic finite element soil-structure interaction analysis was conducted (Section 5.5). In this study, many factors that might potentially affect the tunnel response to seismic effects were examined. The results, however, indicate that the relative stiffness between the soil and the structure is the sole dominating factor that governs the soil-structure interaction effect.

Flexibility ratios, F , were defined to represent the relative stiffness between soils and rectangular structures. Using these flexibility ratios, a well defined relationship was established between the actual tunnel racking response and the free-field shear deformation of the ground (Figures 34 and 35). This relationship allows engineers to perform their design work by using conventional and simple frame analysis programs without resorting to complex and time consuming finite element soil-structure interaction analyses. A detailed step-by-step design procedure using these simplified frame analysis models was given in Section 5.6 of Chapter 5.

REFERENCES

REFERENCES

Agrawal, P. K., et al, "Seismic Response of Buried Pipes and Structural Components," ASCE Committee on Seismic Analysis on Nuclear Structures and Materials, 1983.

American Concrete Institute (*ACI*), *Building Code Requirements for Reinforced Concrete, ACI 318-89.*

American Association of State Highway and Transportation Officials (AASHTO), *Guide Specifications for Seismic Design of Highway Bridges*, 1983 and 1991 Interim Report.

Applied Technology Council (ATC), *Tentative Provisions for the Development of Seismic Regulations for Buildings, ATC 3-06,* 1978.

Bolt, B. A., *Earthquakes: A Primer*, W. H. Freeman and Company, 1978.

Buckle, I. G., Mayes, R. L., and Button, M. R., *Seismic Design and Retrofit Manual for Highway Bridges*, Prepared for Federal Highway Administration, FHWA-IP-87-6, 1987.

Burns, J. Q., and Richard, R. M., "Attenuation of Stresses for Buried Cylinders," *Proceedings of the Symposium on Soil-Structure Interaction*, Tempe, Univ. of Arizona, 1964.

Central Artery/ Third Harbor Tunnel (CA/THT), "Seismic Design Criteria for Underground Structures," 1990.

Converse Consultants, "Seismological Investigation and Design Criteria," prepared for Southern California Rapid Transit District, 1983.

Dobry, R., Oweis, I., and Urzua, A., "Simplified Procedures for Estimating the Fundamental Period of a Soil Profile," *Bulletin of the Seismological Society of America*, Vol. 66, No. 4, 1976.

Douglas, W. S., and Warshaw, R., "Design of Seismic Joint for San Francisco Bay Tunnel," *Journal of the Structural Division, ASCE*, Vol. 97, No. ST4, April 1971.

Dowding, C. H., and Rozen, A., "Damage to Rock Tunnels from Earthquake Shaking," *Journal of the Geotechnical Engineering Division, ASCE*, Vol. 104, No. GT2, February 1978.

Duddeck, H. and Erdman, J., "Structural Design Models for Tunnels," *Tunneling '82*, Institute of Mining and Metallurgy, London, 1982.

East Bay Municipal Utility District, "Seismic Design Requirements," Oakland, California, 1973.

Einstein, H. H., and Schwartz, C. W., "Simplified Analysis for Tunnel Supports," *Journal of the Geotechnical Division, ASCE*, Vol. 105, No. GT4, April 1979.

Fast Lagrangian Analysis of Continua (FLAC), Itasca Consulting Group, Inc., 1989.

Grant, W. P., and Brown Jr., F. R., "Dynamic Behavior of Soils from Field and Laboratory Tests," *Proceedings, International Conference on Recent Advances in Geotechnical Earthquake Engineering and Soil Dynamics*, Rolla, Univ. of Missouri, 1981.

Hadjian, A. H., and Hadley, D. M., "Studies of Apprarent Seismic Wave Velocity," *Proceedings of International Conference on Recent Advances in Geotechnical Earthquake Engineering and Soil Dynamics*, St. Louis, 1981.

Hetenyi, M., *Beams on Elastic Foundation*, The University of Michigan Press, Ann Arbor, Michigan, 1976.

Hoeg, K., "Stresses Against Underground Structural Cylinders," *Journal of the Soil Mechanics and Foundation Division, ASCE*, Vol. 94, SM4, April 1968.

Hwang, R. N., and Lysmer, J., "Response of Buried Structures to Traveling Waves," *Journal of the Geotechnical Engineering Division, ASCE*, Vol. 107, No. GT2, February, 1981.

Japanese Society of Civil Engineers (JSCE), "Specifications for Earthquake Resistant Design of Submerged Tunnels," 1975.

Kuribayshi, E., Iwasaki, T., and Kawashima, K., "Dynamic Behaviour of A Subsurface Tubular Structure," *Proceedings of 5th Symposium on Earthquake Engineering*, India, 1974.

Kuesel, T. R., "Earthquake Design Criteria for Subways," *Journal of the Structural Divisions, ASCE*, Vol. 95, No. ST6, June 1969.

LINOS — A Non-Linear Finite Element Program for Geomechanics and Geotechnical Engineering, User's Manual, by J. P. Bardet, Univ. of Southern California, Los Angeles, California, 1991.

Lyons, A. C., “The Design and Development of Segmental Tunnel Linings in the U. K.,” *Proceedings of the International Tunnel Symposium on Tunneling Under Difficult Conditions*, Tokyo, 1978.

Lysmer, J. et al, “FLUSH — A Computer Program for Approximate 3-D Analysis of Soil-Structure Interaction Problems,” *EERC Report No. 75-30*, Berkeley, Univ. of California, 1975.

Mohraz, B., Hendron, A. J., Ranken, R. E., and Salem, M. H., “Liner-Medium Interaction in Tunnels,” *Journal of the Construction Division, ASCE*, Vol. 101, No. CO1, January 1975.

Monsees, J. E., and Hansmire, W. H., “Civil Works Tunnels for Vehicles, Water, and Wastewater,” Chapter 24.1, *SME Mining Engineering Handbook*, 2nd Edition, 1992.

Monsees, J. E., and Merritt, J. L., “Earthquake Considerations in Design of the Los Angeles Metro,” ASCE Conference on Lifeline Earthquake Engineering, 1991.

Monsees, J. E., “Underground Seismic Design,” *ASCE Structural Group Lecture Series*, Boston Society of Civil Engineers Section, 1991.

Mow, C. C., and Pao, Y. H., “The Diffraction of Elastic Waves and Dynamic Stress Concentrations,” R-482-PR, *Report for the U.S. Air Force Project*, The Rand Corp., 1971

Muir Wood, A. M., “The Circular Tunnel in Elastic Ground,” *Geotechnique 25*, No. 1, 1975.

Nakamura, M., Katayama, T., and Kubo, K., “Quantitative Analysis of Observed Seismic Strains in Underground Structures,” *Proceedings of Review Meeting of U.S.-Japan Cooperative Research on Seismic Risk Analysis and Its Application to Reliability-Based Design of Lifeline System*, 1981.

Newark, N. M., “Problems in Wave Propagation in Soil and Rock,” International Symposium on Wave Propagation and Dynamic Properties of Earth Materials, 1968.

Nyman, D. J., et al, “Guidelines for the Seismic Design of Oil and Gas Pipeline Systems,” ASCE Technical Council on Lifeline Earthquake Engineering, 1984.

O’Rourke, T. D., “Guidelines for Tunnel Lining Design,” ASCE Technical Committee on Tunnel Lining Design of the Underground Technology Research Council, 1984.

Owen, G. N., and Scholl, R. E., *Earthquake Engineering of Large Underground Structures*, prepared for the Federal Highway Administration, FHWA/RD-80/195, 1981.

Paul, S.L., et al, *Design Recommendations for Concrete Linings for Transportation*

Tunnels, Report No. UMTA-MA-06-0100-83-1 and 2, prepared for U.S. DOT, Urban Mass Transportation Administration, Vols. 1 and 2, 1983.

Peck, R. B., Hendron, A. J., and Mohraz, B., "State of the Art of Soft Ground Tunnelling", *Proceedings of the Rapid Excavation and Tunnelling Conference*, Chicago, IL., Vol. 1, 1972.

"Preliminary Seismic Design Guidelines for Pier 300 Container Wharf and Retaining Structures," Port of Los Angeles, 1991.

Richardson, A., and Blejwas T. E., "Seismic Design of Circular-Section Concrete-Lined Underground Openings — Preclosure Performance Considerations for the Yucca Mountain Site," ASCE Symposium on Dynamic Analysis and Design Considerations for High-Level Nuclear Waste Repositories, 1992.

Richardson, A., St. John, C.M., and Schmidt, B., "A Proposed Concrete Shaft Liner Design Method for an Underground Nuclear Waste Repository," *Proceedings of the Conference on Structural Mechanics in Reactor Technology*, Pasadena, 1989.

Rowe, R., "Tunnelling in Seismic Zones," *Tunnels & Tunnelling*, December 1992.

Sakurai, A., and Takahashi, T., "Dynamic Stresses of Underground Pipeline during Earthquakes," *Proceedings of the 4th World Conference on Earthquake Engineering*, 1969.

Schnabel, P. B., Lysmer J., and Seed, B. H., "SHAKE — A Computer Program for Earthquake Response Analysis of Horizontally Layered Sites," *EERC Report No. 72-12*, Berkeley, Univ. of California, 1972.

Schmidt, B., and Richardson, A. M., "Seismic Design of Shaft Linings," ASME Symposium on Recent Development on Lifeline Earthquake Engineering, Honolulu, July 1989.

Schwartz, C. W., and Einstein H. H., *Improved Design of Tunnel Supports: Volume 1 — Simplified Analysis for Ground-Structure Interaction in Tunneling*, Report No. UMTA-MA-06-0100-80-4, Prepared for U.S. DOT, Urban Mass Transportation Administration, 1980.

Seed, B. H., and Idriss, I. M., "Soil Moduli and Damping Factors for Dynamic Response Analysis," *EERC Report No. 70-10*, 1970.

Seed, B. H., and Whitman, R. V., "Design of Earth Retaining Structures for Dynamic Loads," ASCE Specialty Conference on Lateral Stresses in the Ground and Design of Earth Retaining Structures, 1970.

SFBARTD, “Technical Supplement to the Engineering Report for Trans-Bay Tube,” July 1960.

SFBARTD, “Trans-Bay Tube Seismic Joints Post-Earthquake Evaluation,” November 1991.

Sharma, S., and Judd, W. R., “Underground Opening Damage from Earthquakes,” *Engineering Geology*, 30, 1991.

Southern California Rapid Transit District (SCRTD), “Supplemental Criteria for Seismic Design of Underground Structures,” Metro Rail Transit Consultants, 1984.

St. John, C. M., and Zahrah, T. F., “Aseismic Design of Underground Structures,” *Tunnelling and Underground Space Technology*, Vol. 2, No. 2, 1987.

Taipei Metropolitan Area Rapid Transit Systems (TARTS), “Railway Tunnel Investigation — Sungshan Extension Project,” ATC, Inc., 1989.

Torseth, D. O., “Port of Seattle Seismic Waterfront Design,” ASCE Symposium on Lifeline Earthquake Engineering: Performance, Design and Construction,” 1984.

Uniform Building Code (UBC), International Conference of Building Officials, Whittier, California, 1992.

Wang, J. M., “The Distribution of Earthquake Damage to Underground Facilities during the 1976 Tangshan Earthquake,” *Earthquake Spectra*, Vol. 1, No. 4, 1985.

Warshaw, R., “BART Tube Ventilation Building,” *Civil Engineering, ASCE*, December 1968.

Werner, S. D., and Taylor, C. E., “Seismic Risk Considerations for Transportation Systems,” *ASCE Technical Council on Lifeline Earthquake Engineering, Monograph No. 1*, November 1990.

Wittkop, R. C., “Seismic Design for Port of Los Angeles, 2020 Program,” ASCE Conference on Lifeline Earthquake Engineering, 1991.

Wood, J. H., “Earthquake-Induced Soil Pressures on Structures,” *Report No. EERL 73-05*, 1973, California Institute of Technology.

Yeh, G. C. K., “Seismic Analysis of Slender Buried Beams,” *Bulletin of the Seismological Society of America*, Vol.64, No. 5, 1974.

Yong, P. M. F., “Dynamic Earth Pressures Against A Rigid Earth Retaining Wall,” *Central Laboratories Report 5-85/5*, Ministry of Works and Development, New Zealand, 1985.